Department of Precision and Microsystems Engineering

Designing Dutch tunnel ventilation systems dominated by an uncertain fire scenario

Sophie van der Drift

Report no : 2023.093
Coach : -
Professor : Dr. Ir. Lise Noël (TU Delft)
Specialisation : EM
Type of report : Thesis report
Date : 31 October 2023

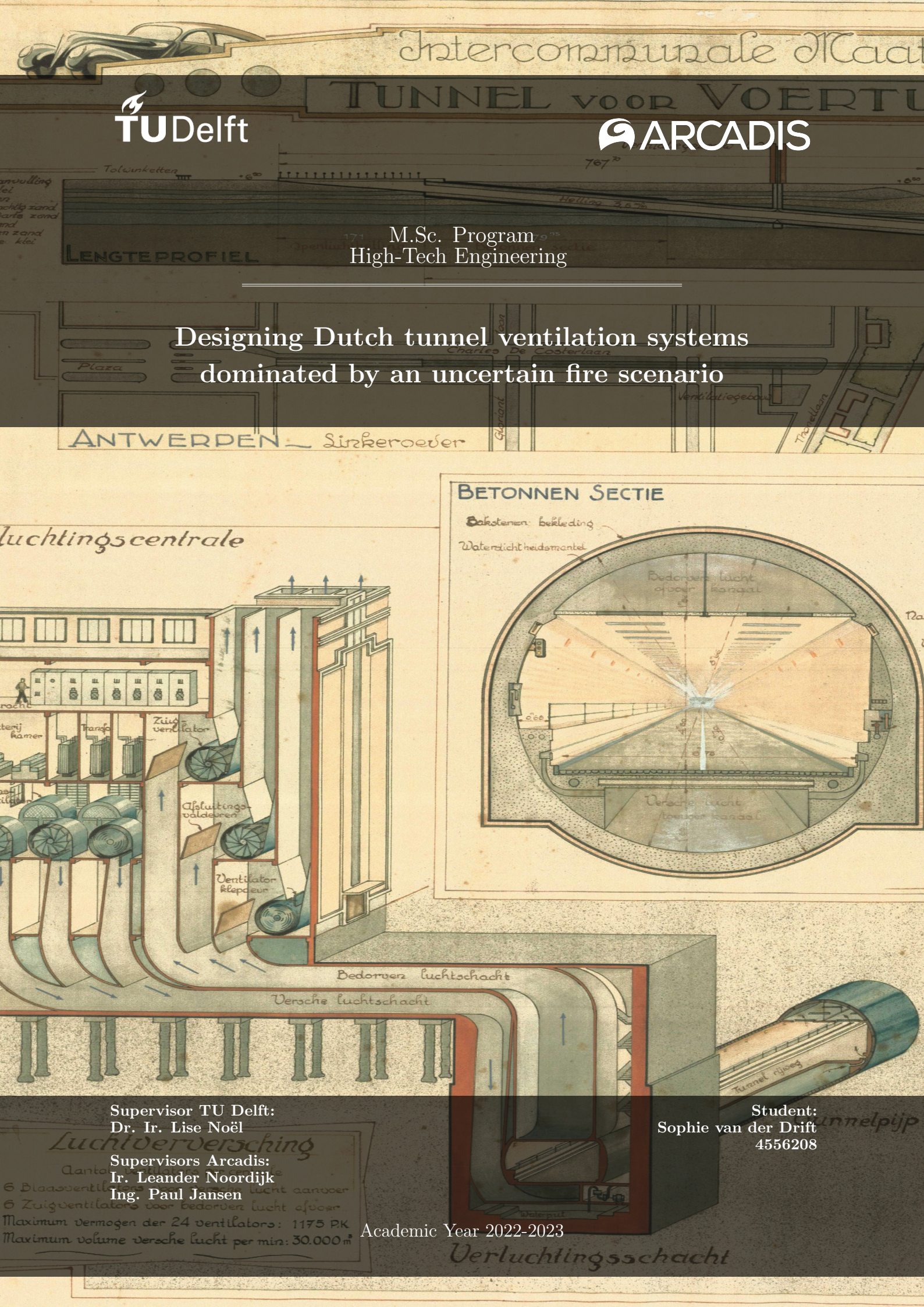

TU Delft

ARCADIS

M.Sc. Program
High-Tech Engineering

Designing Dutch tunnel ventilation systems dominated by an uncertain fire scenario

Supervisor TU Delft:
Dr. Ir. Lise Noël
Supervisors Arcadis:
Ir. Leander Noordijk
Ing. Paul Jansen

Student:
Sophie van der Drift
4556208

Academic Year 2022-2023

Designing Dutch tunnel ventilation systems dominated by an uncertain fire scenario

Master of Science Thesis

For the degree of Master of Science in High-Tech Engineering at Delft University of Technology

by

Sophie van der Drift

October 29, 2023

Faculty of Mechanical, Maritime and Materials Engineering (3mE) · Delft University of Technology

The work in this thesis received support from Arcadis and was conducted under the supervision of ir. Leander Noordijk, ing. Paul Jansen, and dr.ir. Noël of the Precision & Micro-Engineering department at the TU Delft. I would like to express my gratitude for their invaluable cooperation.

Abstract

Adequate mechanical ventilation serves as the first and most important life-saving appliance during a tunnel fire. While engineering for tunnel fire safety contains many aspects, the most severe threat during a tunnel fire is the smoke. Most victims get incapacitated by the smoke, after which they decease from intoxication and/or suffocation. By means of mechanical ventilation, smoke-free escape routes via the central egress corridor are created. A smoke free escape route is accomplished if the smoke flow is uni-directional and the central egress corridor is free of smoke. To carefully design the mechanical ventilation system of a tunnel, two stages are considered. The first stage involves the identification and positioning of jet fans to create a longitudinal ventilation system in the tunnel. The dangerous undesired reverse flow of smoke in the tunnel, back-layering, can be prevented by achieving a minimum critical air velocity. The second stage is a positive pressure establishment in the central egress corridor with respect to the tunnel. This system is essential to prevent smoke flow from the tunnel into the central egress corridor through open escape doors. The longitudinal ventilation system is highly influenced by the position and heat release rate of the fire. Jet fans near the fire are influenced by the temperature, which can lead to reduced efficiency or even complete failure. Given the uncertainty concerning the fire, it is imperative that longitudinal ventilation is designed to consistently meet the back-layering constraint across all possible fire scenarios. For enhanced longitudinal ventilation reliability, jet fan placement at the tunnel entrance is preferable, while positive pressure ventilation benefits from a scattered jet fan layout. This motivates the need for a systematic design method that considers the uncertain fire scenario while finding an optimum between the two objectives. The introduction of a systematic design method has the potential to enhance fire safety for tunnel users and improve the efficiency of ventilation design. To structurally and effectively determine jet fan layouts with the aim of preventing back-layering, a design approach based on the fundamentals of topology optimization is established. To streamline the design of ventilation within the central egress corridor, optimizing longitudinal tunnel ventilation design while minimizing pressure downstream of the fire in the tunnel is advantageous. To prevent energy dissipation, a secondary objective specified as a penalization objective is introduced to promote the required distance between jet fans. This objective determines the placement of jet fans by considering the positioning of nearby jet fans within a specified distance, influenced by a penalization exponent. This approach effectively achieves the desired jet fan distances. To address the fire related uncertainty, a scenario-based approach is applied. This method has the capacity to accommodate multiple fire scenarios simultaneously, where the designer can select the desired quantity. The systematic design approach presented in this thesis has the potential to enhance fire safety for tunnel users and streamline longitudinal ventilation design, effectively achieving the desired jet fan distances, while also addressing fire-related uncertainties.

Contents

1

Introduction

Adequate mechanical ventilation for vehicle tunnels, is crucial in the event of tunnel fires. This has been proven in the past by several disastrous tunnel fires. In March 1999, a fire killed 39 people in the Mont-Blanc Tunnel (Abraham & Dérobert, 2003). More recently in 2009, five lives were lost in the Eiksund Tunnel in Norway (Dagbladet, 2009). In appendix A.1, a comprehensive overview of tunnel fires leading to casualties is provided. Ingason (2016) stated, the most significant risk to tunnel users during operation is the occurrence of fire accidents. These events led to the establishment of rules originating from governmental institutions in Europe and individual countries to increase tunnel fire safety (2004/54/EC, 2004; AVV, 2005).

The fire behaviour in a tunnel is different from an open fire. An open fire has no interaction with surrounding geometries or enclosure (Ingason et al., 2015). Pettersson et al. (1976) described the complex movement of an enclosed fire, which is determined by multiple factors: (*i*) the quantity and location of the fuel, (*ii*) the characteristics of the tunnel such as its geometry, lining and ventilation. The heat released from the fire is transferred to its surroundings through radiation, convection, and conduction. These surroundings include the smoke gasses, the surrounding air, and the construction.

When little to no ventilation is present, the smoke originating from the fire ascends upwards till it reaches the ceiling, after which it propagates in a direction away from the fire. This phenomenon is called *stratification* and is illustrated in Fig. 1.1. After some time, the temperature of the smoke is cooled down by the relatively cold tunnel structure, causing the density difference between the smoke and the surrounding air to decrease. The stratification movements are lost, causing the smoke to descend again (AVV, 2005).

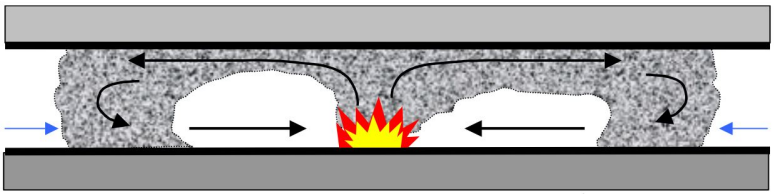

Figure 1.1: Smoke movement during tunnel fire (black arrows) with solely natural ventilation (blue arrows) (AVV, 2005).

Engineering for tunnel fire safety is challenging with respect to many aspects, however the most severe threat during a tunnel fire is the smoke. Only few people fall victim through the fire flames directly. Most victims get incapacitated by the smoke, after which they decease from intoxication and/or suffocation. By means of mechanical ventilation, smoke-free escape routes are established. In addition, the fire brigade can use these smoke-free zones to access the fire, safe people from their vehicles, and prevent further danger risks and damage to the tunnel structure. Therefore, the first and most important life-saving appliance during a tunnel fire is the mechanical ventilation. It allows prevention of smoke flow opposite to the traffic direction and smoke flow into the Central Egress Corridor (CEC). Often, when referring to unidirectional traffic tunnels, the tunnel is made of two tunnel tubes and a CEC located in between. In the event of a fire, people can enter the CEC via escape doors and find their way out through the head doors at the begin and/or end of the tunnel. This route is illustrated by a yellow dotted line in Fig. 1.2. Both the tunnel tubes and the CEC have their own ventilation system.

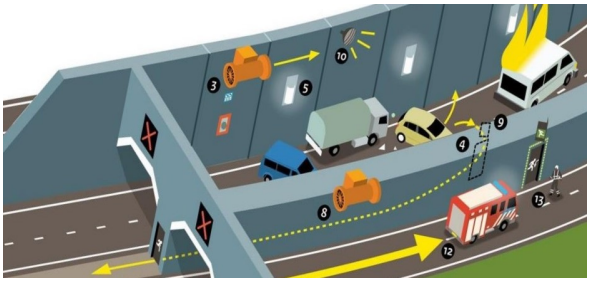

Figure 1.2: A tunnel made of two tunnel tubes and a CEC situated in between. The escape route is illustrated by the yellow dotted line (Scholten, 2016).

1.1 Tunnel Ventilation System

To carefully design the mechanical ventilation system of a tunnel, two stages are considered. The first stage involves the identification and positioning of jet fans to create a ventilation system in the tunnel tube. The second stage is the positive pressure ventilation system, which focuses on the design of the ventilation system in the CEC.

1.1.1 Ventilation System in the Tunnel Tube

The tunnel tube ventilation combines two mechanisms, namely natural-and mechanical ventilation. Natural ventilation occurs through the influence of occasional forces. Examples of such forces are traffic effects, buoyancy forces due to a slope in the tunnel, and wind-and atmospheric conditions. Three main types of mechanical ventilation systems exist. Namely, the longitudinal ventilations, the transverse ventilations, and the semi-transverse ventilations. The longitudinal ventilations create a unidirectional air flow by positioning jet fans at the ceiling of the tunnel tube, see Fig. 1.3a. The transverse ventilations operate perpendicular to the longitudinal axis of the tunnel tube. It removes polluted air and smoke while supplying fresh air. The semi-transverse ventilations only transversely supply fresh air through the ventilation openings. The air flows in the longitudinal direction out of the tunnel. The limited size of the ventilation openings in both transverse ventilation types renders them unsuitable for eliminating smoke from fires with a high heat release rate (HRR). When a tunnel fire occurs and a traffic jam is not present, a queue of vehicles forms upstream of the fire, while vehicles downstream of the fire can exit the tunnel, see Fig. 1.3b. To prevent smoke casualties, the smoke has to be disposed in the exit direction of the tunnel. Longitudinal ventilations create such a unidirectional smoke movement towards the tunnel exit. Therefore, in unidirectional tunnels with limited lengths up to 2.5 to 3 km, longitudinal ventilation is the preferred method. Furthermore, longitudinal ventilation is relatively easy to implement and more energy and cost efficient than the other approaches.

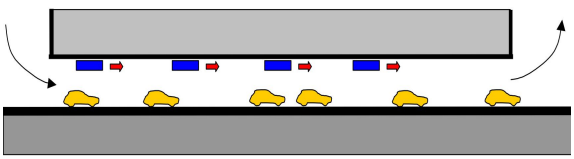

(a) The black arrows show the natural ventilation and the red arrows the longitudinal ventilation (AVV, 2005).

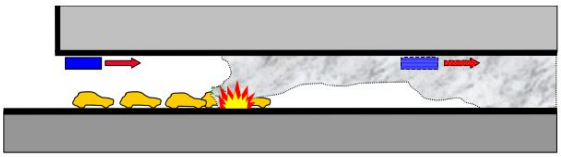

(b) Longitudinal ventilations dispose the smoke in the exit direction of the tunnel (AVV, 2005).

Figure 1.3: Longitudinal tunnel ventilation.

When unidirectional smoke flow toward the tunnel exit fails, it results in the reverse flow of smoke. This phenomenon is called *back-layering*, and is illustrated in Fig. 1.4. It poses a threat to the vehicles upstream of the fire location. In order to prevent back-layering, the longitudinal air velocity has to reach a minimum critical value that depends on the fire HRR (Ingason et al., 2015;

Ntzeremes & Kirytopoulos, 2022). Independent of the tunnel type, the *critical velocity* in a tunnel is generally around 2.5 m/s (AVV, 2005). The number of jet fans required to generate the required air velocity is highly dependent on the problem. However, to offer an initial perspective, a tunnel tube with a length of 1.5 km could require approximately 12 jet fans. For the same tunnel description, the number of fans in the CEC is roughly two or three.

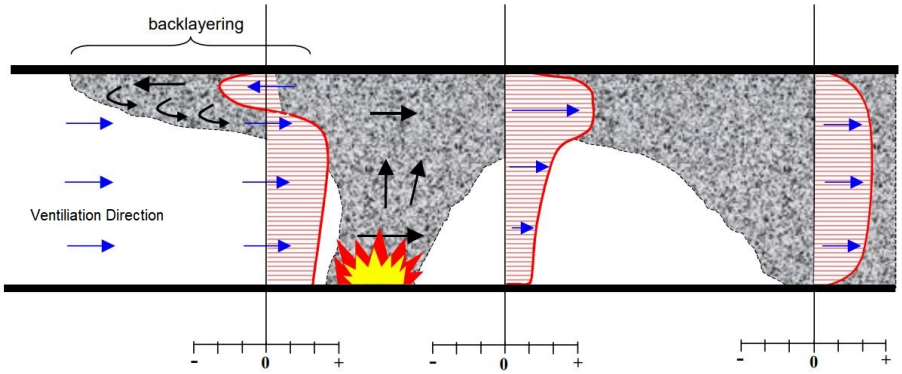

Figure 1.4: In the absence of or with inadequate longitudinal mechanical ventilation, smoke moves against the ventilation direction, resulting in back-layering (AVV, 2005).

The functionality of jet fans in a tunnel reach further than solely the control of smoke movements. Jet fans also regulate the concentration of traffic emissions and the temperature in a tunnel. This report restricts itself to longitudinal ventilation in unidirectional traffic tunnels of limited lengths up to 3 km and ambient air temperatures limited to the boundaries of a moderate maritime climate. Therefore in this research, the traffic emissions and temperature control are not primary variables in the design of the longitudinal tunnel ventilation. Generally, the mechanical ventilation of unidirectional traffic tunnels up to 3 km, is primarily dependent on the fire.

1.1.2 Ventilation System in the CEC

The second stage of the mechanical ventilation design involves designing a positive pressure ventilation system in the CEC. This system is essential to prevent airflow from the tunnel tube into the CEC through open escape doors. To achieve this, the CEC must maintain a positive pressure relative to the tunnel tube. Instead of jet fans, regular axial fans are used in the positive pressure ventilation system, introducing clean outside air. To avoid confusion, it is important to note that jet fans are installed in the tunnel tube, while fans are used in the CEC. A fan positioned in the CEC is illustrated in Fig. 1.5. To achieve the desired positive pressure in the CEC, the required fan specifications need to be determined. The cumulative pressure in the tunnel tube is amongst others,

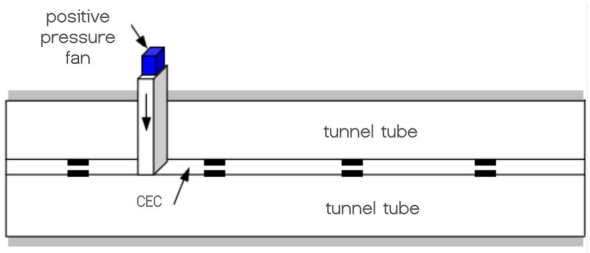

Figure 1.5: A fan positioned in the CEC (AVV, 2005).

dependent on the jet fan spacing and the fire location. The pressure relationship between the CEC and the tunnel tube is explained using a top view illustration presented in Fig. 1.6 of two tunnel tubes with a CEC situated in the center. The continuous line represents the pressure development in

the tunnel tube and the dashed lines the two different pressure levels in the CEC. In order to prevent undesired smoke flow, the dashed line must remain above the continuous line downstream of the fire. In case of CEC pressure value B, the positive pressure requirements are not met. For example, at the position of the fifth black rectangles in the CEC (fifth escape door), the pressure in the tunnel tube clearly exceeds the CEC pressure. Maintaining this positive pressure is particularly critical

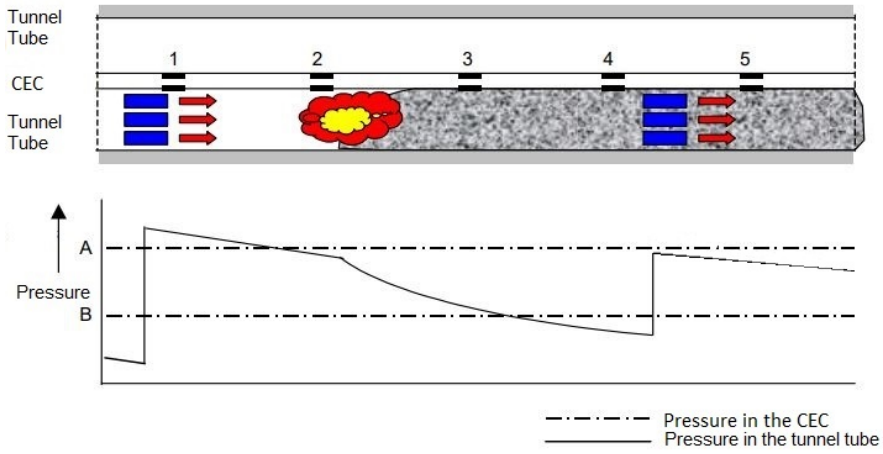

Figure 1.6: Top view of two tunnel tubes with a CEC situated in the center. It shows the pressure relationship between the tunnel tube and the CEC. The blue and black rectangles are the jet fans in the tunnel tube and the escape doors. The red and yellow shape is the fire (AVV, 2005).

downstream of the fire. Since, when the longitudinal ventilation system operates as intended, there is no back-layering of smoke in the tunnel, and no smoke is present upstream of the fire. Therefore, it is not as crucial to maintain positive pressure upstream of the fire.

In the occasion of a fire, it is essential to control smoke movement by reaching the critical air velocity and preventing back-layering, while simultaneously controlling the pressure in the tunnel and the CEC. A carefully designed ventilation is determinant for the safety in a tunnel. Therefore, a design method which accounts for both design objectives simultaneously is key. Since the two objectives are conflicting, creating an effective ventilation design is challenging.

1.2 Uncertain Fire Scenario

The tunnel ventilation performance is highly influenced by the position and HRR of the fire. Jet fans near the fire are influenced by the temperature, which can lead to reduced performance or even complete failure. Given the uncertainty concerning the fire, the longitudinal ventilation must consistently meet the back-layering constraint across all possible fire scenarios. To enhance the reliability of tunnel ventilation, jet fans are preferably positioned at the beginning of the tunnel. This placement allows them to attract cold air from outside the tunnel, while remaining unaffected by the high temperatures from the fire. As a result, a pressure peak is created at the beginning of the tunnel, which the positive pressure ventilation system must exceed to prevent smoke flow into the CEC. Therefore, the positive pressure ventilation benefits from a more scattered jet fan positioning in the tunnel.

1.3 Arcadis

This thesis is performed in collaboration with Arcadis, a global design, engineering, and consulting firm established in the Netherlands in 1888. They specialize in infrastructure, environmental,

and building projects, offering services like architecture, engineering, environmental consulting, and project management. They have a strong presence and expertise in tunnel ventilation design, where they ensure the safety and efficiency of critical underground infrastructure.

The current design approach for tunnel ventilation design at Arcadis is examined to obtain insights into the current design methodology and to identify any shortcomings. The methodology within Arcadis is categorized into sequential components: it begins with the deterministic longitudinal ventilation design approach, where the fire location and HRR are fixed. This is followed by the assessment of the uncertain fire scenario through probabilistic calculations, and the design process concludes with the positive pressure ventilation design.

1.3.1 Deterministic Longitudinal Ventilation Design

The primary objective is to identify a longitudinal tunnel ventilation system that effectively prevents back-layering during a tunnel fire. The design process, as illustrated in Fig. 1.7, starts with the designer selecting a deterministic fire scenario, specifying a fixed fire location and HRR. The designer formulates a longitudinal ventilation design and performs calculations in a design software called ProTuVeM. Subsequently, this design is evaluated against air velocity requirements. If these criteria are not met, the designer adjusts the design, repeating the calculations iteratively until the requirements are satisfied. Consequently, this process is based on the experience of the designer.

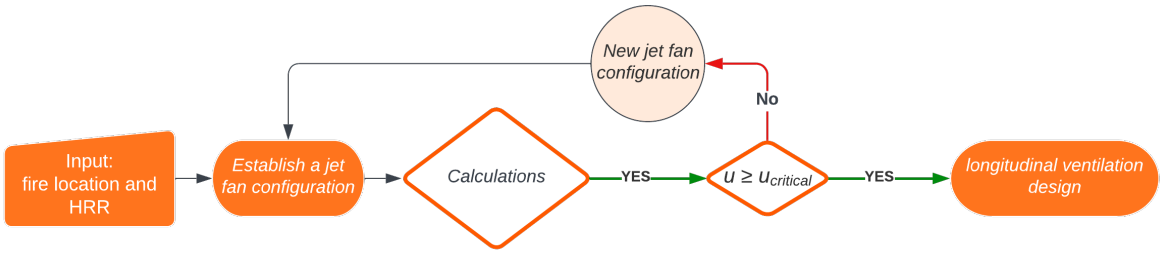

Figure 1.7: The deterministic design process for a longitudinal ventilation design.

1.3.2 Uncertain Fire Scenario

When designing for a deterministic fire scenario, each variable is assigned a fixed value, resulting in a unique solution. To ensure the effective operation of the longitudinal ventilation design, it is crucial to verify if the critical air velocity is reached over a broad range of fire scenarios. This verification involves probabilistic calculations in ProTuVeM with a fixed HRR, considering wind direction, wind velocity, and fire location as stochastic variables. The probabilistic calculations result in failure probabilities concerning the critical velocity requirements. The probability-based calculations serve as verification tool, allowing for the evaluation of the design across a broad range of scenarios. Should the failure probabilities fail to meet the required thresholds, the ventilation design is modified.

1.3.3 Positive Pressure Ventilation Design in the CEC

After identifying a jet fan alignment that meets the constraints of longitudinal ventilation design, the positive pressure ventilation system in the CEC is designed. To prevent smoke flow into the CEC, a positive pressure needs to be established with respect to the tunnel tube. Subsequently, to achieve this, the required fan specifications need to be determined.

A separate mathematical programming sheet is used to calculate the cumulative pressure profile within the tunnel for specific fire scenarios. This is used to asses whether the cumulative pressure profile of the CEC remains above that of the tunnel tube. The pressure level in the CEC is modified by altering the fan type, which, in turn, impacts the air velocity through the escape doors. Air velocity through the escape doors is calculated using a 1D network model. To ensure that individuals

attempting to escape through the CEC are not hindered, it is necessary to adhere to the established requirements described by Rijkswaterstaat & GPO (2023). The requirements are imposed on the air velocity trough the escape doors and on the air velocity in the CEC, and are provided in Table 1.1.

Min. air velocity through escape door [m/s]	Max. air velocity through escape door [m/s]	Max. air velocity in the CEC [m/s]
0.75	12	5

Table 1.1: The air velocity requirements for the positive pressure ventilation system imposed by Rijkswaterstaat & GPO (2023).

Tunnels in the Netherlands are constructed with an escape door every 100 m. To evaluate if the positive pressure ventilation design meets the requirements, several open and closed escape door setups are examined. These setups were established by Rijkswaterstaat & GPO (2023). Following the legal framework in the Netherlands, it is mandatory to consider 30 % of the escape doors opened simultaneously with a minimum of three escape doors, while evaluating the positive pressure conditions. Established by van Oerle (2016) on behalf of Rijkswaterstaat (RWS), approximately 20 different configurations exist. The exact number of configurations to be tested, comprising of different fire scenarios and escape door setups, may vary slightly depending on tunnel specifics. When the air velocity satisfies the requirements, the design for the positive pressure ventilation, as well as the design for the longitudinal ventilation in the tunnel tube, are considered complete.

1.4 Motivation

The preferred design for the longitudinal ventilation often results in a suboptimal, and potentially infeasible, design for the positive pressure ventilation system. Minimizing the number of jet fans, involves concentrating their placement at the tunnel entrance. This leads to a complex and costly (high power) positive pressure ventilation system. Conversely, an optimal design for positive pressure ventilation, with jet fans distributed throughout the tunnel, leads to an expensive longitudinal ventilation system. To prevent rework in later design stages, it is advisable to design a longitudinal ventilation system that not only meets the back-layering constraint but also aims to accommodate the requirements of positive pressure ventilation by preventing unnecessary pressure buildup within the tunnel tube.

The current methodology using ProTuVeM involves iterative designing and relies heavily on the expertise of the designer. Extracting information from ProTuVeM requires providing the program with a jet fan alignment and tunnel specifications to observe its effect. After a complete run, ProTuVeM provides the temperatures, tunnel resistances, and driving forces (jet fans), facilitating problem analysis. However, it lacks additional data on pressure developments and misses flexibility and usability for gaining comprehensive insights into the current problem. Additionally, comparing different ventilation designs is not straightforward. Finally, during probabilistic calculations, ProTuVeM lacks clarity on failure locations. This hinders the identification of ventilation design shortcomings. Therefore, the design approach would benefit from redeveloping ProTuVeM to enhance usability.

To determine the cumulative pressures required for designing the positive pressure ventilation system, a separate mathematical programming sheet is required alongside ProTuVeM. Various critical fire and open and closed escape door scenarios must be considered. However, the mathematical programming sheet is limited to considering only one jet fan design with one fire scenario at a time. Consequently, this method lacks efficiency and ease of use when designing. Hence, the design approach would benefit from a rewritten version of the separate mathematical programming sheet that offers improved flexibility and usability.

1.4.1 Research Proposal

This report focuses on the design of longitudinal ventilation, aiming to enhance the design approach at Arcadis. This process is guided by specific objectives. The first objective involves rewriting

ProTuVeM into a new program with enhanced usability and the integration of cumulative pressure calculations, eliminating the need for a separate mathematical programming sheet. In addition, to release the design approach from its dependence on the expertise of the designer and the iterative design methodology, a systematic design approach is required. This systematic approach should provide a longitudinal ventilation design which prevents back-layering while simultaneously aims to prevent unnecessary pressure buildup within the tunnel tube to serve the positive pressure ventilation design. Furthermore, the systematic design approach must account for uncertainties related to fire scenarios. Finally, it is essential to consider geometric constraints related to jet fan placement to prevent energy loss. These constraints include maintaining a specified inner distance between jet fans in series and positioning them at a specified distance before the tunnel exit.

The development of a systematic design method, has the potential to enhance fire safety for tunnel users and improve the efficiency of ventilation design. Consequently, this could lead to ventilation cost reduction and lower energy consumption in tunnel ventilation systems. The research question for this thesis is defined as: *What systematic design approach can be used to solve the fire safety ventilation design problem dominated by an uncertain fire scenario and how can this approach be practically implemented to enhance fire safety and design efficiency?*

To guide the research, three subquestions are formulated. The first is *What positioning technique is appropriate to find a jet fan alignment in the tunnel tube?* This subquestion seeks to identify a positioning technique that strategically defines the placement of jet fans to effectively prevent the occurrence of back-layering.

The second is *How can both the objectives, back-layering prevention and positive pressure in the CEC with respect to the tunnel tube, be included in the systematic design approach?* As previously discussed, the two objectives are contradictory. During the design stage of the longitudinal ventilation, it is advisable to consider the CEC ventilation design. This helps avoid the necessity for redesigning the longitudinal ventilation system in later design stages.

The third is *How can the two unknown fire parameters, fire HRR and fire location, be included in the systematic design approach?* Given the high influence the fire scenario has on tunnel ventilation performance, it is essential to integrate it into the ventilation design process.

1.5 Outline

The remainder of this report is structured as follows: Chapter 2 discusses the physics and background relevant to tunnel ventilation design and introduces the new tunnel ventilation model. Chapter 3 proposes a novel tunnel ventilation design methodology. Chapter 4 introduces a methodology to account for the uncertain fire scenario in the design process. In Chapter 5, the enhanced tunnel ventilation design method is applied on a ventilation project performed by Arcadis, and the results of both design methodologies are compared. The obtained results are discussed in Chapter 6 to provide insight. Finally, conclusions are drawn in Chapter 7. Chapter 8 offers recommendations for further improving the ventilation design approach.

2

Tunnel Ventilation Model

Limitations were identified and discussed in Chapter 1 regarding the current approach at Arcadis to solve the ventilation design problem. The current ventilation model, ProTuVeM, has shown several shortcomings that hinder the development of a systematic ventilation design approach. To address this, ProTuVeM is rewritten in Python. This chapter provides an in-depth exploration of the underlying physics and background that were used to develop ProTuVeM. Subsequently, the development and validation of the rewritten longitudinal ventilation model is discussed.

2.1 Legal Framework Regarding Tunnel Ventilation Design in the Netherlands

Tunnel designers in the Netherlands have to follow the regulations established by RWS. RWS is the executive agency of the Ministry of Infrastructure and Water Management in the Netherlands. They carried out a thorough research, and collected their findings in the *Aanbevelingen ventilatie van verkeerstunnels* (AVV, 2005), in English referred to as the Recommendations for ventilation of traffic tunnels. The AVV was written in 2005. The AVV describes the background and physics related to tunnel ventilation design. These include effects of wind, ventilator efficiency, and effects of fire on a ventilation system. Before the introduction of low-emission vehicles, the main reason for tunnel ventilation was to regulate the concentration of polluted air. However, since the introduction of low-emission vehicles and the occurrence of the first serious tunnel fires, the focus shifted towards the regulation of fire and smoke. RWS created a design software called ProTuVeM (Derikx et al., 2011), which uses the physics and requirements described in the AVV for tunnel ventilation design. As part of the requirements posed by RWS, it is mandatory to use ProTuVeM directly for the design, or in a post-processing step as verification. The tunnel is represented by a one dimensional model, providing a static overview of the steady-state fire and air movements. The time-dependent behaviour of the smoke spread during the growth phase of the fire is very brief compared to the steady state. This transient behavior is not accounted for in ProTuVeM and is not further discussed in this report.

2.2 Physics Model for the Longitudinal Ventilation

This paragraph provides a comprehensive overview of ventilation in tunnels. First, the fundamental principle of longitudinal ventilation system design is explained, which is the pressure equilibrium. This is followed by temperature calculations. Then, the tunnel resistances and the role of jet fans is examined. Finally, the calculation procedure for longitudinal ventilation is detailed.

2.2.1 Pressure Equilibrium

The basic principle of longitudinal ventilation for the steady state phase is the pressure equilibrium requirement. The equilibrium describes the resistance and driving forces present in a tunnel. The left side of the equilibrium in Eq. (2.1) represents the total positive contribution from jet fans, and the right side represents the pressure losses originating from tunnel resistance effects.

$$\sum_{i=0}^{n}(\Delta p_{jet})_i = \Delta p_{wall} + \Delta p_{in/out} + \Delta p_{traffic} + \Delta p_{meteorologic} + \Delta p_{fire} + \Delta p_{thermostatic}, \quad (2.1)$$

where $(\Delta p_{jet})_i$ represents the pressure contribution from the i-th jet fan from the total of n positioned jet fans, Δp_{wall} are the pressure losses due to wall friction, $\Delta p_{in/out}$ are the pressure losses at the entrance and exit portal, $\Delta p_{traffic}$ is the positive or negative contribution of the traffic to the air flow, $\Delta p_{meteorologic}$ represents the effect of external wind on the air flow in the tunnel, Δp_{fire} is the pressure drop over the fire, and $\Delta p_{thermostatic}$ represents the chimney effect, this refers to the upward force exerted by hot smoke. This upward force may lead to upward motion of smoke towards higher tunnel parts, which can either assist or hinder the intended smoke flow. When performing a deterministic calculation, the fire location and HRR are fixed, as are the prevailing wind direction and force. Therefore, a decision regarding these, otherwise uncertain parameters, has to be made before performing the calculation. Generally, the worst case scenarios are identified and used. An example of such a worst-case scenario involves a 10 m/s adverse wind with a 200 MW fire located in proximity to the positioned jet fans. Some parameter values in the AVV are approximate, rounded from precise scientific values. For instance, the specific heat of air at $10°C$ is specified as 1000, while its exact scientific value is 1005. These values are indicated.

2.2.2 Temperature Calculation

The air temperatures downstream of the fire decrease due to convective and radiative heat transfer from the hot smoke gases to the tunnel walls. The convective and radiative heat transfer coefficients are defined as h_c and h_r, respectively.

$$h_c = \frac{\frac{1}{8}\lambda c_p \rho u_r}{1,07 + 12,7(Pr^{2/3}\sqrt{\frac{1}{8}\lambda})}, \quad h_r = \epsilon\,\sigma(T + T_{wall})(T^2 + T_{wall}^2),$$

where λ is the wall friction coefficient, c_p is the specific heat of air (1000,0 [kJ/kg K]), ρ is the density of the hot smoke gases, u_r is the velocity of the smoke gases, Pr is the Prandtl number (0,71 [-]), ϵ is the wall emissivity (0,7 [-]), σ is the Stefan-Boltzmann constant ($5,669 \cdot 10^{-8}$ [W/m^2K^4]), T is the temperature of the smoke and T_{wall} is the wall temperature. Since downstream of the fire the heat is transferred to the tunnel construction, the temperature of the smoke gasses decreases.

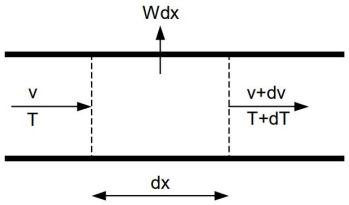

Figure 2.1: Downstream of the fire the air is cooled down by means of convection and radiation.

Based on Fig. 2.1, and the assumption of a uniform temperature distribution in the tunnel, the temperature change dT is calculated over each incremental step in distance dx as:

$$dT\rho_0 c_p v A = hS(T - T_{wall})dx, \tag{2.2}$$

where ρ_0 is the density of the ambient air outside the tunnel, v is the velocity of the supplied air, A is the cross-sectional area of the tunnel, h is the total heat transfer coefficient combining h_r and h_c, and S is the circumference of the tunnel intersection. Subsequently, Eq. (2.2) can be rewritten as:

$$\frac{dT}{dx} = \frac{hS(T - T_{wall})}{\rho_0 c_p v A}. \tag{2.3}$$

Up to the location of the fire, the air temperature within the tunnel corresponds to the ambient outside air temperature. To calculate the temperature for the remaining part of the tunnel, the first step is to discretize the tunnel.

2.2.2.1 Discretization of the Tunnel

The tunnel is discretized starting at the tunnel entrance by two subsequent discretization steps, starting with the discretization into segments followed by smaller sections. This is illustrated in Fig. 2.2, where the red rectangle represents a tunnel which is divided into segments by solid vertical lines. It is further discretized into smaller sections indicated by dotted vertical lines. The orange triangle represents the fire position.

The ventilation designer performs the first discretization step into segments, which serves the purpose of providing ProTuVeM with the essential tunnel and jet fan information. Segment borders are chosen to align with desired jet fan locations and to coincide with changes in tunnel characteristics, such as tunnel slope, traffic lane count, and wall friction coefficient. Thus, these segment borders serve as potential positions for jet fan placement, and the areas between them, referred to as segment lengths, contain the tunnel characteristics for that part of the tunnel. Consequently, segments can have varying lengths, with some segments extending to several hundred meters. Hence, when conducting calculations related to temperature and resistance, it is necessary to use a finer discretization. This second discretization divides the tunnel into smaller sections, where the section borders carry the calculated variables as the temperature and the resistances. Due to the somewhat cumbersome and time-consuming process of inputting segments in ProTuVeM, this two-layered discretization approach is used. This locally refined mesh, division into sections, serves the purpose of automating the inclusion of smaller sections in tunnel areas where temperature and resistances change more rapidly. It follows the principles described: in all segments upstream of the fire, the

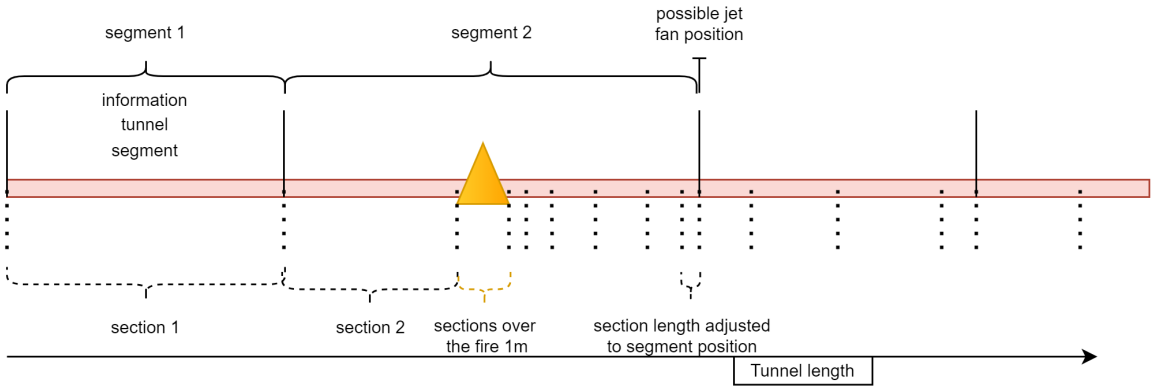

Figure 2.2: The red rectangle represents a tunnel, divided into segments by solid vertical lines. It is further discretized into smaller sections indicated by dotted vertical lines. The orange triangle is the fire. Over the fire length, each section is 1 m.

section borders coincide with the segment borders, and the section lengths are equal to the segment lengths. This is illustrated in Fig. 2.2 upstream of the fire. Each section over the fire length is 1 m, spanning up to a fire length of 10 m, as shown by the orange curly bracket below the fire. Downstream of the fire, each subsequent section is the previous section plus 1.1 times the difference in length between the previous two sections according to:

$$x_{c_{l+1}} = 1.1(x_{c_l} - x_{c_{l-1}}), \tag{2.4}$$

where x_c represents the position from the tunnel entrance of a section border in the tunnel at the $l+1$-th, l-th, and $l-1$-th section borders. This is shown by the increasing distances between the section borders (dotted lines) downstream of the fire. The boundaries of a section always have to coincide with a boundary of a segment (specified by the engineer). If necessary, the section length is adjusted accordingly, meaning that the section becomes shorter than the intended length. The length of the first section within a new segment follows the standard section calculation, using the intended (i.e., uncorrected) length of the preceding section. In cases where the fire position does not align with a segment border, the selection of section lengths must be adjusted to account for the spatial placement

of the fire. This adjustment is necessary to maintain precise alignment with the segment boundaries while accommodating the position of the fire. Consequently, distinct discretization schemes are used within the tunnel. Jet fan placement and tunnel characteristics determine the positions of segment borders, while resistances and temperatures are calculated at the smaller sections.

2.2.2.2 Temperature Calculation at Section Borders

By means of the specified discretization scheme, the temperature at the section borders is computed. The air temperature in the tunnel is determined through the combined use of the approximation of the first-order differential equation expressed in Eq. (2.3) and a relaxation method. First, the solution to the first-order differential equation is outlined, this is followed by an explanation of the used relaxation method. The differential equation is transformed by isolating all the temperature terms on one side and the position terms on the other. The resulting equation is integrated:

$$\int \frac{1}{T - T_{\text{wall}}}\, dT = \int \frac{hS}{\rho_0 c_p v A}\, dx. \tag{2.5}$$

To streamline the notation, the parameters on the right-hand side of Eq. (2.5) are combined into a single parameter denoted as L^*, and defined as:

$$L^* = \frac{\rho_0 c_p v A}{hS}. \tag{2.6}$$

The wall temperature T_{wall} is initially set at the ambient outside air temperature and increases along the fire length according to:

$$T^*_{\text{wall}} = T_{\text{wall}} + \frac{\eta P}{Sh}, \tag{2.7}$$

where P is the HRR, and η is the fraction of the HRR transferred to the smoke, which is 64% for all fire scenarios. Subsequently, the new temperature T_{new} is determined by solving Eq. (2.5):

$$T_{\text{new}} = T^*_{\text{wall}} + (T_{ps} - T^*_{\text{wall}})\, e^{-\frac{dx}{L^*}}, \tag{2.8}$$

where T_{ps} is the temperature at the previous section boundary. The relaxation method aims to iteratively update temperature values until convergence criteria are satisfied. These criteria are met when either one hundred iterations are reached or when the absolute difference between the newly computed temperature value T_{new} and the previously computed temperature value T_{old} becomes smaller than one. This approach uses a relaxation factor, r, with a value of 0.1. It achieves a gradual approach to the solution by considering a weighted average of T_{old} and T_{new} according to:

$$T = (1.0 - r)\, T_{old} + r\, T_{new}. \tag{2.9}$$

Subsequently, the calculated temperature T is produced as the final output. The relaxation method plays a crucial role in smoothing out the solution and promoting convergence by incorporating new information during the temperature calculation process. It enables a more stable and controlled iteration procedure, contrasting with a direct update of temperature values.

2.2.3 Tunnel Resistances

The temperature-dependent parameters are determined by using the temperatures calculated at the section borders. If the longitudinal ventilation operates as expected, the air velocity upstream of the fire has the critical velocity value and the density has a value corresponding to the ambient temperature. When the supplied air approaches the fire location, the air velocity and density change with the increasing temperature. The density decreases, if the temperature increases according to:

$$\rho = \frac{T_0}{T(x)} \rho_0, \tag{2.10}$$

where T and ρ are the temperature and density at position x and T_0, and ρ_0 are the ambient temperature and density. Subsequently, the air velocity changes due to expansion according to:

$$u_t = \frac{\rho_0}{\rho} u_0, \tag{2.11}$$

where u_0 is the initial air velocity in the tunnel. In case of back-layering prevention, u_0 should have the critical velocity value. Over the length of a section, a linear temperature progression is assumed:

$$T_{Asec} = \frac{1}{2}(T_{Bsec} + T_{Esec}), \tag{2.12}$$

where T_{Asec} is the average temperature over a section length, T_{Bsec} and T_{Esec} are the calculated temperatures at the beginning and ending of a section. Based on this assumption, the average values for temperature, velocity, and density are derived over the section lengths. The average values are used in the computation of resistance pressures at the section borders.

The pressure loss between *the in- and exit portal* ($\Delta p_{in/out}$) is dependent on the local velocity and the in-and exit flow coefficients. Possible differences in velocity at the in-and exit portal originate from a changing intersection through the tunnel, and the density and velocity change due to the fire according to Eq. (2.11) and (2.10). This is mathematically described as:

$$\Delta p_{in/out} = \Delta p_{in} + \Delta p_{out}, \qquad \text{with:} \quad \Delta p_{in} = \zeta_{in} \frac{1}{2} \rho_0 u_0^2, \quad \Delta p_{out} = \zeta_{out} \frac{1}{2} \rho u_t^2. \tag{2.13}$$

where ζ_{in} is the inflow coefficient (0,2 - 0,4 [-]) and ζ_{out} is the outflow coefficient (1 [-]). The density and velocity at the end of the last segment are used to compute the pressure loss at the exit portal.

The pressure losses due to *wall friction* are describes as:

$$\Delta p_{wall} = \lambda \frac{dx}{D_h} \frac{1}{2} \rho u_t^2, \tag{2.14}$$

where ρ and u_t are the average values over the sections, and D_h is the hydraulic diameter. This diameter term is used to describe the deviation of the tunnel cross-section with respect to a neatly round cross-section. This means it is a fictional diameter of the tunnel cross-section with equal resistance to the original cross-section. It is calculated according to:

$$D_h = 4 \frac{A}{S}. \tag{2.15}$$

The *traffic* can either resist or enhance airflow, depending on the driving direction and velocity. The total traffic resistance or aerodynamic drag is the sum of the individual vehicle resistances, see Eq. (2.16). Vehicles located downstream of the fire have the capacity to exit the tunnel, while those upstream of the fire can not. Therefore, in absence of any traffic jams, no vehicles are present downstream of the fire when the static calculations are performed. The velocity of the remaining traffic is zero. This changes how the vehicles experience flow in the tunnel. As opposed to stationary vehicles, driving vehicles experience a front flow. When the velocity of a vehicle is zero, the flow experienced is reduced to the mechanical ventilation. This results in a back flow.

$$\Delta p_{traffic} = \sum_{i=1}^{n_c} \frac{f_{sh} c_w A_v}{(1 - \frac{A_v}{A_t})^2} \frac{\frac{1}{2} \rho (u_t - u_v) |u_t - u_v|}{A_t}, \tag{2.16}$$

where n_c is the number of cars in the tunnel, f_{sh} is the shadow factor, c_w is the flow coefficient, A_v is the frontal inflow surface of the vehicles, and u_v is the current traffic velocity, which during the steady-state fire calculation is 0. In the traffic, three types of vehicles are distinguished: passenger cars, delivery vans, and heavy good vehicles (HGV). The passenger cars, delivery vans are denoted as light traffic vehicles (LTV). The parameter values depend on the vehicle type and are presented in Table 2.1.

Vehicle Type	A_v $[m^2]$	Vehicle Length $[m]$	C_w During front flow $[-]$	C_w During back flow $[-]$
Cars	2,5	4,5	0,4	0,55
Vans	5	4,5	0,5	0,8
HGV	10	15	0,8	1,0

Table 2.1: Parameter values for the dimensions and front-and-back flow of distinct vehicle types (AVV, 2005).

When vehicles are in close proximity to each other, the individual influence on the flow decreases. This phenomenon is referred to as the drafting effect or slipstream effect. The magnitude of the drafting effect depends on the distance between the vehicles and the vehicle type. The correlation between the shadow factor f_{sh} and the distance between vehicles is illustrated in Fig. 2.3. The curves have been approximated using polynomial functions. The shadow factor for a passenger car behind a HGV f_{hgv} is equal to the shadow factor for a HGV behind a HGV, see the VA-VA curve. The shadow factor f_{car} for a HGV following a passenger car is identical to the shadow factor for a passenger car following another passenger car, see the PA-PA curve. When the traffic is formed exclusively of LTV, the shadow factor for each individual LTV is equal to f_{car}. It is assumed that the resistance of each individual LTV is only influenced by the vehicle immediately in front of it (or the first vehicle upstream of the LTV). If the traffic consists only of HGVs, the same applies, but related to the shadow factor f_{hgv}.

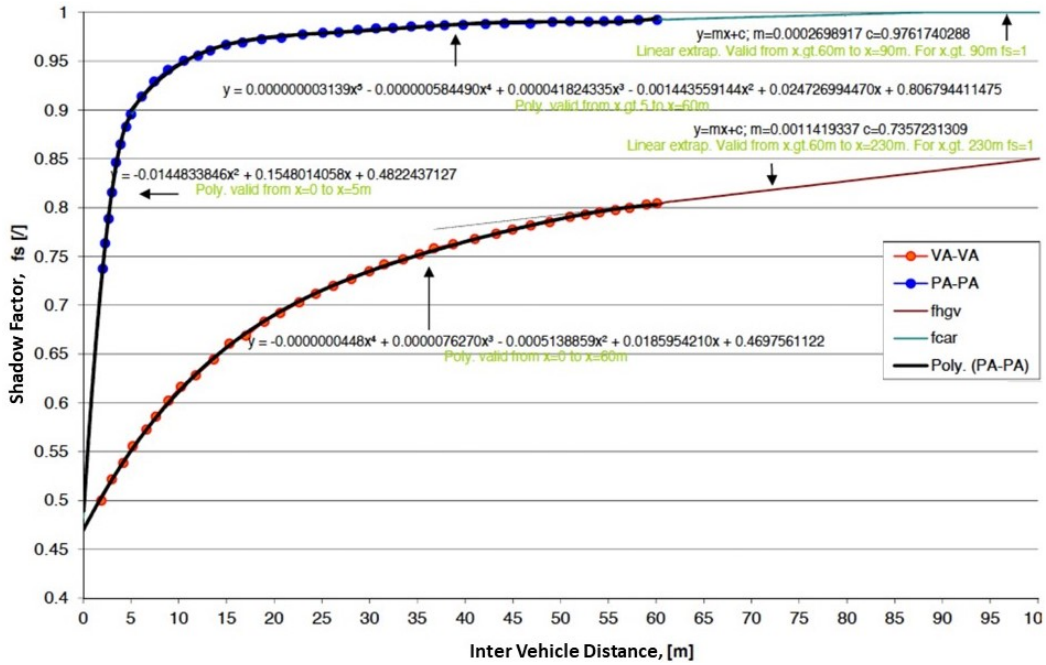

Figure 2.3: The blue curve indicates the shadow factor for vehicles behind a car and the red curve indicates the shadow factor for vehicles positioned behind a heavy good vehicle (AVV, 2005).

In mixed traffic, the shadow factor of each vehicle is equal to either the shadow factor f_{car} resulting from the LTV immediately in front of the vehicle or the shadow factor f_{hgv} resulting from the first HGV upstream of the vehicle. The smaller value of the two is selected. The traffic composition is tunnel dependent, where the engineer puts the ratio of cars, vans, and HGVs into ProTuVeM. It is assumed that the different types of traffic are evenly distributed over the distance to the fire. For instance, if a lane is occupied by 80% light traffic and 20% heavy traffic, the traffic distribution would appear as indicated in Fig. 2.4. Considering that the wake of a HGV can extend over multiple LTVs, it is essential to calculate the shadow factor f_{hgv} for each LTV positioned behind

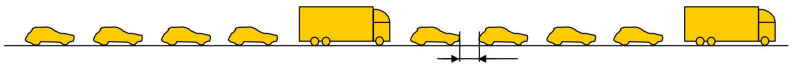

Figure 2.4: Traffic arrangement for a ratio of 80% light traffic and 20% heavy traffic (AVV, 2005).

a HGV (that is, situated between two HGVs). The total number of vehicles in the calculations is determined by the specified traffic ratios and the tunnel length over which vehicles are situated. As a result, the number of vehicles may not necessarily be an integer value. If the total number of vehicles n is not an integer, but expressed as $n + a$, where a represents the deviation from an integer value, the number of vehicles is rounded up to the nearest integer $n + 1$. Subsequently, the f_{hgv} value is determined for each of the $n+1$ vehicles, and the final shadow factor value is based on the minimum of the f_{hgv} and f_{car} values. The shadow factor of the last vehicle $n + 1$ is then multiplied by the fraction a. The average shadow factor value for the LTV is equal to the sum of the shadow factor values of the $n + 1$ LTVs divided by $n + a$. This average shadow factor value is then assigned to each LTV in the formula for calculating the total traffic resistance. The traffic density is dependent on the traffic velocity, which decreases for higher velocities. During zero vehicle velocity, the traffic density is assumed maximum. The aerodynamic resistance of the traffic is consistently computed at the ambient temperature, under the assumption that the traffic is invariably positioned upstream of the hot smoke, with no occurrence of back-layering.

The *meteorologic* effects are determined by the shape of the portal, the tunnel surroundings, and the current windrose, i.e., wind speed and direction. The combined effects lead to a wind pressure for a given meteorologic condition, described as:

$$\Delta p_{wind} = \xi_{wind} \frac{1}{2} \rho u_w^2 + \xi_{wind\&tunnel} \rho u_w u_t, \tag{2.17}$$

where ξ_{wind} is the wind factor describing the wind conditions, $\xi_{wind\&tunnel}$ defines the interaction between the wind and the tunnel air, and u_w is the wind velocity measured at 10 m above the ground level. The values and determination of the parameters describing the meteorological effects are provided in the AVVb (2005). The meteorologic effects are essentially independent of the fire location. The fire is only secondary included through the air velocity in the tunnel.

The *fire* increases the local temperature, which causes an increased velocity of the smoke gases. Therefore, depending on the HRR, a pressure drop follows over the length of the fire. The fire length is specified in the AVVb (2005) and is 10 m. Extra pressure loss follows from flow turbulence, and if the fire is caused by a vehicle, the space a burning vehicle occupies. According to outcomes from computational fluid dynamics simulations provided in AVV (2005), this fire resistance coefficient adopts a value of 1.5 for tunnel cross-sections below 30 m^2 and takes a value of 2 for tunnel cross-sections exceeding 45 m^2. The coefficient progresses linearly within the specified range from 30 m^2 to 45 m^2. The pressure loss over the fire is computed according to:

$$\Delta p_{fire} = f_{fres} u_0 \frac{\eta P}{A c_p T_0}, \tag{2.18}$$

where f_{fres} is the fire resistance coefficient.

Thermostatic effects represent the chimney-effect, influencing smoke movement in tunnels based on the tunnel slope. During flow along a positive slope, the rising smoke contributes to the air flow. While in case of a negative slope, extra pressure is required from ventilation to achieve the desired flow direction. A tunnel slope with its corresponding parameters is illustrated in Fig. 2.5. The influence of the slope is calculated at the section borders using the average temperature over the sections and is described as:

$$\frac{dp}{dx} = -\rho_0 (1 - \frac{T_0}{T(x)}) g \, tan(\phi), \tag{2.19}$$

where ϕ is the angle of inclination, and g is the gravitational acceleration.

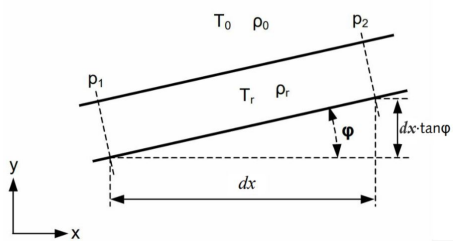

Figure 2.5: The chimney-effect influencing smoke movement based on the tunnel slope (AVV, 2005).

2.2.4 Jet Fans

According to Eq. (2.1), the addition of jet fans is required until the overall pressure loss is adequately compensated to prevent back-layering. The contribution of a single jet fan is defined as:

$$\Delta p_{jet} = \frac{F}{A} = \frac{\eta_{stp}\,\eta_{def}\,\eta_{thr}\,\rho_m\,Q\,(u_{fan} - u_{air})\,cos(\alpha)}{A}, \tag{2.20}$$

where F is the force exerted by one jet fan, η_{stp} is the setup efficiency of the jet fan, η_{def} is the efficiency from possible deflector vanes, η_{thr} is the thrust efficiency, ρ_m is the density of the medium going through the jet fan, u_{fan} is the jet fan discharge velocity, and Q is the flow rate at the jet fan outlet. The jet fan performance changes with the temperature and the local air velocity. With increasing temperatures, the jet fan performance decreases until it completely stops operating. This is associated with a lower medium density passing through the jet fan and a higher medium velocity, as indicated by ρ_m and u_{air} in Eq. (2.20). A jet fan is delivered with a maximum operating temperature, which generally is around $300°C$ or $400°C$. This is specified by the supplier. The temperature influence on the jet fan performance is illustrated in Fig. 2.6 with a fire located at 500 m from hte tunnel entrance for different HRRs. The jet fan type used for this problem has a flow rate of $27.26m^3/s$, an air velocity of $34.70m/s$, and a maximum operating temperature of $300°C$. For the remaining jet fan efficiency parameters, η_{stp}, η_{def}, and η_{thr}, a value of one is assumed. This jet fan type is used for all the analysis in this report unless specified otherwise. The temperature is shown by the blue line. The performance of the jet fan is shown for different HRRs: a pink dashed line for 20 MW, a red dotted line for 100 MW, and a green dash-dotted line for 200 MW. The jet fan efficiency must be considered during tunnel ventilation design.

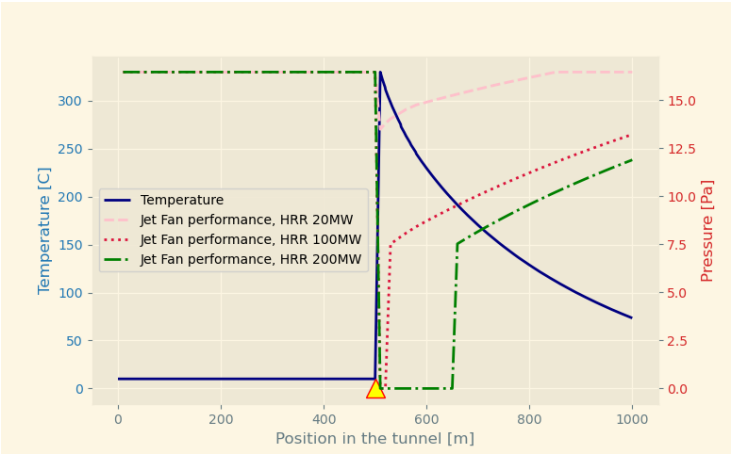

Figure 2.6: Jet fan performance for an HRR of 20 MW (pink dashed line), 100 MW (red dotted line) and 200 MW (green dash dotted line), with a fire at 500 m.

2.2.4.1 Jet Fan Positioning

The jet fan efficiency depends on both local temperature and its relative position to other jet fans. Some restrictions concerning jet fan positioning are discussed. Practical experience and experiments prove that clustering *jet fans in parallel* improves performance. Pei & Pan (2014) also concluded this, after their research on optimizing air velocity in a tunnel with a longitudinal ventilation system. Caution is necessary to avoid that the total air volume through the jet fans does not exceed the total volume flow through the tunnel tube. This could lead to a reverse airflow beneath the cluster of jet fans, as shown in Fig. 2.7. In the occasion of a fire, this would result in the reverse flow of smoke. The specific threshold to prevent this is tunnel-and jet fan dependent.

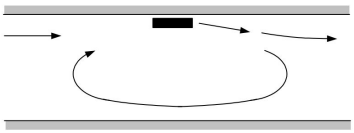

Figure 2.7: Reverse flow underneath a cluster of jet fans (AVV, 2005).

The distance between *jet fans, or jet fan clusters, in serie* in the longitudinal direction are restricted to a minimum value. It is crucial that the exit flow from one jet fan, drawn in by the subsequent jet fan, is reduced to the air velocity of the tunnel. Failure to achieve this results in the dissipation of energy, as untransferred energy remains unused. To prevent this energy loss, Osborne et al. (1954) advised to space jet fans at intervals of ten or more hydraulic diameters. At Arcadis, a longitudinal spacing of 100 m is employed. This value is used in this report.

2.3 Calculation Procedure for the Longitudinal Ventilation

To perform a deterministic calculation, it is essential to solve the equilibrium equation, which entails computing both sides of the equation where the air velocity is the variable of interest. This requires a designed jet fan ventilation system and the tunnel specifications. Once these are established, evaluating both sides of the equilibrium equation involves introducing a fire scenario and applying a starting value for the air velocity. This evaluation confirms whether the equilibrium equation holds true for the specified air velocity. This evaluation validates the validity of the equilibrium equation at the specified air velocity. If the equation is not satisfied, it undergoes iterative resolution until equilibrium is achieved.

2.3.1 Calculating the Tunnel Resistances

To clarify the process of calculating tunnel resistances for the equilibrium equation, a visual representation is presented in Fig. 2.8. The fire is located at 500 m with a HRR of 200 MW. Initially, the temperature and density adopt the value corresponding to the outside ambient temperature. By means of the input parameters in the most left solid line block and Eq. (2.3), the temperature over the tunnel length is calculated and indicated by the blue line. The variation in density and air velocity over the tunnel length are indicated by the purple and green line, and are determined through using the temperature development and Eq. (2.10) and Eq. (2.11). Subsequently, the emerging resistances along with the contribution from the jet fans are computed.

2.3.2 Tunnel Ventilation Requirements for Different Fire Scenarios

Naturally, before a fire takes place in a tunnel, the fire location and HRR are unknown to the tunnel ventilation designer. For different fire scenarios, the pressure-and constraint conditions change. Nevertheless, the final ventilation design must satisfy the requirements for each fire scenario. Therefore, the uncertainty of the fire HRR and location must be accounted for during the longitudinal

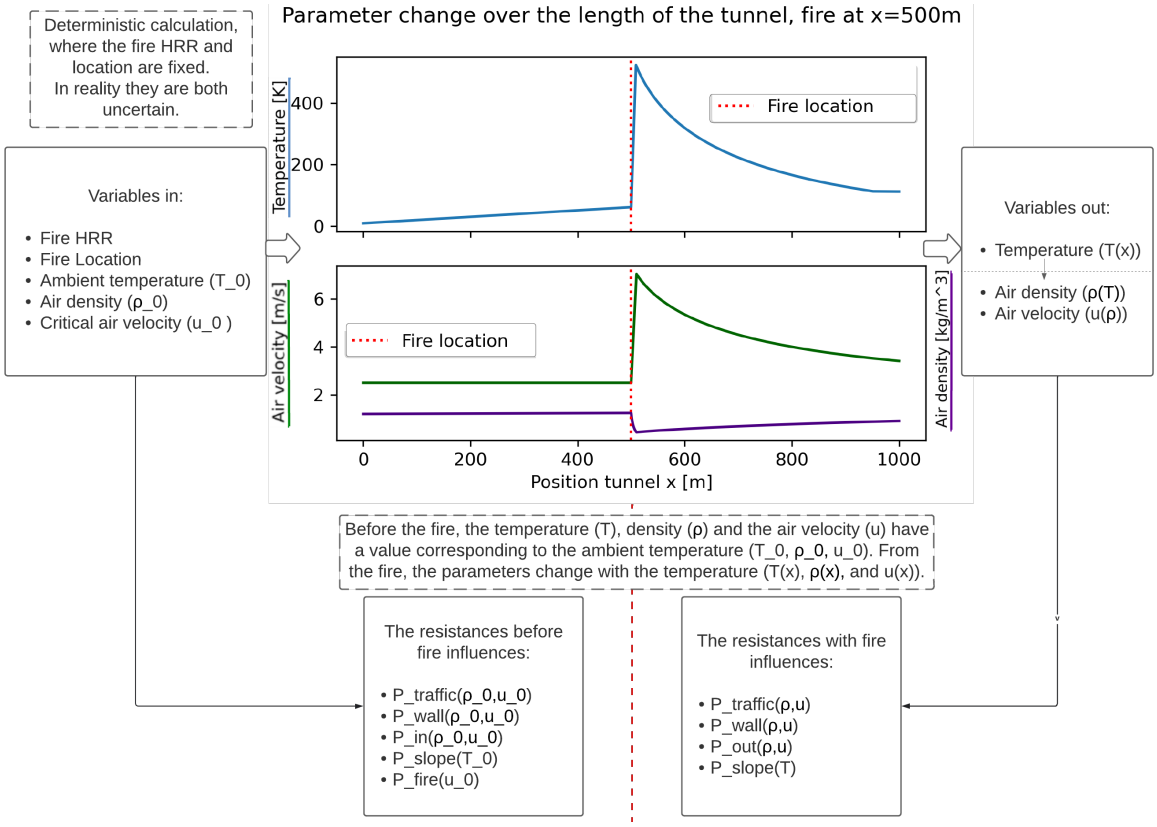

Figure 2.8: Calculation procedure for a deterministic calculation. The most left solid line block shows the input variables, followed by two figures illustrating the change of the temperature, density and air velocity over the x-axis resulting from the fire influence. With the graphs representing the changes of the variables, the resistances over the tunnel are calculated.

ventilation design stage. For specific HRRs, varying levels of failure probability are allowed, as outlined in the AVV (2005). As previously noted, the air velocity required to prevent back-layering is HRR-specific as well. An overview of the requirements for various fire scenarios is presented in Table 2.2.

Maximum allowed chances for the ventilation system				
HRR [MW]	Critical air velocity [m/s]	Relative chance fire power [%]	Failure allowance back-layering velocity [-]	Technical and velocity failure [-]
5	1,5	100	-	-
20	1,8	20	1×10^{-3}	16×10^{-3}
50	2,25	5	5×10^{-3}	20×10^{-3}
100	2,5	1	15×10^{-3}	30×10^{-3}
200	2,5	0,01	50×10^{-3}	65×10^{-3}

Table 2.2: Tunnel ventilation requirements for different fire scenarios as determined by RWS (AVV, 2005).

2.4 Rewritten Longitudinal Tunnel Ventilation Model

To enable precise control of the ventilation model and integrate the cumulative pressure calculations, ProTuVeM is rewritten in Python, following the physics outlined in this chapter. The new model allows for the extraction of additional data, providing critical design insights. Consistently verifying the results against ProTuVeM outcomes, for a tunnel with a constant cross-section, ensures adherence to the legal framework. Therefore, first, the validation of the rewritten longitudinal ventilation model is performed. This is followed by the integration of cumulative pressure calculations.

2.4.1 Validation of the Rewritten Longitudinal Tunnel Ventilation Model

For ProTuVeM 2 to be considered valid for application, a validation process is performed. Three validation cases are presented, each characterized by varying tunnel lengths, segment lengths, and fire scenarios. The remaining tunnel parameters are constant across the three cases: the cross-sectional area of the tunnel A is 64 m^2, the circumference of the cross-section S is 32 m, the tunnel tube has two traffic lanes, the traffic composition considered is as follows: cars 28 %, Vans 15 %, and HGV 57%. The wall friction coefficient λ has a value of 0.018. The inflow coefficient ξ_{in} and exit flow coefficient ξ_{out} have a value of 0.2 and 1. A 0.6 deg slope is used for both the descending and ascending segments of the tunnel, with the lowest point in the middle. To streamline the presentation of ventilation calculations in this report, these remaining tunnel parameter values are consistently used in this report, unless specified otherwise. The varying parameters used in the three cases are given in Table 2.3. ProTuVeM has a constraint wherein a maximum of 49 segments can be used as input. This is considered while choosing the tunnel lengths and the number of segments for the validation cases. Manually inputting a large number of segments into ProTuVeM is time consuming.

Validation scenario	Tunnel Length [m]	Segment lengths [m]	Fire HRR [MW]	Fire location [m]
1	1000	10 segments of 100	100	200
2	400	40 segments of 10	50	200
3	1000	[40,150,200,310,300]	200	500

Table 2.3: Three different cases to validate the new model, ProTuVeM 2, against ProTuVeM.

Hence, an automated clicker file was developed in Python to improve comparability between the two models. The file is named ProTuVeM_A_Click.py and provided in Appendix A.1. The validation is performed by comparing the resulting resistance forces for both models. The results are given in Table 2.4. Developed in Python, ProTuVeM 2 provides solutions with higher decimal precision compared to ProTuVeM, which offers only one decimal place. The results from ProTuVeM 2 are presented using three decimal places. To focus on the primary research questions, the scope of ProTuVeM 2 was limited, resulting in the exclusion of wind effect calculations Δp_{wind}. Instead, a constant value of -0.3 N, which means almost no wind effects, is used. Therefore, this is not included in Table 2.4. The relative difference for all resistances is below 0.5%. Therefore, ProTuVeM 2 is considered valid for use.

	Validation 1		Validation 2		Validation 3	
Resistances [N]	ProTuVeM	ProTuVeM 2	ProTuVeM	ProTuVeM 2	ProTuVeM	ProTuVeM 2
Tunnel Wall	73,5	73,452	388,6	388,212	413,9	413,983
Traffic	33,8	33,761	515,3	515,339	434,4	143,214
In/Out	30,6	30,716	421,9	421,797	194,1	194,110
Fire	361,6	363,045	704,3	707,374	1636,9	1644,300
Chimney	707,4	707,716	178,4	177,489	854,8	854,775

Table 2.4: Three sets of resistance force results to compare and validate ProTuVeM 2 against ProTuVeM.

2.4.2 Integration of the Cumulative Pressure Calculations in the Rewritten Model

To eliminate the need for the separate mathematical programming sheet that calculates the static cumulative tunnel pressures, the calculations of these pressures is examined. The static pressure distribution within the tunnel is characterized by its cumulative nature, described as:

$$P_{static} = \sum_{i=1}^{N_s} p_i, \tag{2.21}$$

where p_i represents the pressure at the i-th section border, and P_{static} is the cumulative sum up to the total number of section borders N_s. The cumulative approach deviates from the prior approach used for the equilibrium equation, where the pressures could be readily summed. The difference between the cumulative pressure and the previous pressure calculations are shown in Fig. 2.9. In Fig. 2.9a the calculated pressure values at the section borders are shown, while Fig. 2.9b presents the cumulative pressures. The prominent grey dotted line depicts the chimney effect for a 0.6 deg slope, with the lowest point at the midpoint of the tunnel. The remaining resistance components are indicated by, the dashed pink line (wall), the green dashdotted line (fire), the purple dotted line (traffic), the yellow line (in portal), and the thicker red line (total resistance).

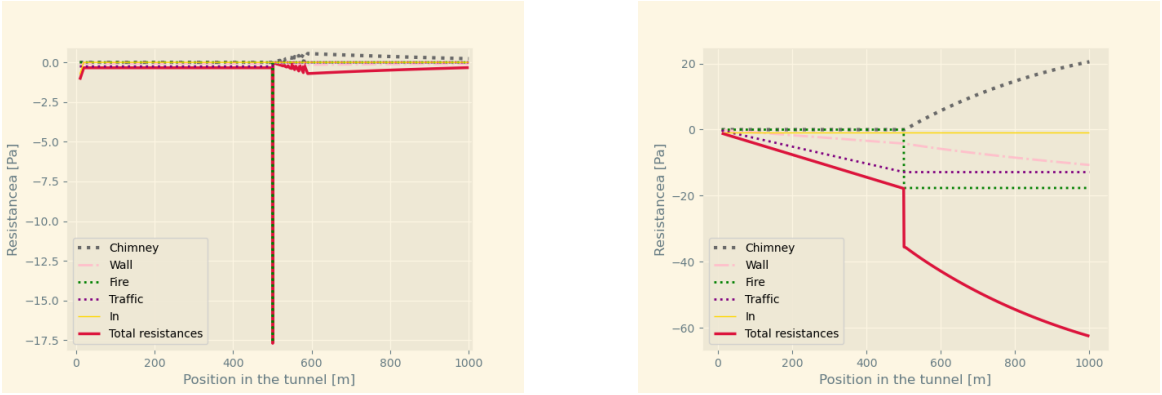

(a) Calculated resistance pressure values.

(b) Cumulative resistance pressure values.

Figure 2.9: The difference between the calculated pressure values and the cumulative pressure values.

In order to use the cumulative resistances for ventilation calculations, it is essential to consider both the static pressure caused by resistances and the dynamic pressure arising from air movement according to:

$$P = P_{static} + P_{dynamic}, \qquad \text{with} \quad P_{dynamic} = \frac{1}{2} \cdot \rho \cdot u_{air}^2. \tag{2.22}$$

Additionally, the pressure drop at the exit portal, caused by the air leaving the tunnel, is not considered in the cumulative pressure calculation. In conclusion, to determine the total tunnel pressure, the cumulative effect of the jet fans must be added with the resistances.

3

Deterministic Longitudinal Ventilation Design

The experience-based methodology for tunnel ventilation system design at Arcadis exhibits several shortcomings. The desire for a systematic design approach was presented. The enhancements to the current design approach aim at achieving increased fire safety and reduced tunnel ventilation design expenses. ProTuVeM 2, introduced in Chapter 2.4, is used in the new design methodology due to its enhanced usability and increased data extraction possibilities. This chapter presents an explanation of the revised tunnel ventilation design methodology, focusing on addressing a deterministic fire scenario with a fixed fire HRR and location. First, the updated deterministic longitudinal ventilation design approach is elaborated upon. Second, compliance with the positive pressure ventilation design is discussed. Lastly, an approach to obtain the required distance between jet fans is discussed.

3.1 Revised Methodology

To formulate a systematic design method, literature related to tunnel ventilation design is considered. Substantial research has been carried out in the field of tunnel ventilation design. However, the new systematic design method must comply with the physics and requirements specified by RWS. The proposed tunnel ventilation design problem, while simultaneously considering the positive pressure ventilation in the case of an uncertain fire scenario, is very specific. In fact, the CEC is a Dutch design. Therefore, the associated design problem is not largely explored in literature. Generally in tunnel ventilation problems, only one main objective is present: back-layering prevention. With the introduction of the CEC, a second objective, which conflicts with the first is introduced.

To address the ventilation design problem in a more structured manner, this report introduces the use of the fundamental principles of topology optimization (TO), a design approach introduced by Bendsøe & Kikuchi (1988). TO is a systematic design process which optimizes the layout or distribution of materials or components within a design space. It aims to find a configuration that optimizes the specified objectives while adhering to established constraints. It helps designers make informed decisions regarding their design challenges. The design methodology is revised to enhance automation and improve the design process. This eliminates the need for experience-based jet fan selection and iterative evaluations to obtain a compatible ventilation design.

3.1.1 Critical Air Velocity as Ventilation Model Input

The existing design approach is centered on specifying a jet fan alignment, which allows for solving both sides of the equilibrium equation to find the unknown, the air velocity, and subsequently assess whether it meets the minimum critical value. To eliminate the need of manual jet fan selection in the design approach, a different approach to solving the equilibrium equation is desired. The objective is to shift from calculating the air velocity to determining the required number of jet fans. A methodology is developed based on inputting the required critical air velocity, which enables the determination of the necessary number of jet fans. This means, the critical air velocity is used as the air velocity of the tunnel, rather than specifying a jet fan alignment as model input. Using this approach, the right-hand side of the equilibrium equation (Eq. (2.1)) can be solved. To satisfy the equilibrium, the pressure provided by jet fans must equate the tunnel resistances. Using this information, the number of jet fans necessary can be identified.

It is essential to emphasize that by using the critical air velocity as model input, the remaining tunnel specifications, resistances, and jet fan performance are computed for the specified critical air velocity. As a result, these values are assumed fixed for the specified problem. In the event of a perfect jet fan design to the equilibrium equation, the air velocity is equal to the critical air velocity. Should the pressure exerted by jet fans surpass the resistance pressures, the air velocity is slightly elevated. Consequently, this approach requires that the jet fan pressure always remains equal to or exceeds the resistances. Otherwise, the air velocity constraint is not met and the design is not valid.

3.1.2 Tunnel Discretization

In ProTuVeM 2, a tunnel is discretized by means of segments and smaller sections, similar to ProTuVeM. Tunnel specifications are defined on a segment-by-segment basis. In the current design approach at Arcadis, segments are manually selected based on two criteria: first, where variations in tunnel characteristics such as slope and wall resistance occur, and second, to align with the intended jet fan placements. In practice, this can result in four segments of varying lengths in a 50 m tunnel, as depicted in the top figure of Fig. 3.1. In the revised methodology, jet fan positions are optimized to aim for effective ventilation. To enable the placement of jet fans throughout the entire tunnel length, a structured grid is established by keeping segment lengths uniform in the tunnel discretization. This is illustrated in the bottom figure of Fig. 3.1, where segment lengths of 10 m are used. Given that the revised methodology uses a different approach to position segment borders, which involves creating a structured grid, in the revised methodology these segment borders are referred to as nodes. Reducing segment lengths increases the number of nodes, subsequently expanding the potential jet fan positions.

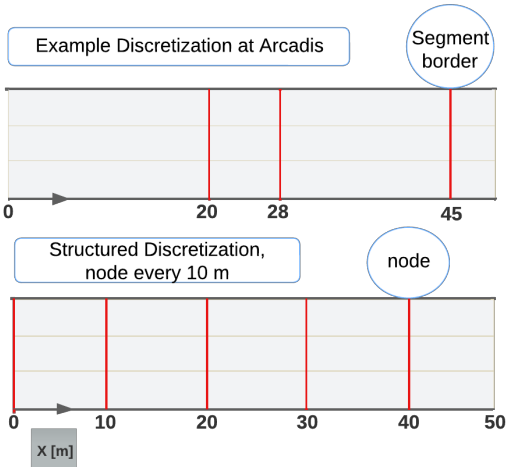

Figure 3.1: Top: discretization using the current design approach at Arcadis, where segments are chosen manually. Bottom: structured discretization where the discretization borders are referred to as nodes.

3.1.3 Jet Fan Presence as Design Variable at the Nodes

The tunnel is discretized by a structured grid, where jet fans can be positioned along the grid lines referred to as nodes. The number of jet fans that fit over the width of the tunnel at the nodes along the tunnel length are determined by the tunnel specifications, such as tunnel dimensions and other constraints that might hinder jet fan placement. The maximum number of jet fans that fit at a node is denoted by $N_{max}(x)$. To provide a comprehensive explanation of the revised ventilation design methodology, Fig. 3.2 illustrates an overview of a tunnel with the design variable at the nodes, where each node n is assigned a jet fan density ρ_n. The illustration shows a ventilation design problem, where the left rectangle represents a filled design space before optimization and the right after optimization with the optimized density values at the nodes. The tunnel has a length of 50 m,

with a fire at 35 m, shown by a yellow-red diamond shape. In this illustration, a maximum of three jet fans can be positioned across the width of the tunnel along the entire length, denoted by the yellow N_{max}. The light blue arrows indicate the densities of the design variable at the nodes. The tunnel borders define the boundaries of the design space. In tunnel ventilation design, it is preferred to position jet fans in clusters. This is related to practical considerations, including the installation of power cables. Therefore, the design variables representing the jet fan densities at the nodes range from 0 to 1, rather than ranging to the maximum allowable jet fans, from 0 to $N_{max}(x)$. This also aligns with the common practice within TO, where the design variables typically range from 0 to 1. Thus, the jet fan densities at the nodes range from 0 to 1, but this does not necessarily mean that represents the number of jet fans at the nodes to range from 0 to 1. It is desired to apply gradient-based algorithms; therefore, the density values can be $0 \leq \rho_n \leq 1$.

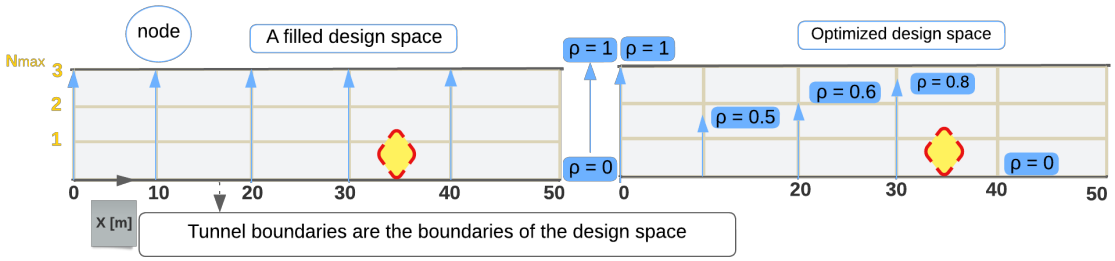

Figure 3.2: Tunnel design space before (left) and after (right) optimization. The 50 m tunnel has a fire at 35 m (yellow-red diamond shape). The design variable is the jet fan density at the nodes, denoted by the light blue arrows. The maximum number of allowed jet fans at the nodes is described by the yellow N_{max}.

3.1.4 Jet Fan Pressure Interpolation Scheme

The maximum achievable jet fan pressure P_{JF} at position x is determined by three factors: the jet fan type, the number of jet fans allowed to be positioned across the tunnel width at that node $N_{max}(x)$ and the local temperature, which influences the jet fan performance at position x. As explained in Chapter 2.2, the jet fan performance decreases for increasing temperature and they are delivered with a maximum operating temperature T_{max}. This influence was illustrated in Fig. 2.6. The maximum achievable jet fan pressure P_{JF} at position x is described as:

$$P_{JF}(x, T(x)) = \begin{cases} N_{\max}(x) P_{JF0}(x, T(x)) & \text{if } T(x) < T_{max}; \\ 0 & \text{if } T(x) \geq \mathrm{T_{max}}, \end{cases} \tag{3.1}$$

where $P_{JF0}(x, T(x))$ is the pressure a single jet fan delivers dependent on the local temperature, as outlined in Eq. (2.20). To include this in the systematic design approach, the relation with the jet fan densities at the nodes is introduced in Eq. (3.2). This leads to the formulation of the jet fan pressure interpolation scheme:

$$P_{JFn}(\rho_n) = \begin{cases} N_{maxn} \rho_n P_{JF0n} & \text{if } T_n < T_{max}; \quad \rho_n \in [0, 1] \\ \text{1e-6} & \text{if } T_n \geq T_{max}. \end{cases} \tag{3.2}$$

Instead of setting P_{JFn} to zero for higher temperatures than T_{max}, a value of 1e-6 is assigned, ensuring differentiability and continuity in the interpolation function.

3.2 Optimization Problem and Sensitivity Analysis

The ventilation design problem is reconsidered as an optimization problem, characterized as a multi-objective (MO) problem influenced by an uncertain fire scenario. A general formulation of the

problem is provided in Eq. (3.3). The objective of the optimization problem is to determine a jet fan layout that satisfies the back-layering constraint, while aiming to accommodate the requirements of positive pressure ventilation design by preventing unnecessary pressure buildup within the tunnel. The first objective in this optimization problem is described as minimize the maximum pressure present in the tunnel, downstream of the fire. The requirements must be met, while simultaneously minimizing the number of jet fans. Therefore, the second objective is to minimize the total number of jet fans in the tunnel. This problem is subject to the inequality constraint following from Eq. (2.1), where jet fan pressures must equate or exceed the resistance pressures in the tunnel. Each of the objective functions is associated with a weighting coefficient. The weights sum to one, $\sum_{i=1}^{m} w_i = 1$, where m is the number of objective functions, and w_i the weights associated with objective f_i.

$$\begin{aligned} min: & \sum_{i=1}^{m} w_i f_i(\boldsymbol{\rho}) \\ s.t.: & \sum_{j=1}^{l} c_j(\boldsymbol{\rho}) \geq 0, \end{aligned} \tag{3.3}$$

where f_i is the i-th objective, and c_j represents the j-th inequality constraint, with a total of l inequality constraints. First, two problem formulations are provided with the focus solely on the longitudinal ventilation design. This implies that the objective concerning the positive pressure ventilation system is currently excluded. The first formulation aims to minimize the number of jet fans while satisfying the equilibrium constraint. This formulation is provided in Chapter 3.2.1. The second formulation aims to maximize jet fan efficiency while providing designers the flexibility to adjust the maximum allowable number of jet fans. This is further discussed in Chapter 3.2.2.

The design variable is updated by means of the Method of Moving Asymptotes (MMA) introduced by Svanberg (1993). This method is often used in TO applications and is easily available. It effectively handles both equality and inequality constraints.

3.2.1 Design For Minimal Number of Jet Fans

The proposed formulation offers insights into the minimum pressure required from jet fans for a given tunnel and fire scenario. The objective is to minimize number of jet fans (f_1) while meeting the equilibrium constraint (c_1). This provides the required jet fan positioning and is defined as:

$$\begin{aligned} min: \quad & Num_{fans} = \frac{\sum_{n=1}^{N} N_{maxn}\rho_n}{N\sum_{n=1}^{N} N_{maxn}} \\ s.t.: \quad & 1 - \frac{\sum_{n=1}^{N} P_{JFn}\rho_n}{P_{res}} \leq 0, \\ & 0 \leq \rho_n \leq 1, \end{aligned} \tag{3.4}$$

where ρ_n is the jet fan density at node n, N is the total number of nodes used to discretize the design domain, P_{res} is the total resistance value for the specified deterministic fire scenario, and Num_{fans} represents the total number of positioned jet fans. It is subject to the pressure equilibrium constraint according to Eq. (2.1). To ensure that the optimization process starts within a region of the design domain where the inequality constraint is not violated, the process starts with a value of ρ_n set to 0.1 at the nodes. This starting value is used for all the analyses performed in this report for this problem formulation. For this problem specification, the specific starting value does not impact the solution.

3.2.2 Design for Maximum Jet Fan Efficiency

This formulation facilitates the exploration of different configurations for increased jet fan usage or a more conservative design. In this approach, the objective is to maximize the jet fan efficiency (f_2)

while meeting a volume fraction constraint (c_2) according to:

$$\begin{aligned} max: \quad & P_{fans} = \frac{\sum_{n=1}^{N} P_{JFn}\rho_n}{\sum_{n=1}^{N} P_{JFn}} \\ s.t.: \quad & \frac{\sum_{n=1}^{N} N_{maxn}\rho_n}{vf \ \sum_{n=1}^{N} N_{maxn}} - 1 \leq 0, \\ & 0 \leq \rho_n \leq 1, \end{aligned} \tag{3.5}$$

where $P_{JFn}\rho_n$ represents the pressure exerted by jet fans at node n, P_{fans} is the total pressure provided by jet fans, and vf is the volume fraction, indicating the allowable number of jet fans relative to the total number of available jet fan positions. It is crucial to carefully select the volume fraction vf to prevent the equilibrium constraint is not met or unnecessary pressure is buildup in the tunnel. This can be accomplished through two approaches. The optimization formulation presented in Eq. (3.4) can be applied to the same tunnel and fire scenario to obtain the minimum number of jet fans needed to satisfy the equilibrium constraint. Alternatively, trial and error can be employed to determine the volume fraction at which the jet fans balance the equilibrium constraint. This is not a straightforward approach of solving the ventilation design problem. However, it is included due to its direct control of the number of jet fans to be positioned. This can be important when aiming for a more conservative result, or when analyzing the impact of positioning more or less jet fans compared to what is required according to the equilibrium equation.

3.2.3 Sensitivity Analysis Objectives and Constraint Functions

The sensitivities of objective f_1 and the constraint function c_1, as presented in Eq. (3.4), with respect to the node densities ρ_n are given by:

$$\begin{aligned} \frac{\partial f_1}{\partial \rho_n} &= \frac{N_{maxn}}{N \sum_{n=1}^{N} N_{maxn}}, \\ \frac{\partial c_1}{\partial \rho_n} &= \frac{P_{JFn}}{P_{res}}. \end{aligned} \tag{3.6}$$

The sensitivity information with respect to objective f_2 and constraint c_2, as presented in Eq. (3.5), are according to:

$$\begin{aligned} \frac{\partial f_2}{\partial \rho_n} &= \frac{P_{JFn}}{\sum_{n=1}^{N} P_{JFn}}, \\ \frac{\partial c_2}{\partial \rho_n} &= \frac{N_{maxn}}{vf \ \sum_{n=1}^{N} N_{maxn}}. \end{aligned} \tag{3.7}$$

3.2.4 Stopping Criteria

Two distinct optimization formulations are presented in Eq. (3.4) and Eq. (3.5). These formulations aim to provide solutions that align, in the case where the volume fraction in Eq. (3.5) is adjusted to meet the requirements of the equilibrium constraint. To ensure proper alignment of the solutions for both formulations despite their initial conditions, a stopping criterion based on the absolute change in design variables is used. The stopping criterion ensures consistent termination of the optimization process for both formulations, enabling comparability of the solutions. Termination is imposed when the maximum absolute change in design variables is below the specified threshold, denoted as ω set to 0.001. This is described as:

$$||\rho_k - \rho_{k-1}|| \leq \omega, \tag{3.8}$$

where ρ_k and ρ_{k-1} are the densities at the nodes for the k-th and k-1-th iterations.

3.2.5 Optimization Longitudinal Ventilation Design

The solutions of both formulations are presented through a sequence of two figures shown in Fig. 3.3. The left column shows the solution for the formulation in Eq. (3.4): with objective f_1 and constraint c_1. The right column displays the formulation from Eq. (3.5): with objective f_2 and constraint c_2.

For both formulations, an identical tunnel and fire scenario are used. The tunnel has a length of 1 km, nodes every 10 m, and the fire is situated at 200 m from the tunnel entrance with a HRR of 200 MW. In Chapter 2.2.4 and Chapter 2.4.1, values for the jet fan type characteristics and the remaining tunnel parameters were provided, and it was specified that these values would be used throughout the remainder of the report. The maximum number of jet fans that fit across the tunnel width N_{max} is set to one at every node. This value is used throughout this report. The volume fraction used for the formulation in Eq. (3.5) is 0.038. This leads to a comparable number of jet fans to the formulation provided in Eq. (3.4), resulting in a similarity in the figures.

In the first row in Fig. 3.3, the blue line represents the temperature along the tunnel length, the red dotted line shows the affected jet fan performance by the fire over the tunnel length, the orange dashdotted line displays the pressure generated by jet fans for the optimized jet fan layout, and the yellow triangle indicates the position of the fire. The second row, provides the design variable after optimization. It is important to note that forces resulting from wind effects were excluded in the calculations, as discussed in Chapter 2.4.1. Consequently, the total resistance forces are reduced, leading to a lower number of required jet fans compared to what might be expected.

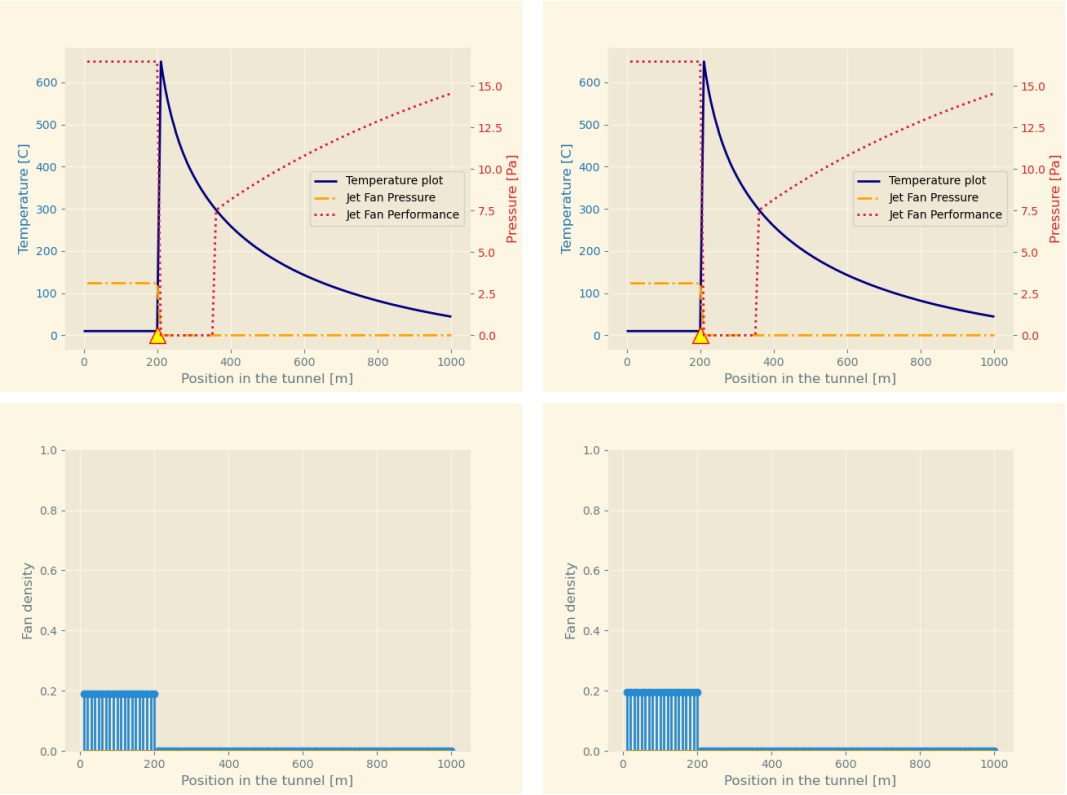

(a) Objective f_1 while meeting constraint c_1

(b) Objective f_2 while meeting the constraint c_2

Figure 3.3: Left column: objective f_1 while meeting constraint c_1. Right column: objective f_2 while meeting constraint c_2. The tunnel length is 1 km. A fire at 200 m from the tunnel entrance with a HRR of 200 MW, indicated by a yellow triangle in the top figures. Second row: optimized jet fan layout, where the jet fan densities are shown at the nodes.

3.2.5.1 Discussion Solutions

It can be observed that jet fans are solely positioned upstream of the fire. In this tunnel and fire scenario, the jet fan performance is influenced by the fire for the entire remaining downstream tunnel length, as depicted by the red dotted line in the first row showing the jet fan performance. To minimize the required number of jet fans for this fire scenario, it is effective to position jet fans upstream of the fire. This ensures their maximum performance. The uniform density of all jet fans upstream of the fire is a consequence of the critical air velocity as model input and the configuration of the model. Consequently, the performance of jet fans upstream of the fire remains consistent, and positioning a jet fan at, for example, 100 m or 200 m has the same effect.

Due the configuration of the model, jet fans are positioned where the fire appears to have already started. In Fig. 3.3, this implies that a jet fan is positioned at 200 m, coinciding with the location of the fire. To explain, with a fire at 200 m, the temperature calculation starts over the first m, ranging from 200 to 201 m. Consequently, at 200 m, the temperature remains at the ambient level.

3.2.6 Allowing for More Jet Fans than fit Upstream of the Fire

When more jet fans are allowed or required than fit upstream of the fire, the same positioning strategy persists: jet fans are placed where their performance is least affected by fire effects. To investigate this, the formulation presented in Eq. (3.5), where the objective is f_2 and constraint is c_2, is used for this analysis. This formulation allows for easy control of the maximum jet fans to be positioned. A volume fraction of 0.5 is used. The tunnel length is 1 km, with a 200 MW fire at 200 m. The solution is provided in Fig. 3.4, which shows that jet fans are placed as far from the fire as feasible. Further down the tunnel, the performance of jet fans improves compared to when they are closer to the fire.

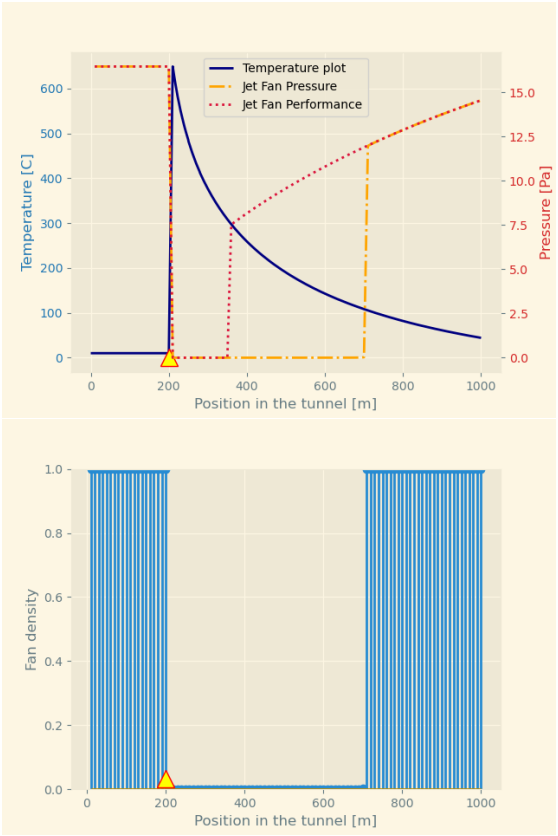

Figure 3.4: Optimized solution for the problem in which objective f_2 is optimized while meeting constraint c_2 with a volume fraction of $v_f = 0.5$. Tunnel length is 1 km, with a 200 MW fire at 200 m. Bottom figure: optimized jet fan density. The value of v_f for this tunnel and fire scenario allows for more jet fans than required to satisfy equilibrium.

3.2.7 Effect of Different Fire HRR on Jet Fan Positioning

For the formulations in Eq. (3.4) and (3.5), jet fans are strategically placed to minimize fire effects and maximize performance. This does not necessarily require positioning jet fans upstream of the fire. Lower HRRs lead to less significant temperature increases over shorter distances in comparison to higher HRRs. The impact of different HRRs is provided in Fig. 3.5. It shows the problem formulation presented in Eq. (3.4), where f_1 is the objective and c_1 the constraint, for three distinct HRRs: 5 MW, 100 MW, and 200 MW. These HRR values were selected from Table 2.2, with the lowest, middle, and highest values chosen for this analysis. In all three scenarios, the fire is located at 300 m from the tunnel entrance. As the fire HRR increases, more jet fans are placed to compensate for the increased pressure drop caused by the fire.

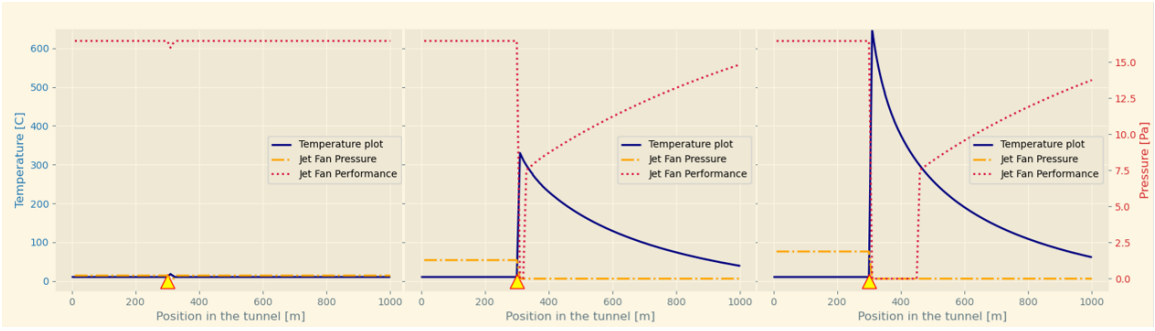

(a) Temperature, Jet fan performance, and exerted jet fan pressure for the different fire HRR.

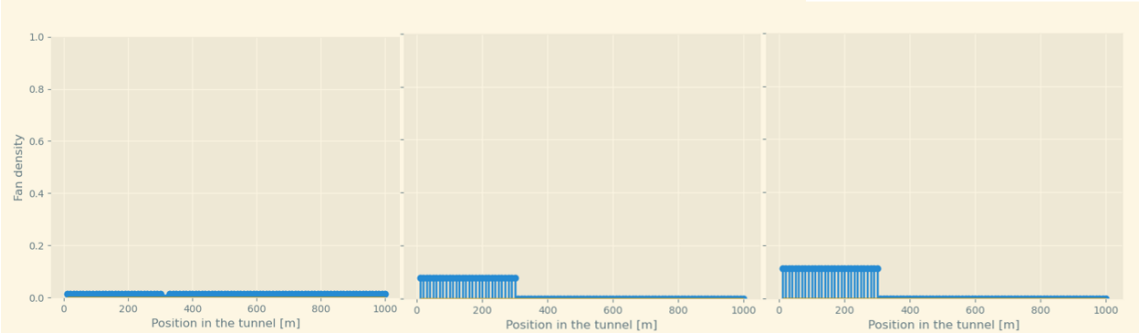

(b) The optimized jet fan layouts.

Figure 3.5: Solutions: objective f_1 while meeting constraint c_1. Jet fan positioning for a fire HRR of 5 WM (left), 100 MW (middle), and 200 MW (right). The fire in all scenarios is positioned at 300 m from the tunnel entrance.

3.2.7.1 Discussion Solutions

When comparing the jet fan performance for the three different HRRs, it can be concluded that the decrease in jet fan performance increases for higher HRR. Jet fans are positioned where their performance is least affected by the increased temperature. For a lower HRR, the jet fan performance decreases only slightly and over a shorter distance, as shown left in Fig. 3.5. Consequently, the corresponding jet fan densities show positioning along the entire tunnel length, with a slight interference at the location of the fire. This is in contrast to the outcomes observed for the 100 MW and 200 MW HRR, where the performance of jet fans is influenced for the entire remaining tunnel length downstream of the fire. Consequently, in these scenarios, jet fans are exclusively positioned upstream of the fire.

3.2.8 Effect Diverse Tunnel Configurations

To investigate the effect of different design spaces, three distinct tunnel configurations are formulated and presented in Table 3.1. For each, the same fire scenario is applied: a 100 MW fire located at

Tunnel case	Tunnel Length [km]	Negative slope [deg]	Lowest tunnel point [m]	Positive slope [deg]
1	3	-1	1500	1
2	1	-3	750	4
3	1	-4	250	1

Table 3.1: Three tunnel cases to investigate the effect of various design spaces.

the midpoint of the tunnel. The used problem formulation is presented in Eq. (3.4), where f_1 is the objective and c_1 the constraint. The results are presented in Fig. 3.6. The first row shows

the temperature, jet fan performance, and exerted jet fan pressure. The second row represents the optimized jet fan layout for the specified deterministic conditions. Tunnel case 1 is represented in the left column, tunnel case 2 in the middle column, and tunnel case 3 in the right column. The solutions demonstrate that, for various tunnel configurations, jet fans are positioned where their performance is least affected by fire effects. In tunnel case 1, the tunnel length is three times longer than the other two tunnel cases. Consequently, the tunnel length allows for the temperature to return to ambient levels before the end of the tunnel. Therefore, jet fans are positioned downstream of the fire. The impact of the slope is visible when comparing tunnel case 2 and 3. As shown in Table 3.1, Tunnel case 2 features a longer part of the tunnel with a negative slope. Specifically, 750 m with a -3 deg slope, compared to Tunnel case 3, which shows a 250 m length with a -4 deg slope. This results in a stronger chimney effect and a greater need for jet fans to achieve equilibrium.

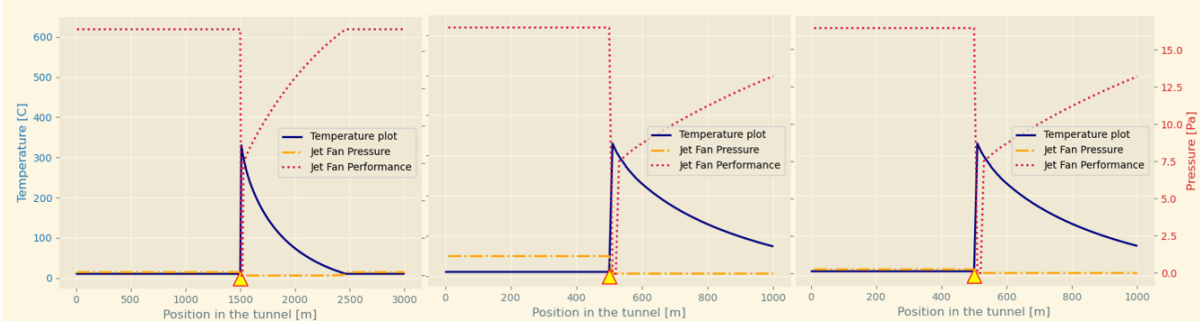

(a) Temperature, Jet fan performance, and exerted jet fan pressure for the different fire HRR.

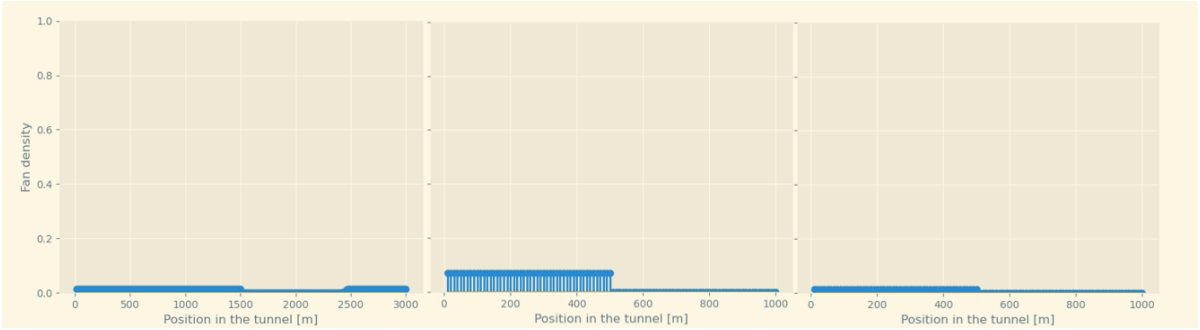

(b) The optimized jet fan layouts.

Figure 3.6: Three tunnel cases with a 100 MW fire at midpoint. First column: A 3 km tunnel with a 1 deg slope up and down, reaching its lowest point in the middle. Second column: A 1 km tunnel with a -3 deg and 4 deg slope, with the lowest point at 750 m. Third column: A 1 km tunnel with a -4 deg and 1 deg slope, with the lowest point at 250 m. Second row: optimized design variable.

3.3 Considering the Positive Pressure Ventilation System

The CEC needs to maintain a positive pressure with respect to the tunnel. To accommodate the requirements of positive pressure ventilation, the objective is to prevent unnecessary pressure buildup within the tunnel. This reduces the need for the positive pressure ventilation system to meet impractical or undesirable pressure levels in order to exceed the tunnel pressures. Therefore, as discussed in Chapter 3.2 a second objective is introduced; namely, to minimize the maximum pressure downstream of the fire. Subsequently, the maximum pressure in the tunnel must be determined. The design variable is situated at the nodes, while the pressure resistance data is located at the section borders. In order to sum the jet fan and resistance values, the resistance values at the nodes are obtained. An evaluation was conducted to assess whether the use of resistance information at nodes, with nodes spaced every 10 m, might lead to the loss of essential information. In order to investigate,

the resistances are plotted for a tunnel of 1 km with a fire of 200 MW situated at 200 m from the tunnel entrance. The resistance values are plotted at the section borders and at the nodes in Fig. 3.7. The red dotted line shows the resistance values over the nodes and the orange line the resistances over the sections. The two lines show minimal distinction, leading to the assumption that using resistance information at the nodes is sufficient for this purpose.

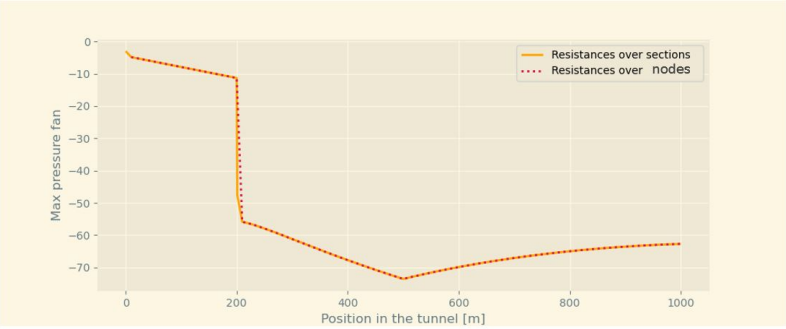

Figure 3.7: Difference cumulative resistance pressures in the tunnel at the nodes and section borders, where nodes are positioned at 10 m intervals.

3.3.1 Positive Pressure Ventilation Objective Longitudinal Ventilation Design

To incorporate the objective of minimizing the maximum pressure in the tunnel (f_3), it is essential to obtain the maximum value. Gradient-based optimization techniques rely on the availability of derivatives (gradients) to guide the optimization procedure. The maximum value itself is not a function and lacks the necessary gradient information. Therefore, to identify the maximum pressure while still enabling the use of gradient-based optimization methods, a function is used which provides an estimate of the maximum value. Two common functions for this purpose are the P-norm, introduced by Arnold (1985), and the Kreisselmeier-Steinhauser (KS) function proposed by Kreisselmeier & Steinhauser (1979). After experimenting with both functions, it was observed that the KS function offered more accurate approximations of the maximum value compared to the P-norm. Therefore, the KS function is used for the ventilation problem. Objective f_3 is incorporated into the problem formulation provided in Eq. (3.4), which optimizes f_1 while ensuring compliance with c_1. For this analysis, the problem formulation presented in Eq. (3.5) is set aside temporarily due to its less straightforward usability. Objective f_3 transforms the optimization problem in Eq. (3.4) into:

$$\begin{aligned} min: \quad & Num_{fans} = \frac{\sum_{n=1}^{N} N_{maxn}\rho_n}{N\sum_{n=1}^{N} N_{maxn}} \\ min: \quad & P_{\max} = \frac{1}{k}\frac{\ln(\sum_{n=1}^{N} e^{kP_n})}{P_{jfm}} \\ s.t.: \quad & 1 - \frac{\sum_{n=1}^{N} P_{JFn}\rho_n}{P_{res}} \leq 0, \\ & 0 \leq \rho_n \leq 1, \end{aligned} \tag{3.9}$$

where P_n is the cumulative pressure at node n, P_{jfm} represents the maximum pressure level within the tunnel when all the jet fans needed to achieve equilibrium are positioned upstream of the fire. This is where their performance remains unaffected by fire effects. Therefore, this value represents the maximum pressure under these specific tunnel and fire conditions. Additionally, k controls the smoothness of the approximation. Higher values of k result in better approximations of the maximum value. However, also cause rapid variations of the gradient due to sensitivity to outliers

and extreme vector values. This can negatively influence the convergence of the optimization process. Subsequently, the MO function is transformed into a single objective function:

$$min: \qquad \sum_{i=1}^{m} w_i f_i(\boldsymbol{\rho}), \tag{3.10}$$

where m is the number of objectives equal to two, f_i is the i-th objective, and w_i is the weight associated to objective f_i. The weights w_1 and w_3 are associated with the specified objectives f_1 and f_3. The weights determine the trade-off between f_1 and f_3. Instead of obtaining a single solution, this approach uncovers a range of Pareto-optimal solutions. First, a solution is offered to examine the impact of introducing f_3. Subsequently, a range of Pareto-optimal solutions is provided in Chapter 3.3.5. A starting value of 0.1 for ρ_n is used to analyse this problem formulation, and it appears that the used starting value does not significantly affect the solutions for this problem specification.

3.3.2 Sensitivity Analysis Minimize Maximum Pressure Objective

The sensitivities of objective f_3 with respect to the node densities ρ_n are given by:

$$\frac{\partial f_3}{\partial \rho_n} = \frac{\sum_{n=1}^{N} e^{kP_n} \frac{\partial P_n}{\partial \rho_n}}{\sum_{n=1}^{N} e^{kP_n} P_{jfm}} = \frac{\sum_{n=1}^{N} e^{kP_n} P_{JFn}}{\sum_{n=1}^{N} e^{kP_n} P_{jfm}}. \tag{3.11}$$

3.3.3 Stopping Criteria

The optimization terminates for the established stopping criteria, as detailed in Chapter 3.2.4, with ω set at 0.001.

3.3.4 Optimizing with the Positive Pressure Ventilation Objective

To examine the impact of introducing f_3, an optimization is performed with and without f_3 using the same tunnel and fire scenario for both optimizations. To emphasize the effect of f_3 and highlight the differences in outcomes, weights $w_1 = 0.1$ and $w_3 = 0.9$ are used in the optimization with both f_1 and f_3. This is compared to solutions where f_3 is excluded. The tunnel scenario used is a 1 km tunnel with a 100 MW fire located at 300 m from the tunnel entrance. The solutions are shown in Fig. 3.8, where the left column presents the solution for an optimization with solely f_1 as objective, while the right column shows the results with objectives f_1 and f_3. The figures are structured into a sequence of three rows. The first row illustrates temperatures, jet fan performance, and jet fan pressures. In the second row, the optimized jet fan densities are shown. Lastly, the third row represents the cumulative pressures, where the orange dash-dotted line corresponds to jet fan pressures, the red dotted line represents resistances, and the brown line illustrates the total tunnel pressures.

3.3.4.1 Discussion Solutions

When considering the second row in Fig. 3.8, in absence of f_3, jet fans are uniformly positioned where their performance remains unaffected. However, with the introduction of f_3, a shift in jet fan placement occurs. Jet fans are positioned just upstream of the fire and further down the tunnel. Immediately upstream of the fire, the jet fan performance remains unaffected (as indicated by the red dotted line in the first row), while resistances cause a pressure reduction (as shown by the red dotted line in the third row). Further down the tunnel, the tunnel resistances result in a pressure drop, while the jet fan performance improves. When examining the brown lines in the third row, the formulation with objective f_3 exhibits a maximum cumulative tunnel pressure of 4 Pa. Conversely, the problem without objective f_3, results in a maximum pressure of 23 Pa. In summary, the introduction of objective f_3 results in a lower maximum pressure level in the tunnel. Consequently, it seems to positively influence the process of positive pressure ventilation design.

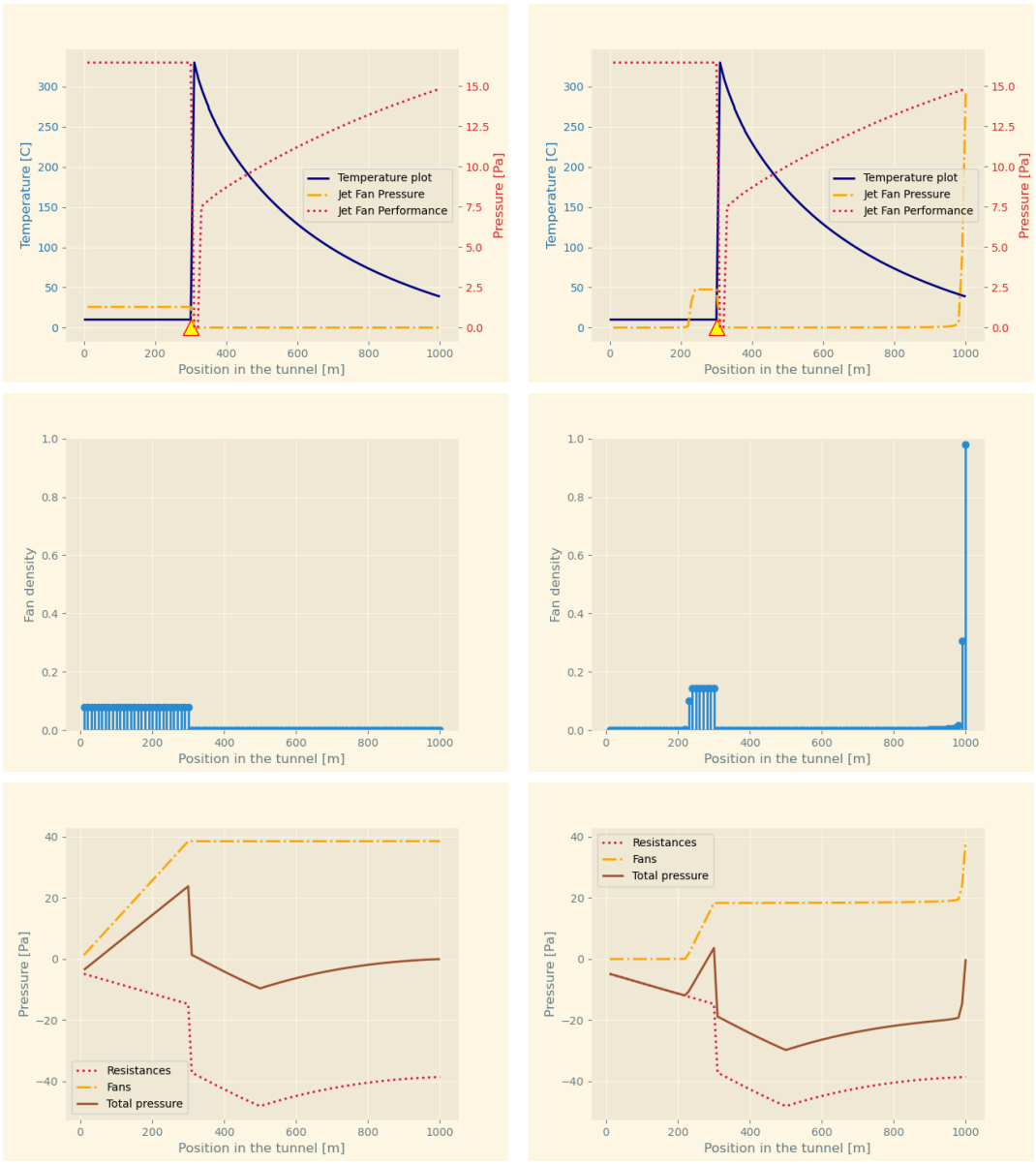

(a) Objective f_1 with constraint c_1.

(b) Objectives f_1 and f_3 and weights $w_1 = 0.1$ and $w_3 = 0.9$.

Figure 3.8: Left column: optimizing objective f_1 with constraint c_1. Right column: MO problem with objectives f_1 and f_3 and weights $w_1 = 0.1$ and $w_3 = 0.9$. The tunnel length is 1 km with a fire at 300 m from the tunnel entrance with a HRR of 100 MW (yellow triangle in the top figures). Second row: optimized jet fan layout. The third row: the cumulative pressures showing the jet fan pressures (orange dash-dotted line), the resistances (red dotted line), and the total tunnel pressure (brown line).

3.3.5 Weight Analysis between Two Ventilation Systems Design

The weights are determined before the optimization process, based on the preferences of the designer and the specific requirements of the design assignment. To further investigate the effect of the introduction of objective f_3, as presented in Eq. (3.9), and the effect of different weight allocations, a Pareto-front is built. It is built for a 1 km tunnel with a fire of 100 MW at 800 m from the tunnel entrance and provided in Fig. 3.9. The legend shows the values of w_1. As w_3 increases, there is a

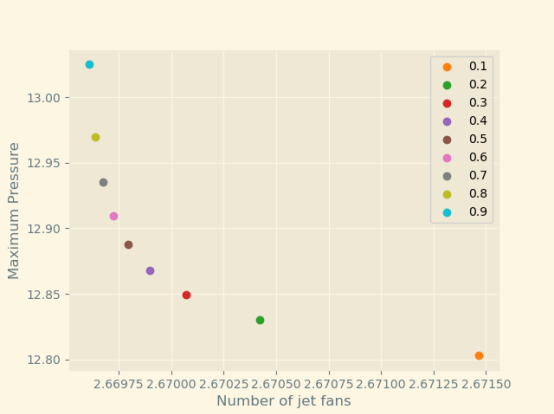

Figure 3.9: Pareto-front for a tunnel of 1 km with a fire HRR of 100 MW situated at 800 m from the tunnel entrance. The legend shows the values of w_1.

noticeable decrease in the maximum pressure, with a slight increase in the number of jet fans. In the case of this fire location, as w_3 increases, the previously uniform distribution of jet fans upstream of the fire transitions into a more concentrated placement just upstream of the fire location, this is shown in Fig. 3.10. In Fig. 3.10a, jet fans are positioned starting at 200 m, whereas in Fig. 3.10b, positioning starts at 300 m. This means that jet fan placement moves towards the fire location. This expected shift is driven by the increasing tunnel resistances when moving further down the tunnel. Given that jet fan positioning remains upstream of the fire, increasing w_3 does not result in a substantial increase in the total number of jet fans. In scenarios involving steeper tunnel slopes, a steeper resistance plot arises, primarily due to the chimney effects. As slopes become steeper, the difference in resistance pressures between two tunnel locations grows. Consequently, positioning jet fans closer to the fire location results in a more pronounced influence on the final pressure.

3.4 Solutions for Practical Applicability

To ensure the practicality and applicability of the solutions obtained with the enhanced ventilation design methodology, it is essential to decrease the presence of intermediate densities. Additionally, it is necessary to ensure a minimum distance of 100 m between jet fan clusters and between jet fan clusters and the tunnel exit. To address these limitations in the current results, first the application of the power law is explored. This is followed by the proposition of a method that guides the optimization process towards a practical solution.

3.4.1 Applying the Power Law to Promote Binary Solutions

To enhance the practical applicability of the solutions, the power law is introduced to promote convergence towards binary solutions. In earlier problem formulations, without objective f_3 (Eq. (3.4) and (3.5)), the introduction of the power law would not promote desired solutions. Since all intermediate densities are penalized equally. However, the formulation including objective f_3 requires precise jet fan placement within the tunnel. The introduction of the power law changes the jet fan pressure interpolation scheme according to:

$$P_{JFn}(\rho_n) = \begin{cases} N_{maxn}\rho_n^p P_{JF0n} & \text{if } T_n < T_{max}; \qquad \rho_n \in [0,1] \\ \text{1e-6} & \text{if } T_n \geq T_{max}. \end{cases} \tag{3.12}$$

where p is the penalization factor. The impact of using penalization factor values of 2 and 3 is examined. The impact of incorporating the power law into the problem with objectives f_1 and f_3 for both values of p is shown in Fig. 3.11. To facilitate comparability, the left column presents the

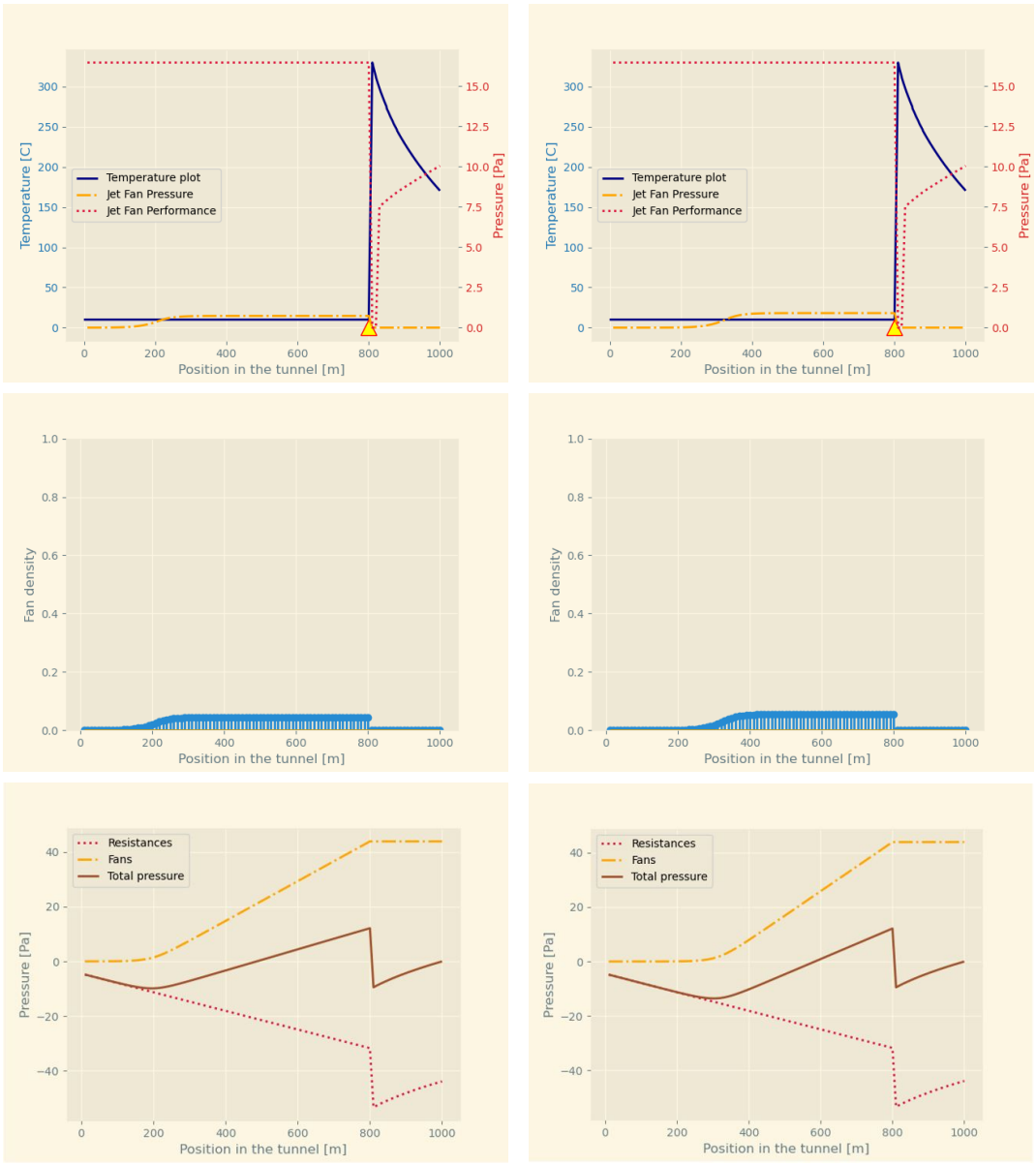

(a) $w_1 = 0.8$ and $w_3 = 0.2$.

(b) $w_1 = 0.5$ and $w_3 = 0.5$

Figure 3.10: Allocating the weight between objectives f_1 and f_3. Left column: $w_1 = 0.8$ and $w_3 = 0.2$. Right column: $w_1 = 0.5$ and $w_3 = 0.5$. The tunnel length is 1 km with a fire at 300 m with a HRR of 100 MW (yellow triangle in first row). Second row: optimized jet fan layout. Third row: cumulative pressures showing the jet fan pressure (orange dash-dotted line), the resistances (red dotted line), and the total tunnel pressure (brown line).

solution without the power law, as was presented in Fig. 3.8. The solutions for $p = 2$ and $p = 3$ are shown in the middle and right column.

When comparing the solution without the power law to the solutions with the power law, it becomes evident that the intermediate densities between 200 m and 300 m are absent, and higher-density values are distributed further down the tunnel. Therefore, it appears that introducing the power law leads to a reduction in intermediate densities. Furthermore, in the solutions that include the power law, the maximum pressures are lower in comparison to those without the power law, with values of 2 and 1 Pa, as opposed to 4 Pa. When analyzing the results for a p value of 2 compared to

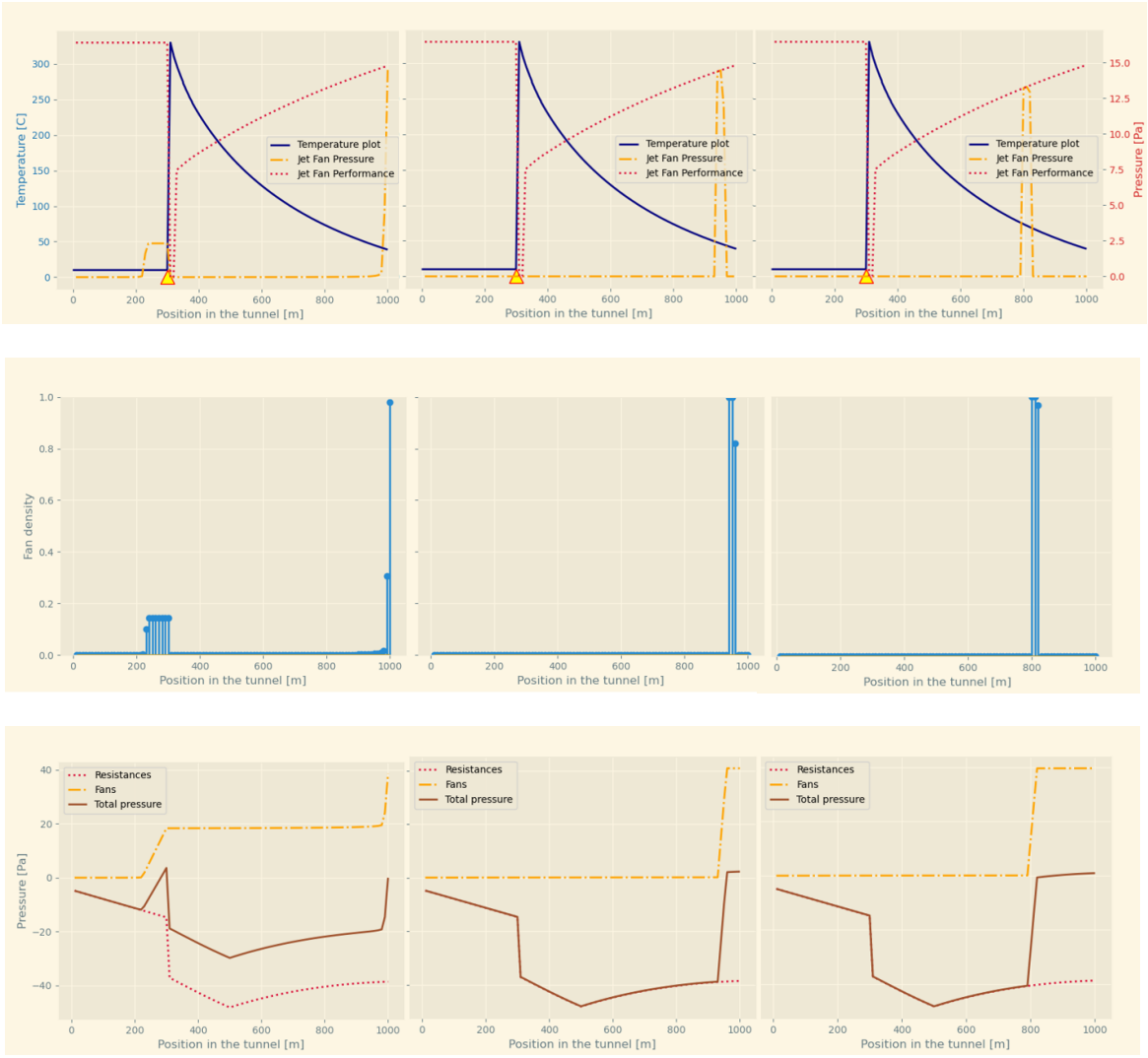

Figure 3.11: Effect of introducing the power law in MO problem, with objectives f_1 and f_3 and weights w_1 = 0.1 and w_3 = 0.9. Left: no power law. Middle and Right: solutions influenced by the introduction of the power law, with $p = 2$ (middle) and $p = 3$ (right). The tunnel length is 1 km with a 100 MW fire at 300 m from the tunnel entrance.

3, it can be observed that $p = 3$ shows a further reduction in the presence of intermediate densities and a slightly lower maximum pressure value. The decrease of intermediate densities and maximum pressure value indicate a positive influence of the power law on the solutions, especially for $p = 3$ in this case.

3.4.2 Distance Requirement Between Jet Fan Clusters

The introduction of the power law was observed to have a positive effect on reducing the presence of intermediate densities in the solutions. To further improve the practicality and applicability of the solutions, it is essential to guarantee a minimum distance between jet fan clusters and between the tunnel exit and jet fan clusters. A method is needed which influences the distribution of jet fans. The feasibility of positioning jet fans with respect to the inner distance requirement, relies on the densities at the surrounding nodes. Consequently, it is chosen to base the densities at the nodes on

the densities of the surrounding nodes. The proposed method draws parallels to the concept of a density filter introduced by Bruns & Tortorelli (2001). This filter acts as a smoothing operation by considering both the density of the node and the densities of neighboring nodes to modify the overall density distribution in the design space.

3.4.3 Penalization Objective in Ventilation Design

A method is proposed that uses the principles of the power law in combination with concepts derived from the density filter. With the introduction of the proposed method, the use of the power law as introduced in Eq. (3.12) is disregarded. Unlike the density filter, the proposed method does not directly affect the design variable; instead, it introduces an additional objective that aims to easily control the influence of the distance requirement. The objective imposes constraints on the positioning of jet fans by penalizing the densities at the nodes based on the densities at the surrounding nodes. This means, the objective operates as a penalization objective. The penalization objective f_q calculates the total sum over the nodes, where, for each node, the sum over the surrounding densities within a specified distance is computed. The inclusion of the density of the node itself, as in the density filter, is omitted to avoid that nodes penalize their own densities. The surrounding densities are subjected to the exponential q, which promotes the distance between jet fans and binary solutions. The penalization objective f_q is described as:

$$f_q = \sum_{n \in N} \sum_{i \in N_n} {\rho_i}^q, \tag{3.13}$$

where N_n is the set of nodes i for which the distance $\Delta(n, i)$ to node n is smaller than the required distance, N is the total number of nodes in the design space, and q, compared to the power law, is the penalization factor which influences the rate of convergence. To further explain f_q, the values 3 for q and 3 for distance are assumed. To maximize the value of objective f_q, it is more advantageous to assign a density of 1 to a single jet fan rather than distributing a density of 0.167 among six jet fans (three on the left and right). This is supported by the following calculations: $1^3 + 5(0^3) = 1$, and $6(0.167)^3 = 0.0279$, which align with the principles of the power law as illustrated in Fig. 3.12.

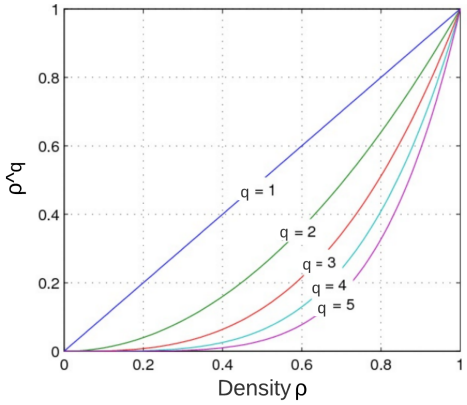

Figure 3.12: The power law relation with exponent q.

For additional clarification, Fig. 3.13 illustrates the computations of f_q at the first four nodes after optimization. It is shown in a grid structure, to highlight which ρ_n contributes to the calculations of which f_{qn}. Densities with a value of one are marked beige. The sums are computed based on the density values raised to the power q within the distance $\Delta(n, i)$ for each node n. In Fig. 3.13, ρ_1 and ρ_5 have a density of one. Higher-density values penalize lower-density values, implying that the density values used in the computation of f_q at the first node, for instance, should be relatively low to enable ρ_1 to attain a higher density value. Given that ρ_1 and ρ_5 are not included in the calculations of f_q at nodes one and five, they can both have a density value of one. Conversely, the remaining ρ_n

are included in these calculations and converge to zero. This ensures the required distance between jet fans.

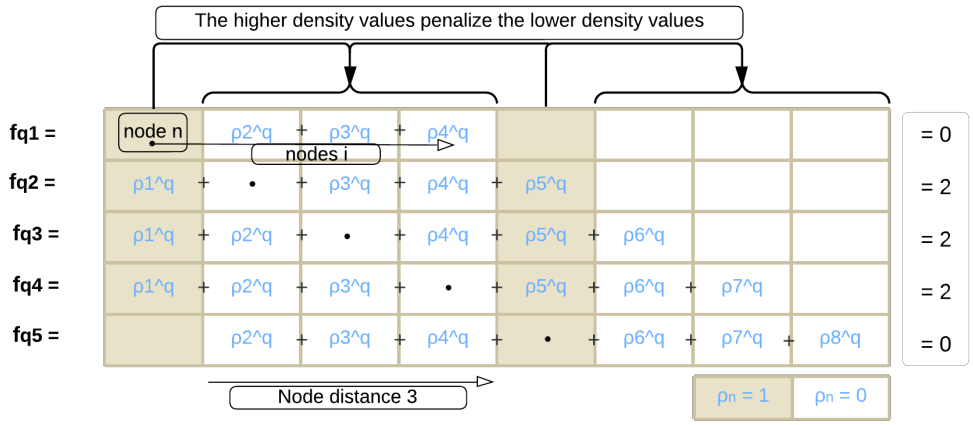

Figure 3.13: Values of f_q at the first four nodes after optimization. Densities with a value of one are marked beige. The sums are computed based on the density values raised to the power q within the distance $\Delta(n, i)$ at each node n. Densities ρ_1 and ρ_5 are equal to one. The required node distance is three.

To illustrate the relation between ρ_n and f_{qn} for an optimized ventilation design, Fig. 3.14 is provided. The stem plot shows the densities at the nodes, and the light blue dotted line represents f_q at the nodes. The tunnel length is 1 km, and the required distance between jet fans is 100 m. It is evident that when ρ_n equals one at certain nodes, f_{qn} is zero, and as a result, at neighbouring nodes within the required distance, f_{qn} is one. In certain instances, such as at 780 m, the node is positioned within the required distance of two nodes where the density value equals one, resulting in a f_{qn} value of two.

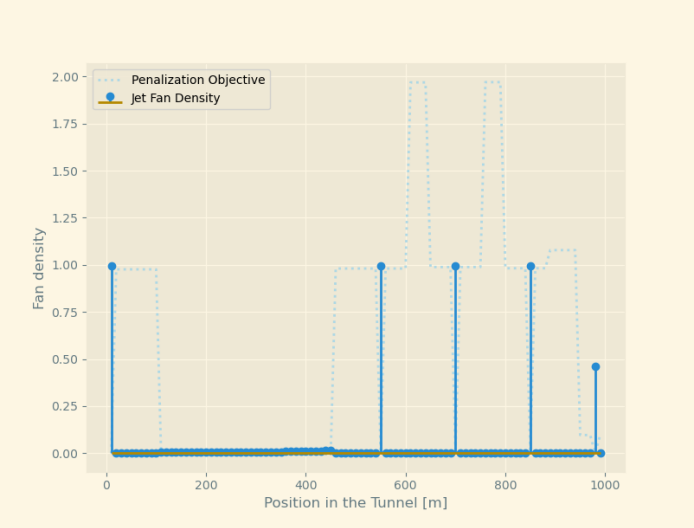

Figure 3.14: The densities and the values of the objective f_q at the nodes. The required distance between jet fans is 100 m.

Ventilation design objectives aim to optimize the positioning of jet fans, while the objective f_q aims to concentrate densities around a single node, taking into account the required distance. If there are more jet fans allowed to be positioned than what fits in the tunnel given the required inner distance, it means more than one ρ_n within the specified distance could converge to a higher density value than zero. Consequently, this approach necessitates a volume control. This method aims to

improve the solutions for the ventilation design problem through promoting the necessary separation between jet fans. Additionally, the characteristics of the power law in the objective f_q encourages convergence toward binary solutions.

3.4.4 Optimization with the Penalization Objective

With the introduction of objective f_q into the ventilation design problems described in Eq. (3.4), which optimizes objective f_1, and Eq. (3.5), optimizing objective f_2, both problems are transformed into MO problems. Since f_1 is minimized, while f_2 and f_q are both maximized, objectives f_1 and f_2 are in relation with f_q according to:

$$\begin{aligned} f_{t1} &= w_1 f_1 - w_q f_q, \\ f_{t2} &= w_2 f_2 + w_q f_q, \end{aligned} \tag{3.14}$$

where w_q is the weight associated with f_q, and f_{t1} and f_{t2} are the total sums of the objectives. The introduction of f_q transforms the formulation in Eq. (3.4) into:

$$\begin{aligned} min: \quad & Num_{fans} = \frac{\sum_{n=1}^{N} N_{maxn}\rho_n}{N\sum_{n=1}^{N} N_{maxn}} \\ max: \quad & N_{dfans} = \frac{\sum_{n\in N}\sum_{i\in N_n} {\rho_i}^q}{2N(d_{fans}-1)} \\ s.t.: \quad & 1 - \frac{\sum_{n=1}^{N} P_{JFn}\rho_n}{P_{res}} \leq 0, \\ & 0 \leq \rho_n \leq 1, \end{aligned} \tag{3.15}$$

where d_{fans} is the required node distance between jet fans, and N_{dfans} is the total sum over the nodes, where for every node the sum over the surrounding densities is taken within the range of d_{fans}. The relation between d_{fans} and the required distance between jet fans in m is determined by the discretization size. The relation is shown in Fig. 3.15, which illustrates a discretized tunnel with node distances of 10 m. A node distance d_{fans} of 5 corresponds to a distance of 60 m in the tunnel.

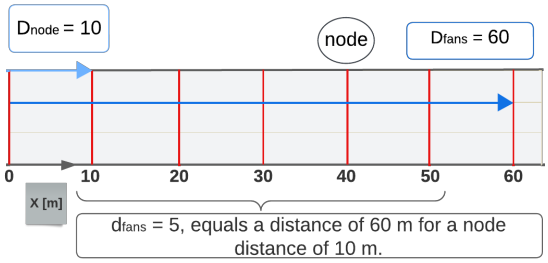

Figure 3.15: relation between d_{fans} and the distance in the tunnel in m.

This relation is described as:

$$d_{fans} = \frac{D_{fans}}{D_{node}} - 1, \tag{3.16}$$

where D_{fans} is the required distance between jet fans in m, and D_{node} is the distance in m between nodes. The starting value of ρ_n used for the optimization of the formulation presented in Eq. (3.15) remains 0.1. It seems that the initial value used for this optimization formulation has a negligible

impact on the solutions. The formulation in Eq. (3.5) transforms into:

$$\begin{aligned} max: \quad & P_{fans} = \frac{\sum_{n=1}^{N} P_{JFn}\rho_n}{\sum_{n=1}^{N} P_{JFn}} \\ max: \quad & N_{dfans} = \frac{\sum_{n\in N}\sum_{i\in N_n} {\rho_i}^q}{2N(d_{fans}-1)} \\ s.t.: \quad & \frac{\sum_{n=1}^{N} N_{maxn}\rho_n}{vf\ \sum_{n=1}^{N} N_{maxn}} - 1 \leq 0, \\ & 0 \leq \rho_n \leq 1. \end{aligned} \tag{3.17}$$

3.4.4.1 Sensitivity Analysis Penalization Objective

The sensitivities of objective f_q with respect to the densities ρ_n are given by:

$$\frac{\partial f_q}{\partial \rho_n} = \sum_{n\in N} \frac{\partial f_q}{\partial \rho_i}\frac{\partial \rho_i}{\partial \rho_n} = \frac{\sum_{n\in N}\sum_{i\in N_n} q{\rho_i}^{q-1}}{2N(d_{fans}-1)}. \tag{3.18}$$

3.4.4.2 Stopping Criteria

The optimization terminates for the established stopping criteria, as detailed in Chapter 3.2.4, with ω set at 0.001.

3.4.5 Solutions with and without the Penalization Objective

The solutions for the optimization formulation presented in Eq. (3.17) are presented in Fig. 3.16. The formulation in Eq. (3.17) is used because of its ability to control the number of placed jet fans, which is valuable when examining the weight allocations between the objectives. The tunnel has a length of 1 km, with a fire of 200 MW at 300 m from the tunnel entrance. The required distance between jet fans is 100 m. The weights for both objectives in this illustration were determined through gradually shifting towards the ventilation objective starting at an equal weight allocation. Chapter 3.4.6 provides a more in depth investigation of different weight allocations. The weights used are $w_2 = 0.6$ and $w_q = 0.4$. Both penalization values, 2 and 3, were considered and resulted in identical solutions. However, a q value of 3 showed faster convergence, 51 iterations compared to 70 iterations for 2. Less iterations does not necessarily signify better convergence. Nonetheless, to illustrate the impact of the penalization objective, a value of $q = 3$ was selected. Additionally, when applying the power law to the ventilation problem, which shares fundamental characteristics with the penalization objective, a penalty value of 3 appeared to generate more desirable solutions. Chapter 3.4.9 explores the influence of q in greater detail. The left column displays the results without objective f_q, whereas the right column presents the results with f_q.

It can be observed that the distance requirement is met with the introduction of f_q. By introducing the distance requirement, a reduced number of jet fans fit upstream of the fire. Therefore, jet fans are also positioned downstream of the fire, at positions where their performance is minimally influenced by the fire effects. Additionally, the solution shows a significant decrease in the presence of intermediate densities.

3.4.6 Weight Allocation Ventilation-and Penalization Objective

It is important to carefully consider the weight allocation between the ventilation objective and objective f_q. Assigning a small value to weight w_q can cause the optimization process to fail in meeting the distance requirement. Conversely, when objective f_q is heavily emphasized, the optimization process might provide suboptimal solutions. To increase insight into the problem, a weight investigation is performed between objectives f_2 and f_q. When the solution provides solely jet fan densities of one, the penalty objective results with its maximum value for the specified problem.

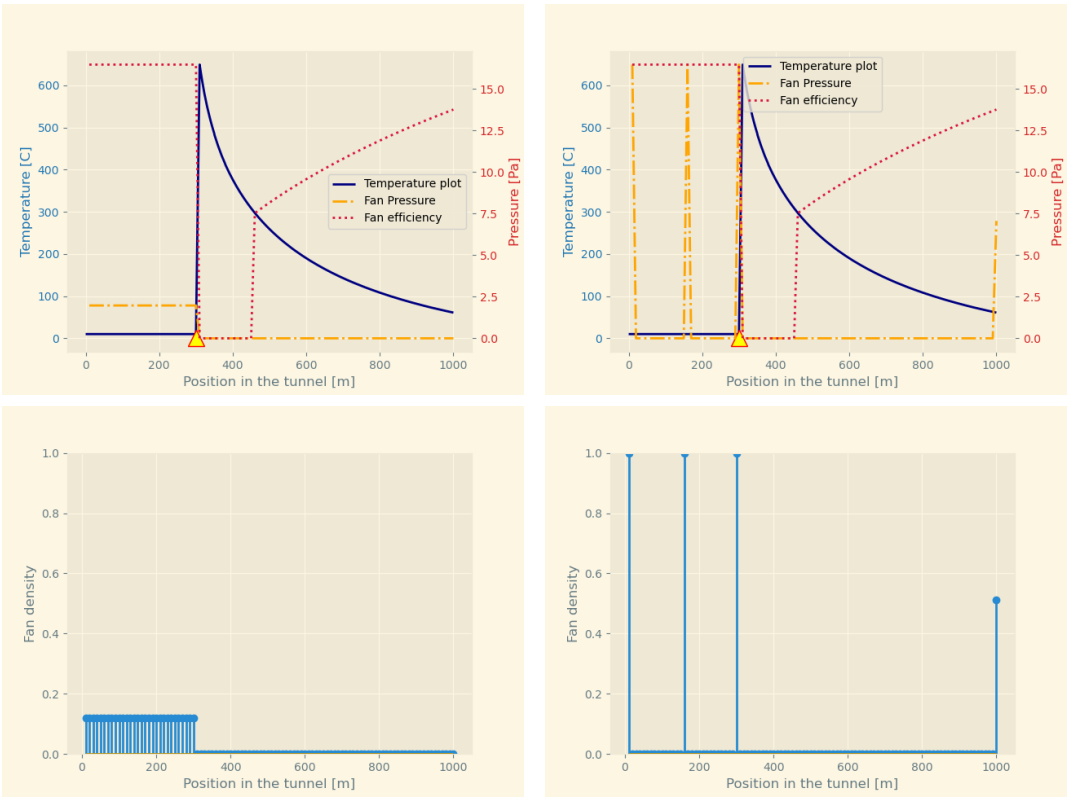

(a) Optimization of f_2 while meeting c_2.

(b) Optimization of f_2 and f_q, with $w_2 = 0.6$ and $w_q = 0.4$.

Figure 3.16: Left column: problem optimizing solely f_2 while meeting c_2. Right column: optimizing for both f_2 and f_q, with weights $w_2 = 0.6$ and $w_q = 0.4$. The required distance between jet fans is 100 m, and $q = 3$. The tunnel length is 1 km, a fire at 300 m with a HRR of 200 MW.

This does not indicate whether the jet fans are optimally positioned in the tunnel. Downstream of the fire, the optimal positioning is furthest away from the fire position, while meeting the distance requirement. Hence, the distance between the downstream-positioned jet fans serves as a measure to assess if the influence of f_q is excessive and results in suboptimal solutions. The distances between all the positioned jet fans are measured to asses whether the distance requirement is met.

3.4.7 Weight Allocation Analysis

To investigate the effects of different weight allocations, the tunnel and fire scenario used are: a tunnel of 1 km, with a 100 MW fire located 200 m from the tunnel entrance. A jet fan spacing of 60 m is used to demonstrate the effectiveness of f_q across varying distances. For this investigation, the formulation provided in Eq. (3.17) is used, which optimizes both f_2 and f_q. A value of 3 is maintained for q. The objective is to evaluate whether the weight allocation in the optimization process effectively positions the maximum possible number of jet fans upstream of the fire while optimizing the placement of downstream jet fans. Thus, the downstream jet fans should be positioned as far away from the fire while adhering to the required distance. Therefore, a specific volume fraction is selected, allowing for the placement of three jet fans upstream of the fire and two downstream. Consequently, for this specified jet fan distance, the two downstream jet fans should optimally be located at 1 km and 940 m from the tunnel entrance. Given that the nodes are separated by 10 m in a 1 km tunnel, this results in a volume fraction of 0.05. The investigation of the weight allocation is provided in Fig. 3.17a, where the total jet fan performance is provided against the node distance between the two downstream jet fans for different weight allocations. The left column in the legend shows the investigated values of

w_2 and the right column shows the number of iterations till optimization termination. Dots represent outcomes meeting the minimum distance requirement, while crosses indicate non-compliance with the requirement. In cases of non-compliance, the jet fan(s) that would not fit upstream of the fire due to the required distance provided are still positioned upstream. In such cases, the vertical axis represents the difference between the intended downstream node distance of 100 and the nearest upstream jet fan position to the fire, resulting in a node distance of 80. In this context, the optimal

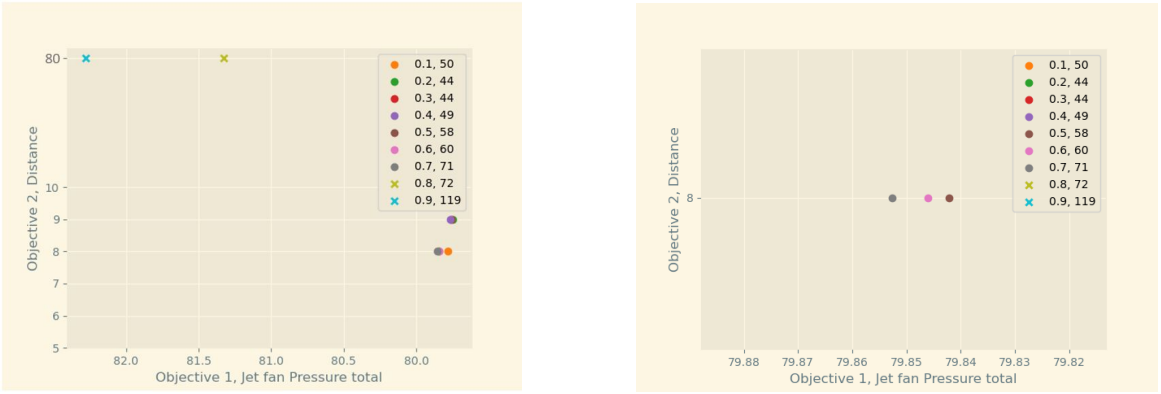

(a) Outcomes different weight allocations.

(b) Zoomed into the optimal weight allocations, where the node distance is eight.

Figure 3.17: Different weight allocations between f_2 and f_q. Vertical axes: node distance between the two downstream jet fans. Left column legend: investigated w_2 values. Right column legend: number of iterations till convergence. Dots indicate compliance with the distance requirement, while crosses indicate non-compliance.

node distance is six. The values on the axes are arranged so that an improvement in the solution is represented by movement toward the lower-left corner. However, in this case, the solution should not drop below six, as this would indicate non-compliance with the distance requirement.

3.4.7.1 Discussion Weight Allocations

It can be observed that for increasing w_2, the total jet fan performance increases. When w_2 is set to 0.8, the distance requirement is no longer satisfied, as indicated by the cross. From Fig. 3.17b can be concluded that at $w_2 = 0.7$ the optimal weight allocation is achieved for this problem. Since for this weight allocation, the majority of the weight is assigned to f_2, and it still satisfies the distance requirement. However, this weight allocation needs a greater number of iterations to achieve convergence compared to using alternative weight values. This is because, for $w_2 = 0.7$, the optimization process must navigate potentially through a more complex decision space between the objectives. It is worth noting that the difference in jet fan performance between the w_2 values of 0.5, 0.6, and 0.7 is nearly negligible. In fact, one could argue that 0.5 is most favourable since it requires less iterations till convergence compared to weights 0.6 and 0.7. Nonetheless, $w_2 = 0.7$ is found the preferred weight allocation as it represents the optimal compromise between the two objectives when compared to the other weights under consideration. However, the node distance achieved between the two downstream jet fans is eight, while the optimal value was discussed to be six. Therefore, an investigation is conducted to assess whether promoting the exploration of the design space through continuous weight allocation between f_2 and f_q could reduce the distance between the two downstream positioned jet fans. This investigation is conducted in Chapter 3.4.8. First, the impact of employing values higher than $w_2 = 0.7$ is demonstrated.

3.4.7.2 Solutions Distinct Weight Allocations

In order to illustrate the effect of using a higher weight than 0.7, Fig 3.18 is provided. This shows the solutions for $w_2 = 0.7$ and $w_2 = 0.9$. The distance requirement is still met in Fig. 3.18a, while

in Fig. 3.18b all the jet fans are positioned upstream of the fire, resulting in a failure of meeting the distance requirement.

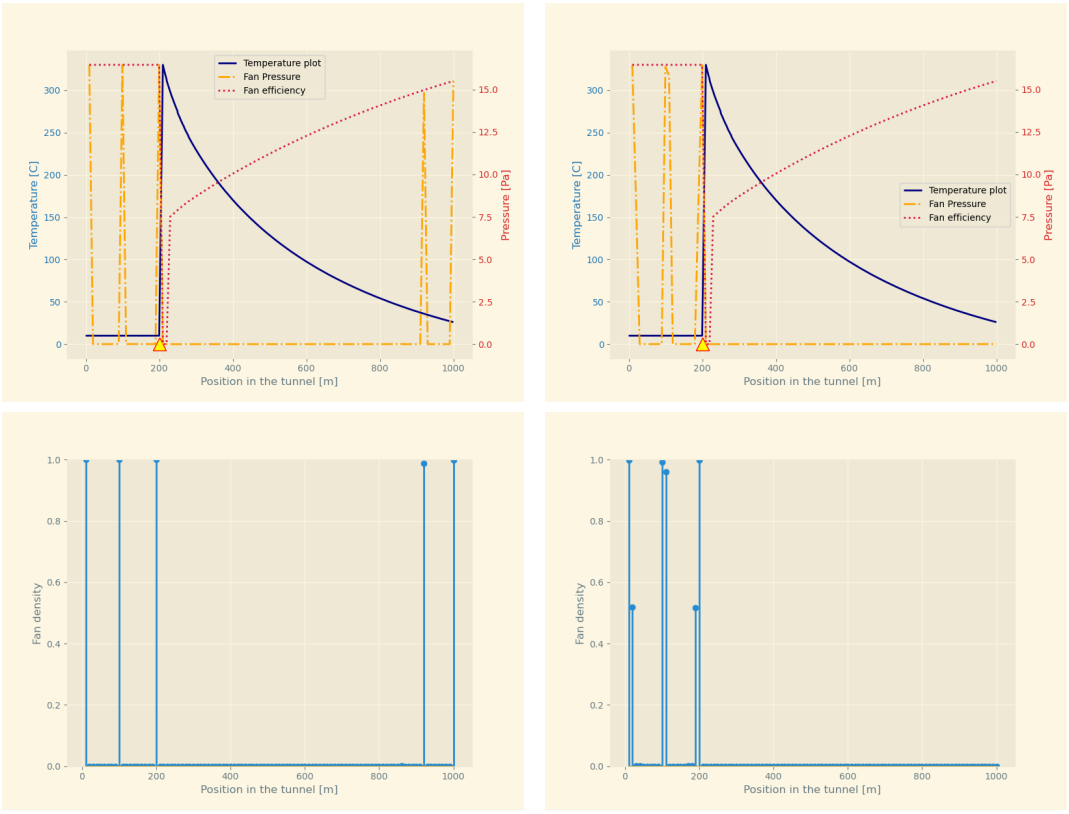

(a) $w_2 = 0.7$ and $w_q = 0.3$.

(b) $w_2 = 0.9$ and $w_q = 0.1$.

Figure 3.18: The results are shown for $w_2 = 0.7$ (left, optimal weight distribution), and $w_2 = 0.9$ (right, distance requirement failure).

3.4.8 Continuous Weight Allocation

Thoroughly exploring the design space has the potential to improve designs. To reduce the node distance between the positioned downstream jet fans for the specified weight allocation of $w_2 = 0.7$ and $w_q = 0.3$, gradual weight allocation is explored. Various weight allocation increments, denoted as w_{in}, are used to investigate the allocation of weights between the two objectives. Every iteration, starting from iteration zero, the weights allocate during optimization according to:

$$\begin{aligned} w_{2_k} &= w_{2_{k-1}} - w_{in}, \\ w_{q_k} &= 1 - w_{2_k}, \end{aligned} \tag{3.19}$$

where w_{2_k}, w_{q_k} and $w_{2_{k-1}}$ are the weights for the k-th and $k-1$-th iterations. The values of w_{in} used for the weight allocation investigation are chosen within the range of 0.001 to 0.009. These values of w_{in} were chosen to strike a balance between a finer weight allocating analysis and computational efficiency. The investigation showing the effects for different values of w_{in} are provided in Fig. 3.19. The left column in the legend shows the different values of w_{in}. The weight allocation terminates when w_2 reaches the value 0.7

It can be observed that, for $w_{in} = 0.002$ and $w_{in} = 0.006$, the distance between the downstream jet fans decreases to six. This indicates that the gradual weight allocation approach in this problem effectively enhances the exploration of the design space during optimization and leads to improved

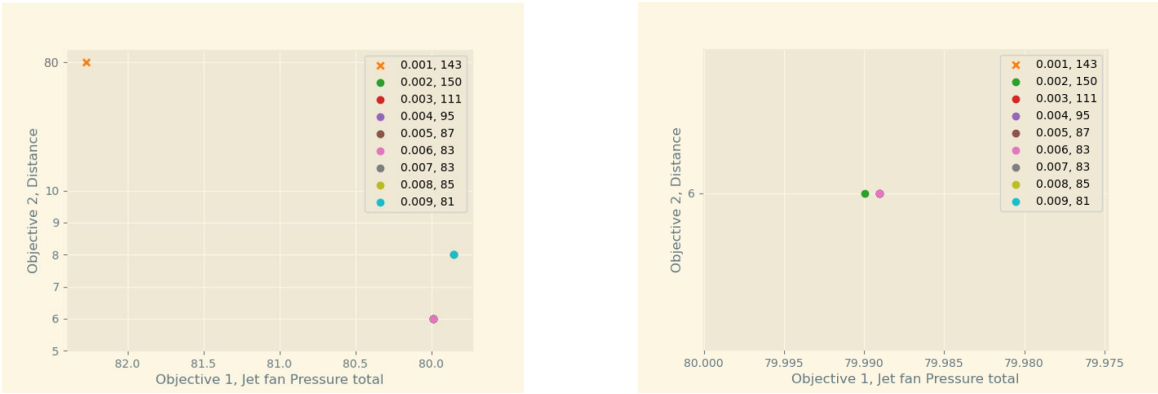

(a) Outcomes different weight increments.

(b) Zoomed into the optimal weight increments, showing a distance of six.

Figure 3.19: Analysis of gradual weight allocation between f_2 and f_q. The values on the vertical axes show the distance between the two downstream jet fans. Left column legend: values of w_{in}. Right column legend: number of iterations till convergence. The dots show the results for which the distance requirement is met, and the crosses for which they are not. A fixed value of $q = 3$ is used.

solutions. Notably, when $w_{in} = 0.006$ the optimization requires significantly fewer iterations to achieve convergence. To further promote and investigate approaches for enhancing the exploration of the design space during optimization, the gradual increase of the factor q is analyzed.

3.4.9 Continuation Strategy for the Penalization Factor

The effect of increasing the value of q during optimization is analyzed. This approach aims to prevent local minimum entrapment by starting the problem unpenalized and slowly increasing the penalization factor. An analysis is performed and shown in Fig. 3.20, showing different q increment values q_{in} to obtain insights. The value of q increases from 1 to 3 every iteration with q_{in}, starting from the first iteration according to:

$$q_k = q_{k-1} + q_{in}, \tag{3.20}$$

where q_k and q_{k-1} are the values of q for the k-th and $k-1$-th iterations. The weight allocation remains fixed at $w_2 = 0.7$. Different values for q_{in} are used and shown in the left column of the legend in Fig. 3.20. The right column in the legend shows the number of iterations till convergence. It appears that when a value of $q_{in} = 0.09$, the highest one analyzed, is used, a node distance of eight between the two downstream jet fans is observed. This indicates that promoting design space exploration, using this value, does not lead to a further decrease in the node distance between the two downstream jet fans compared to when no continuation method is applied. However, for all values of q_{in} lower than 0.09, the gradual increment of the q value appears to decrease the node distance to six. Since the two downstream jet fans are positioned at the same locations in the tunnel for the different values of q_{in}, the total jet fan pressure shows negligible differences. Among the analyzed values of q_{in}, 0.06 requires the least number of iterations while resulting in a node distance of six. The number of iterations required is 71. This means, less iterations are required to reach convergence compared to that achieved through the gradual weight allocation method. When the complexity of the problem grows, it is advisable to expand exploration of the design space. This can be achieved by using both continuous methods in succession of each other. Therefore, this is analyzed.

3.4.10 Continuation Methods in Both Weight Allocations and Penalization Increments

The effect of using the continuation methods in succession is investigated. Naturally, while $w_2 = 1$ and $w_q = 0$, f_q has no influence in the optimization. Therefore, solely the effect of continuously

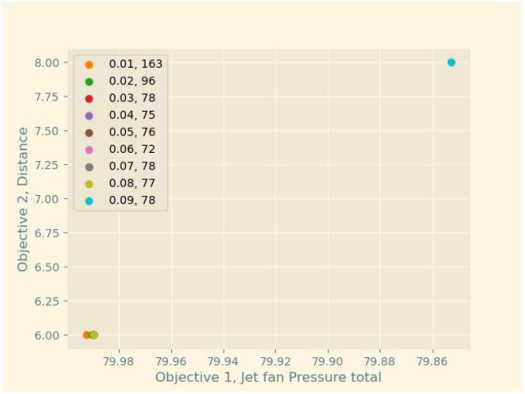

(a) Outcomes the different penalization increments.

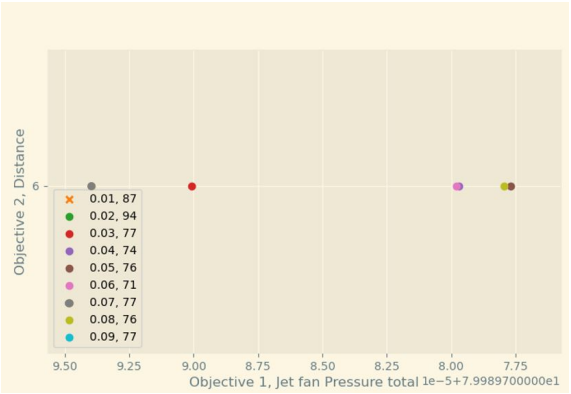

(b) Zoomed into the optimal penalization increments, showing a node distance of six.

Figure 3.20: Analysis of a gradual penalization value increment ranging from 1 to 3. Vertical axes: distance between the two downstream jet fans. Left column legend: values of q_{in}. Right column legend: number of iterations till convergence. The dots show the results for which the distance requirement is met, and the crosses for which they are not.

allocating the weight followed by a continuous increase of q is investigated. The continuation methods use the values presented in this chapter: weight allocation uses $w_{in} = 0.006$ and stops when $w_2 = 0.7$. Penalization increment commences at $w_2 = 0.7$, ranging from $q = 1$ to $q = 3$, with $q_{in} = 0.06$. The convergence behavior of both continuous methods separately and when applied successively, is presented in Fig. 3.21. The dark and light green solid lines show the convergence behaviour of the ventilation objective, in this case f_2, and the penalization objective f_q where both the weight allocation and the penalization increment are continuous in succession during optimization. The dark and light dotted blue lines, f_2 and f_q, show the convergence behaviour where solely the weight allocation is continuous and q remains fixed. The purple and pink dashdotted lines, f_2 and f_q, shows the convergence behaviour where the weight allocation remains fixed at $w_2 = 0.7$, and q increases during optimization.

3.4.11 Discussion Solutions

The convergence behaviors of f_2 for different continuation methods are quite similar, with the primary difference being the number of iterations required to achieve convergence. As previously noted, continuous penalization shows the least number of iterations till convergence, while both parameters continuously shows the highest number of iterations. When assessing the convergence behavior of f_q, distinct patterns are observed. Continuous penalization results in a more rapid fluctuation in objective f_q, compared to the other two continuation approaches. Continuous weight allocation begins with a gradual optimization process, followed by a steep ascent towards convergence. In contrast, when both methods are applied continuously, the convergence seems more steady. Despite requiring more iterations for convergence, the continuous methods in succession appears to exhibit greater stability.

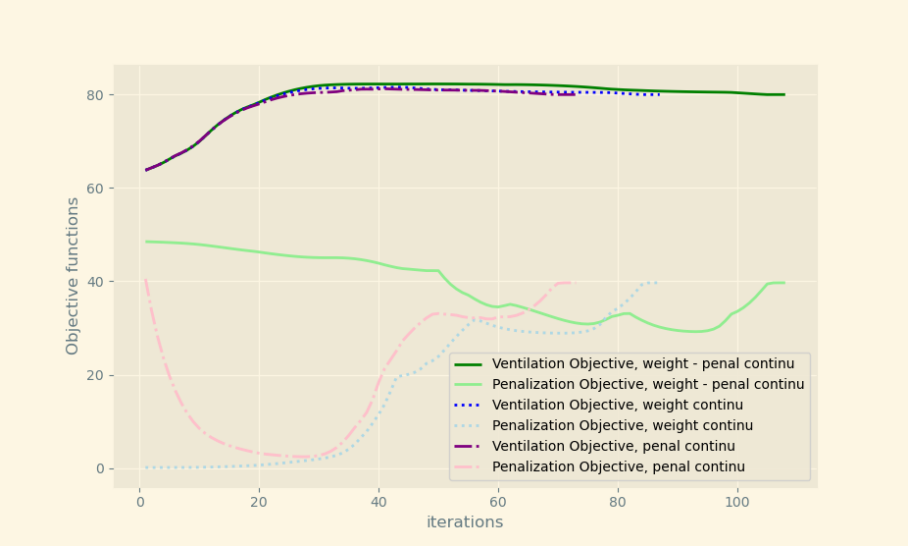

Figure 3.21: Convergence behavior with continuous weight allocation, using $w_{in} = 0.006$ terminating at $w_2 = 0.7$, and continuous increase of q ranging from 1 to 3, with $q_{in} = 0.06$. Convergence behavior of the continuation methods separate and in succession are shown. Ventilation objective: f_2, penalization objective: f_q. Weight - penalization continu: both weight allocation and q are in succession continuously adjusted. Weight continu or penalization continu: one is fixed while the other is continuously updated.

4

Design for an Uncertain Fire Scenario

When a deterministic optimization is performed, the result is pushed towards a highly specialized solution for the specified deterministic problem. However, this implies little about the applicability in other scenarios. Before a tunnel fire occurs, it is impossible to know what fire scenario to design for. The fire scenario determines the tunnel temperatures, influencing tunnel pressure and, consequently, the performance of the longitudinal ventilation system. Including fire uncertainty into the design process, leads to solutions different from a deterministic approach. An uncertainty approach ensures compliance with constraints across a range of scenarios, rather than optimizing for a single scenario.

This chapter begins with a general introduction to the concept of designing while taking uncertainty into account. This is followed by applying an uncertainty approach to the ventilation design problem. In conclusion, an analysis is conducted to compare the design obtained through the deterministic approach with that obtained using the uncertainty approach.

4.1 Design with Uncertainties

When addressing uncertainty, it is often unclear what exact uncertainty to design for. In such cases, a probability distribution centered around a mean value is often assumed. This allows for the meaningful construction of a worst-case scenario, which can be used for optimization. Zhu et al. (2020) discussed two well-known methods using this approach to represent uncertainty, Reliability-Based Optimization (RBO) and Robust Design Optimization. RBO and Robust Design Optimization focus on identifying worst-case scenarios in reliability assessment. However, in ventilation design problems, the uncertainty linked to the fire location has a uniform distribution. This characteristic hinders the pursuit of identifying an effective and usable worst-case scenario for optimization purposes. Relying solely on this approach could lead to failure in other scenarios. Hence, in the context of the ventilation problem, RBO and Robust Design were not further considered. An alternative method for addressing uncertainty is the fail-safe approach, explored by Jansen et al. (2014). This method approaches the problem through a scenario-based setup. It manages local failures individually through a min-max formulation, minimizing the worst-case performance. The incorporation of multiple scenarios during optimization aims to satisfy constraints across various scenarios. In a further investigation into approaches which consider multiple scenarios during optimization, Dembo (1991) introduced the scenario-based methodology. This method optimizes for all specified scenarios simultaneously, as opposed to utilizing a min-max formulation. In ventilation design, it is desired the uncertainty approach considers all the specified scenarios simultaneously during optimization to obtain a final design that satisfies constraints across all plausible fire scenarios. Therefore, the scenario-based methodology seems to align with the requirements of ventilation design and is used to solve the ventilation design uncertainty problem.

4.2 Scenario-Based Methodology

The scenario-based methodology uses a discrete set of fire scenarios to represent the uncertainty. The critical HRR in longitudinal ventilation design is 200 MW, as this requires the most pressure from jet fans. Consequently, the selected fire scenarios maintain a fixed HRR of 200 MW, varying only the positions. The selection of these scenarios determines the number of equilibrium constraints, in contrast to the single constraint outlined in Eq. (3.4), where f_1 is optimized while meeting constraint

c_1. This is described as:

$$\begin{aligned} min: \quad & Num_{fans} = \frac{\sum_{n=1}^{N} N_{maxn}\rho_n}{N\sum_{n=1}^{N} N_{maxn}} \\ s.t.: \quad & 1 - \frac{\sum_{s\in S}(\sum_{n=1}^{N} P_{JFn}\rho_n)_s}{\sum_{s\in S}(P_{res})_s} \leq 0, \\ & 0 \leq \rho_n \leq 1, \end{aligned} \tag{4.1}$$

where s is the scenario within the set of scenarios S. The design can be considered feasible when it satisfies the scenario constraints, which implies the minimization of:

$$\sum_{s\in S} || \sum_{n=1}^{N} (P_{JFn})_s \rho_n - (P_{res})_s ||. \tag{4.2}$$

Therefore, conform scenario-based optimization, Eq. (4.1) is reformulated to minimize the uncertainty constraints represented as distinct scenarios. The differences are squared to amplify the influence of large errors and eliminate the sign. The objective function presented in Eq. (4.1) is reformulated to serve as the constraint. This is described as:

$$\begin{aligned} min: \quad & \frac{\sum_{s\in S} p_s || \sum_{n=1}^{N} (P_{JFn})_s \rho_n - (P_{res})_s ||^2}{P_{MaxDiff}^2} \\ s.t.: \quad & \frac{\sum_{n=1}^{N} N_{maxn}\rho_n}{vf \sum_{n=1}^{N} N_{maxn}} - 1 \leq 0, \end{aligned} \tag{4.3}$$

where p_s is the weight associated with each scenario, and $P_{MaxDiff}$ is the difference between the jet fan pressures and the resistances in case of a filled design space. The fire position follows a uniform probability distribution; therefore, the probability p_s has a value of one for every scenario. Given the nature of the objectives, the optimization process aims to meet the necessary equilibrium constraint for every scenario. Therefore, it avoids placement of jet fans beyond what is required. Consequently, the inclusion of a volume fraction constraint primarily serves to guide the optimization process and shape the evolution of the design, rather than imposing a limit on the number of jet fans.

4.2.1 Sensitivity Analysis of the Scenario-Based Objective

The sensitivities of the scenario-based objective function f_s with respect to the densities ρ_n are given:

$$\frac{\partial f_s}{\partial \rho_n} = \frac{\sum_{s\in S} 2p_s(\sum_{n=1}^{N}(P_{JFn})_s(\sum_{n=1}^{N}(P_{JFn})_s - (P_{res})_s))}{P_{MaxDiff}^2} \tag{4.4}$$

4.2.2 Stopping Criteria

During analysis of the scenario-based methodology used in the ventilation design problem, it was noted the optimization does not terminate for the specified convergence criteria. To investigate, the convergence behaviour of objective f_s and of the absolute change in design variable are presented against the number of iterations in Fig. 4.1. The optimization process is terminated after 100 iterations. It is observed that the objective f_s seems to reach a state of convergence with minimal observable change, after approximately 70 iterations. Concurrently, the design variable seems to exhibit consistent fluctuations around a value of 0.003. This suggests that minor changes in the design variable result in negligible changes in the objective function. This scenario-based methodology optimizes for 99 objectives; therefore, the limited improvement in objective value observed can be a result of reaching a region where further enhancements in the objectives are challenging. Which might contribute to the inability of full stabilization. While the optimization does not seem to achieve the

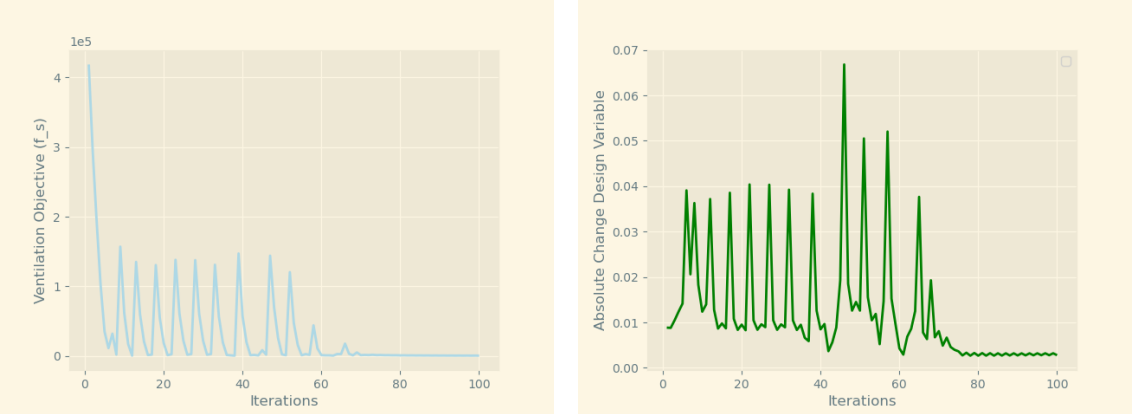

(a) Convergence behaviour f_s over 100 iterations. (b) Absolute difference design variable over 100 iterations.

Figure 4.1: Convergence behaviour scenario-based methodology.

absolute change in design variable as initially specified, namely $\omega = 0.001$, the optimization process seems to achieve a state of convergence, considering that the absolute change in the design variable remains around 0.003, and the objective value exhibits minimal change. Before performing this scenario-based optimization, determining an appropriate absolute change in the objective function value might be challenging. Therefore, the optimization process is terminated when the relative change in objective function is below a specified threshold, denoted as ω_f set to 0.1. This is according to:

$$\frac{||f_k - f_{k-1}||}{||f_{k-1}||} \leq \omega_f, \tag{4.5}$$

where, in this case, f_k and f_{k-1} represent the objective values for the k-th and $(k-1)$-th iterations of the objective function f_s.

4.2.3 Fail-Safe Regions

To perform the scenario-based optimization, for each fire scenario the total resistances $(P_{res})_s$ and jet fan performance along the tunnel length $(P_{JF})_s$ are obtained. This is used to identify a jet fan alignment that minimizes the objective for each fire scenario. The fire locations within the set of scenarios S are shown in Fig. 4.2 against the total pressure resistances for each scenario s, for a fixed HRR of 200 MW. This means, for a fire located at 400 m, the total resistances in the tunnel are 50 Pa. The red line is a collection of the total resistance for all the specified fire scenarios. In accordance with the equilibrium requirement as presented in Eq. (2.1), the back-layering constraint is met when the pressure from jet fans equals or exceeds the total resistances for a given fire scenario. This means, the pressure from the jet fans should operate at or above this red line for all fire scenarios. This indicates that if the jet fans operate below the red line, they are in the fail region, and when they operate above it, they are in the safe region. These fail-safe regions are illustrated in Fig. 4.2. For the remainder of this chapter, a HRR of 200 MW is used. Ideally, the jet fan pressure line should closely align with the resistances line to avoid unnecessary pressure build-up. Which is desired to serve the positive pressure ventilation system design and to avoid the use of an excessive number of jet fans to prevent back-layering.

The greatest pressure required from jet fans is observed at the entrance and final part of the tunnel. This can be primarily attributed to the impact of chimney effects, with the influence determined by the length over which it is present and whether this effect has a negative or positive impact on the intended smoke flow.

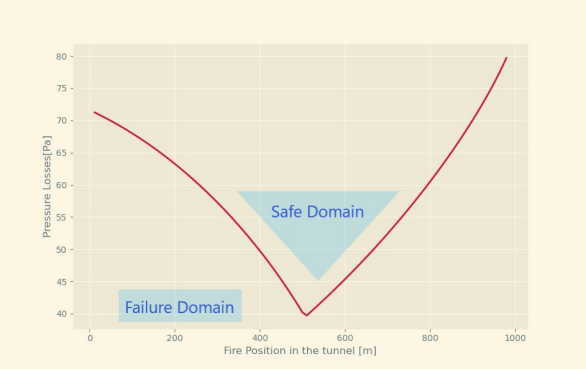

Figure 4.2: The fail-safe regions to consider when designing in the presence of uncertainty. The red line signifies the total resistances for all the specified fire locations.

4.3 Scenario-Based Longitudinal Ventilation Design

For the same tunnel specifications as used in Chapter 3, the scenario-based optimization is performed, presented in Fig. 4.3. For this optimization, nodes are selected as the fire locations for the scenarios. In this context, this means a fire location every 10 m starting from the tunnel entrance, resulting in a total of 99 fire locations. The fire locations at 0 km and 1 km are excluded, as they correspond to the entrance and exit of the tunnel. Positioning the fire locations at the nodes is not a requirement, and the designer is free to choose the fire locations.

The problem described in Eq. (4.3) is solved for the specified fire location scenarios. In Chapter 3.2.5, a volume fraction vf of 0.038 was used to solve the problem described in Eq. (3.5), for the same tunnel and fire scenario. Since the volume fraction in this problem does not serve the function of limiting the number of jet fans during optimization, a volume fraction of 0.1 is used to facilitate exploration of the design space.

In Fig. 4.3a, the pressures associated with the optimized design variable are presented. The orange line represents the total jet fan pressure, and the red dotted line represents the total resistances, both for every fire location. In order to offer valuable insights into the problem and provide critical design information for the overpressure ventilation system, the maximum cumulative pressures for each fire scenario are presented. The green dashdotted line is the maximum pressure downstream, and the pink dashed line is the maximum pressure over the entire tunnel length. The resulting jet fan densities at the nodes are shown in Fig. 4.3b.

(a) Tunnel pressures for the optimized jet fan layout.

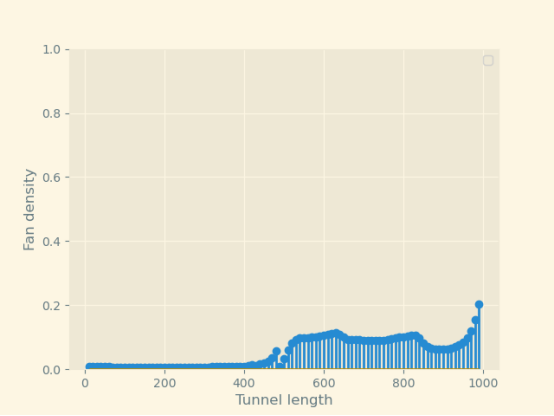

(b) The optimized jet fan layout.

Figure 4.3: Scenario-based volume-constrained optimization with objective f_s. Tunnel length is 1 km, a fire is situated every 10 m starting at the tunnel entrance with 200 MW HRRs.

4.3.1 Discussion Solution

The result indicates that, for each predefined fire scenario, the jet fan alignment approaches the total resistances. This means, near compliance with the equilibrium constraints. This suggests that there exists a ventilation solution that closely matches the required equilibrium constraint for every specified fire scenario. It seems that achieving this solution involves positioning jet fans in the second half of the tunnel, where the tunnel shows a positive slope.

The intuitive approach for dealing with uncertain fire scenarios involves positioning jet fans near the tunnel entrance, where the chances at exposure to fire effects is minimized. However, it seems placement is particularly in areas of the tunnel with a positive slope. A hypothesis is formulated to provide an explanation for this observation. To explain the hypothesis Fig. 4.4 is provided, which shows the total resistances for the specified fire locations indicated by the red line. Four fire positions are denoted by yellow diamond shapes, each marked with a number. The main positioning of jet fans in the tunnel is indicated by the blue squares in the second half of the tunnel.

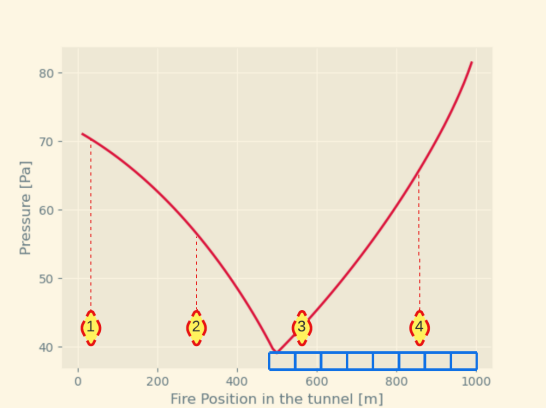

Figure 4.4: Four fire positions represented by numbered yellow diamond shapes. The primary placement of jet fans in the second half of the tunnel is marked by blue squares.

To prevent the longitudinal ventilation failing for fire location 1, jet fans are strategically positioned further down the tunnel, where they are least influenced by the effects of the fire. As the fire moves further down the tunnel to position 2, it moves closer to the positioned jet fans, decreasing their performance. However, mainly due to the decreasing length over which the chimney effect negatively influences the smoke movement, the total resistance value also decreases. At fire position 3, the jet fans are located downstream and in close proximity to the fire. This leads to a significant influence by the fire effects. However, this fire position also corresponds to the lowest total resistance value. As the fire position moves toward position 4, total resistances increase. Simultaneously, the number of jet fans positioned upstream of the fire grows. This is where they remain unaffected by the fire effects. Consequently, the overall pressure generated by the jet fans increases. In conclusion, it appears that this positioning strategy effectively aligns the placement of jet fans with the required pressure for specific fire locations.

By using this approach, ventilation designers have the potential to adjust their designs to meet the pressure requirements for each fire scenario. This could potentially lead to the use of fewer jet fans, as the solution indicates that jet fan pressures closely align with the resistances for each scenario. Consequently, this approach seeks to prevent unnecessary pressure accumulation while striving to meet the equilibrium constraints. It appears to lead to constrained maximum tunnel pressures, especially when analyzing the maximum downstream pressures shown in Fig. 4.3b, with a maximum value of 3 Pa. Since this approach aims to prevent unnecessary pressure accumulation, it seems to effectively serve the minimization of the downstream pressure. Therefore, it can be assumed that this uncertainty approach serves both the longitudinal ventilation design and the positive pressure ventilation system design.

4.4 Distance Requirement Between Jet Fan Clusters

It is essential to maintain a separation of at least 100 m both between jet fans and 100 m between jet fans and the tunnel exit, to prevent energy loss. The tunnel used for the illustration in Fig. 4.3 is 1 km, this implies that jet fans can be maximally located at 900 m from the tunnel entrance.

4.4.1 Penalization Objective in the Scenario-Based Approach

To meet the separation between jet fans, f_q, introduced in Chapter 3.4, is used. This changes the optimization formulation provided in Eq. (4.3) into:

$$\begin{aligned} min: \quad & \frac{\sum_{s\in S} p_s || \sum_{n=1}^{N} (P_{JFn})_s \rho_n - (P_{res})_s ||^2}{P_{MaxDiff}^2} \\ max: N_{dfans} = & \frac{\sum_{n\in N} \sum_{i\in N_n} {\rho_i}^q}{2N(d_{fans}-1)} \\ s.t.: \quad & \frac{\sum_{n=1}^{N} \rho_n}{vf\ V_0} - 1 \leq 0, \\ & 0 \leq \rho_n \leq 1. \end{aligned} \tag{4.6}$$

The conclusions drawn from the weight investigation and continuation method discussed in Chapter 3.4.10 are used for this problem. This implies that the weight associated with the ventilation objectives, in this case w_s, decreases with 0.006 each iteration until it reaches a value of 0.7. Subsequently, q is incremented from 1 to 3 each iteration, with q_{in} set at 0.06. To avoid the placement of jet fans within the final 100 m of the tunnel, at the nodes between 900 m and 1000 m, the performance of jet fans is decreased to generate zero pressure (0 Pa) for every scenario. The jet fan performance at the nodes P_{JFn} is described as:

$$P_{JFn} = \begin{cases} P_{JFn}, & \text{for } n \leq N-10; \\ \text{1e-6}, & \text{for } n > N-10, \end{cases} \tag{4.7}$$

where $N-10$ indicates the last 10 nodes located in the final part of the tunnel, which represents the last 100 m in the tunnel. This resembles the performance of jet fans operating close to the fire.

The selected volume fraction is 0.1. It appears that the chosen volume fraction does not significantly impact the solutions, provided it remains above the minimum threshold required to meet the equilibrium requirement.

4.4.2 Stopping Criteria

In the context of the optimization problem described in Eq. (4.6), which includes objective f_q, it is worth noting that the stopping criteria defined in Chapter 4.2.2, where the optimization process is terminated when the relative change in the objective value falls below the specified threshold value of ω_f, leads to premature convergence. Conversely, the previously established stopping criteria based on the absolute change in design variables, with ω set to 0.001, has proven to be effective for this problem. Therefore, it is used for the problem formulation provided in Eq. (4.6).

4.4.3 Optimizing with the Penalization Objective

To monitor the impact of the jet fan positioning requirements on the results, the introduction of the requirements is carried out one at a time. Consequently, Fig. 4.5 displays two columns of figures. The results for the introduction of only the distance requirement between jet fan is provided in Fig. 4.5a. Additionally, the introduction of both distance requirements is provided in Fig. 4.5b. The results show that the discussed distance requirements are met. It can be observed that jet fans are predominantly positioned in the second half of the tunnel. Additionally, the top figures show a

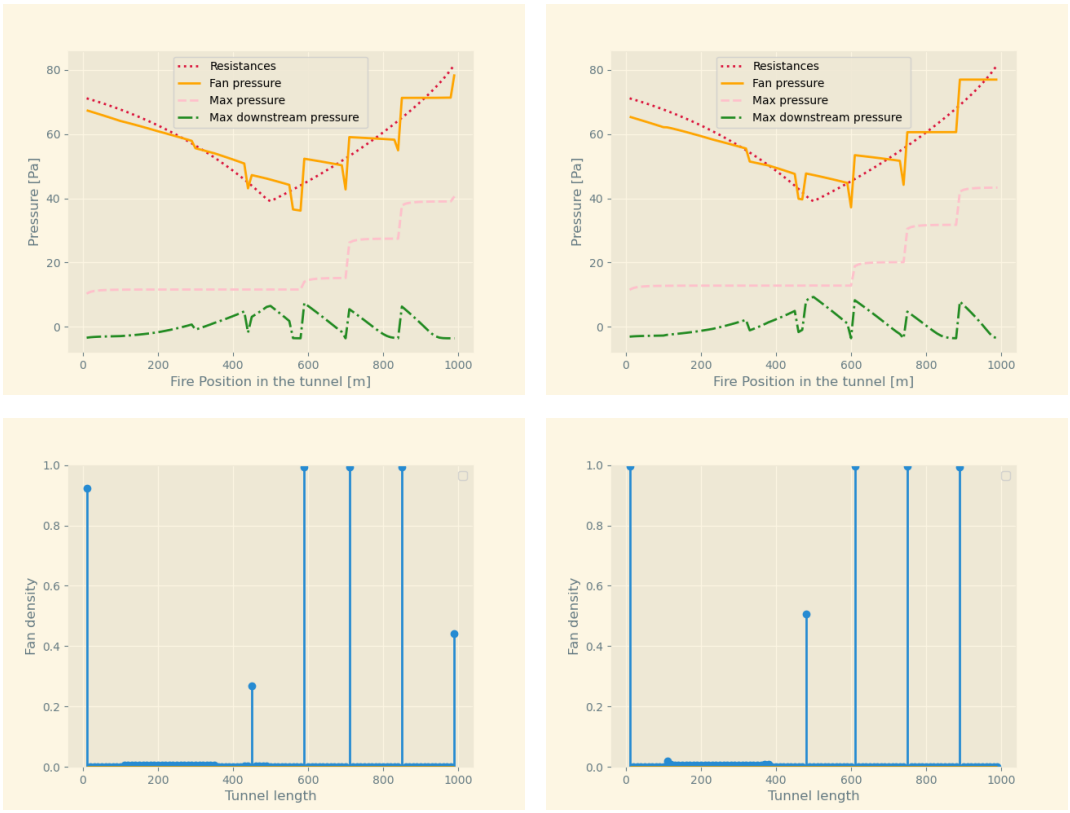

(a) A 100 m spacing between jet fans.

(b) A 100 m spacing between jet fans, with no jet fans in the final 100 m.

Figure 4.5: Solution for the optimization of both f_s and f_q while meeting a volume constraint. Left column: a 100 m spacing between jet fans. Right column: A 100 m spacing between jet fans, with no jet fans in the final 100 m. The tunnel length is 1 km, with a fire situated every 10 m starting at the tunnel entrance with a HRR of 200 MW. The distance between jet fans is 100 m.

staircase pattern in the jet fan pressures, and in the maximum pressures and maximum downstream pressures. When a jet fan is placed downstream of the fire, it decreases in performance or even fails when close enough to the fire. To further explain, the jet fan positioned around 600 m fails for a fire positioned at that same position. This results in a drop in jet fan pressure.

Moreover, as seen in Fig. 4.3, the continuous jet fan densities led to the jet fan performance closely approaching the resistances. With the introduction of f_q, jet fans are restricted in their positioning and are promoted to converges towards binary solutions. This results in the jet fan pressure to fluctuate more intensely around the resistances line compared to what was observed in Fig. 4.3. These fluctuations lead to increased downstream maximum pressure fluctuations for each scenario, in contrast to the smoother variations observed in the continuous solution.

4.4.4 Presence of Intermediate Densities in the Solutions

The presented results in Fig. 4.5 show some remaining intermediate densities. These intermediate densities could be reduced further, for instance, by increasing the penalty term or incorporating a Heaviside projection filter. The effect of increasing the penalty term is analyzed. This choice is driven by two primary considerations. First, increasing the penalty factor fits into the existing framework with minimal changes to the design process. Second, the inclusion of a Heaviside projection filter introduces an additional parameter tuning aspect, in addition to adjusting the weight and penalty term, which is preferably avoided. The effect of increasing the penalty value to 4,5, and 6 was

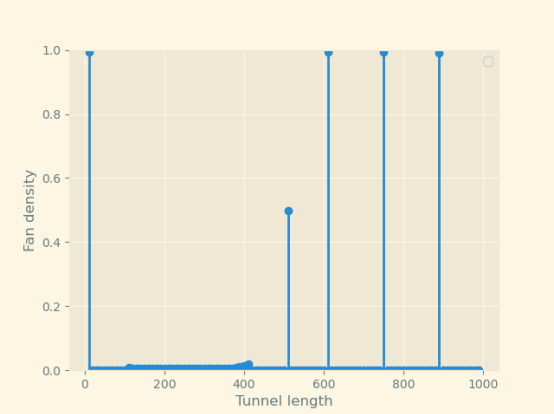

Figure 4.6: Solution for the optimization of both f_s and f_q while meeting a volume constraint. A 100 m spacing between jet fans, with no jet fans in the final 100 m is shown. The tunnel length is 1 km, with a fire situated every 10 m starting at the tunnel entrance with a HRR of 200 MW. The distance between jet fans is 100 m. The penalization increases every iteration from 1 to 4.

analyzed. It was concluded that increasing the penalty value showed minimal change in the final solution. To show, Fig. 4.6 presents the solution of increasing the penal value to 4, which almost exactly resembles the solution shown in Fig. 4.5b.

At present, the decision is made to preserve certain intermediate densities and maintain the current solution. This choice is guided by two reasons. First, in this problem formulation, the maximum allowable jet fans per node N_{max} is set to one. However, in practical tunnel ventilation applications, N_{max} is often higher. This means, an intermediate density of 0.5 would correspond to the placement of one jet fan. While it is preferred to position jet fans in clusters, this is not a significant concern. This permits flexibility, allowing ventilation designers to make the remaining decisions based on the specific requirements of the tunnel ventilation assignment. Secondly, the optimization objective is to minimize differences between jet fan performance and resistance across scenarios. However, not all deviations from the resistance line are equally disadvantageous. Controlling deviations in specific tunnel areas can prove beneficial for both the longitudinal ventilation and the positive pressure ventilation system. For example, the positions of escape doors could be considered.

4.5 Comparing Deterministic and Scenario-Based Approach Solutions

To compare the solutions obtained from the scenario-based methodology with those from the deterministic approach, solutions from both approaches are compared for two fire locations with a fixed HRR of 200 MW. For the scenario-based methodology the solution provided in Fig. 4.5b is used, this was the last obtained solution, where all the geometric constraints are considered. For the deterministic approach, a solution is provided that addressed the problem with a fire located at 300 m, considering the geometric constraints as well.

The comparison involves two fire locations: one at 300 m and the other at 100 m. These locations were selected for specific reasons: the 300 m location served as the basis for optimization in the deterministic approach, while the choice of the 100 m location is included to highlight the limitations of the deterministic approach. In the deterministic approach, jet fans are positioned primarily upstream of the fire where their performance is least effected by fire effects for that scenario. When the fire location is moved closer to these positioned jet fans, their performance decreases.

4.5.1 Ventilation Design Approach Comparison for a 300 m Scenario

Solutions for both approaches are presented in Fig. 4.7 for a fire located at 300 m. The left column shows the solution for the deterministic approach, and the right for the uncertainty approach. The

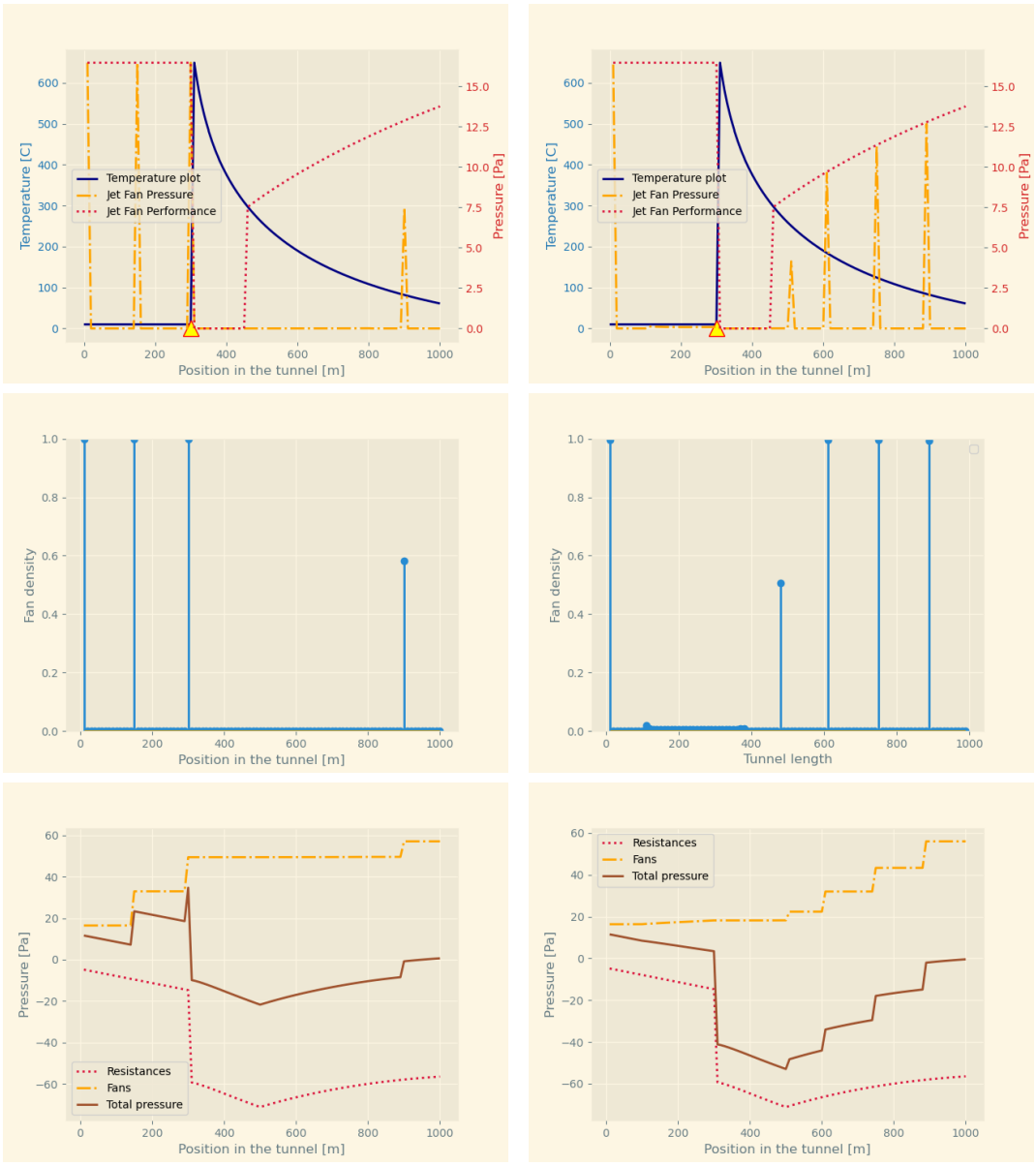

(a) Deterministic approach.

(b) Scenario-based methodology.

Figure 4.7: Comparison of the solutions from the the deterministic approach (left column) and the scenario-based methodology (right column). A fire is situated at 300 m, with a HRR of 200 MW.

total pressures of both solutions terminate at a pressure of approximately 0 Pa, as shown in the third row of Fig. 4.7. This means, both solutions satisfy the equilibrium constraint for this fire location. As expected, the deterministic approach positions less jet fans to achieve equilibrium in comparison to the scenario-based approach. This is because the deterministic approach is optimized for this fire scenario, where jet fans are positioned at their most efficient locations, resulting in a reduced requirement of jet fans.

4.5.2 Ventilation Design Approach Comparison for a 100 m Scenario

For this comparison, a fire location at 100 m is considered for the same ventilation solutions. The solutions for both approaches are presented in Fig. 4.8. When considering the final total pres-

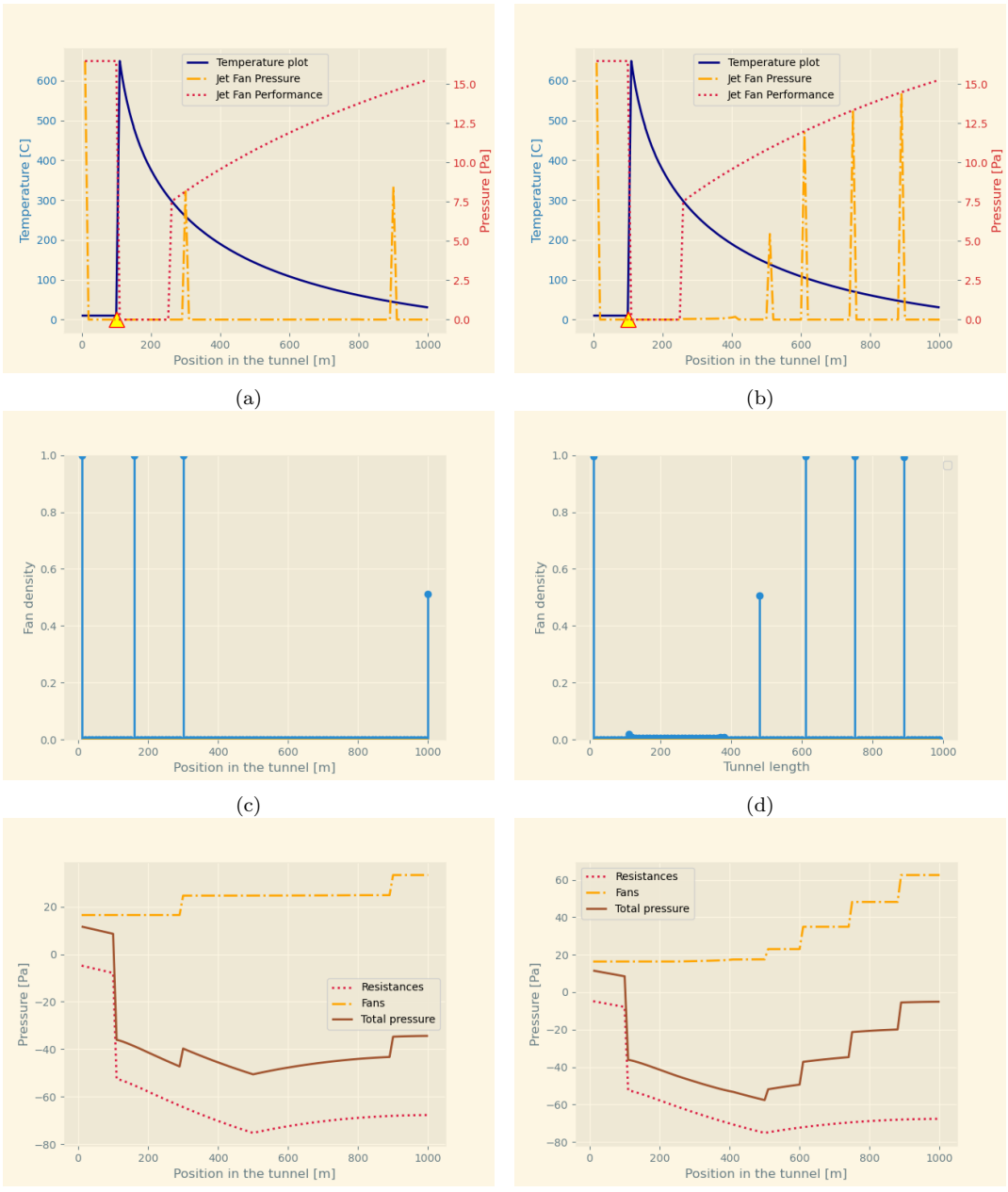

Figure 4.8: Comparison of the solutions from the the deterministic approach (left column) and the scenario-based methodology (right column). A fire is situated at 100 m, with a HRR of 200 MW.

sures again, it is observed that for the deterministic approach the pressure terminates at -38 Pa. This indicates that the equilibrium requirement is not satisfied, and the critical air velocity is not achieved, which in turn means that this design is not feasible for this fire location. Contrarily, in the scenario-based methodology, the pressures reach the 0 Pa boundary, indicating that the equilibrium requirement and the corresponding critical air velocity are almost achieved. The pressure terminates

slightly below the 0 Pa boundary, due to the scenario-based formulation, which aims to minimize the difference rather than always ensuring neat operation above the resistances. This is also evident in Fig. 4.5b, where the jet fans (represented by the orange line) operate slightly below the resistances line for the fire location at 100 m. However, as Fig. 4.5b demonstrates, the equilibrium requirement is approached for every fire location for this worst-case fire HRR of 200 MW, leading to solutions that exhibit significantly improved feasibility for all the fire locations compared to the solution obtained using the deterministic approach.

This comparison demonstrates that, although a minor increase in jet fan pressure is required to achieve equilibrium for this fire scenario, the scenario-based methodology outperforms the deterministic approach at this location in terms of achieving the critical air velocity and obtaining a feasible design. This comparative analysis can be extended to more fire locations. This will demonstrate that although the deterministic solution is more efficient for certain fire locations, requiring fewer jet fans while still meeting the equilibrium requirement, the scenario-based methodology consistently approaches the equilibrium constraint. In contrast, the deterministic approach fails significantly for a subset of the fire locations. In conclusion, the scenario-based methodology offers longitudinal ventilation designs that reach the equilibrium constraint across a wide range of scenarios without introducing unnecessary pressure build-up in the tunnel.

5

Comparative Analysis Tunnel Ventilation Design Approaches

This report proposes a systematic design approach for the design of longitudinal ventilation systems. Instead of relying on an experience-based methodology to develop tunnel ventilation designs, this approach employs a systematic method to discover optimized solutions for ventilation problems. The design approach for both the deterministic and uncertain design approach are outlined in Appendix A.3. The corresponding Python files are located in an attached folder.

To evaluate the effectiveness of the newly introduced approach and to gain deeper insights into the results, the outcomes of the systematic design approach are compared with a design created by Arcadis. The tunnel selected for this comparative analysis is the Beveren Tunnel, located near Antwerpen. First the specifications of the Beveren Tunnel are provided, which serve as the basis for the ventilation design. Then, the longitudinal ventilation design developed by Arcadis is provided. Subsequently, the results obtained through the newly developed approach are shown. Finally, a comparison and discussion of the results derived from both design methodologies is provided. The comparison is based on two ventilation design characteristics: the number of positioned jet fans and the failure probability, determined by means of the probabilistic calculations using ProTuVeM. It is important to acknowledge that this comparative review has its limitations. It focuses on evaluating the number of jet fans used in the ventilation design and employs the ProTuVeM probability of failure tool to assess performance. This analysis does not completely cover all the aspects of ventilation design. For example, the effect of the final designs on the positive pressure ventilation is not thoroughly investigated. Nevertheless, it does provide an initial impression of the performance.

5.1 Tunnel Specifications Beveren Tunnel

The Beveren Tunnel consists of two tunnel tubes, one leading toward Gent and the other toward the Netherlands. During the design process, one tube is considered at a time. For the purpose of this comparison, one tunnel tube is used for evaluation. The tunnel tube which experiences more wind effects is the tube which runs in the direction of Gent. This tunnel tube requires increased performance from jet fans, making it a slightly more complex ventilation design compared to the other tube. Therefore, this tube is used for the comparison. The geometric information for this tunnel tube is provided in Table 5.1. Furthermore, the traffic tunnel longitudinal profile which indicates the tunnel slope and driving direction is shown in Fig. 5.1.

Description	Characteristic
Intersection	79 $[m^2]$
Circumference	41 $[m]$
Number of traffic lanes	2
Tunnel length	1120 [m]
Orientation North portal	25°
Orientation South portal	205°

Table 5.1: Geometric facts Beveren tunnel, tunnel tube direction Gent.

The remaining relevant information concerning Beveren tunnel is provided: The traffic composition for the considered traffic tube, is as follows: cars 28 %, Vans 15 %, and HGV 57%. The wall

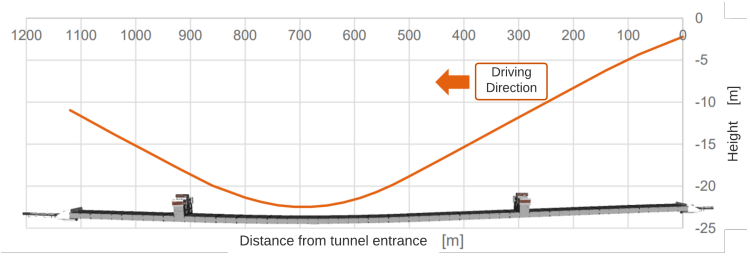

Figure 5.1: Traffic tunnel longitudinal profile, driving direction from Netherlands to Gent.

friction coefficient λ has a value of 0.018. The inflow coefficient ξ_{in} and exit flow coefficient ξ_{out} have a value of 0.2 and 1. The surrounding grounds around the tunnel contain virtually no obstacles. This means that the wind correction factor, ξ_{wind} has a value of 1. The IOWA data (*Iowa Environmental Mesonet*, 2021) is used to construct a wind table providing a worst case air velocity of 10 m/s, which is used for design. The fire HRR that is used for designing is 200 MW.

Two types of jet fans are used for this ventilation system. The tunnel entrance allows the use of larger-sized jet fans compared to the interior of the tunnel. At the tunnel entrance five jet fans fit, within the tunnel two jet fans within a single cluster are allowed by the tunnel dimensions of the specified jet fan type. The two types of jet fans and their relevant specifications for designing are provided in Table 5.2.

Ventilator Type	Maximum Operating Temperature $[°C]$	Flow Rate $[m^3/s]$	Discharge Velocity $[m/s]$
ø1120	300	36,17	36,00
ø800	300	20,76	42,00

Table 5.2: Jet fan specifications of the two types of jet fans used in the Beveren Tunnel. The jet fan type in the first row is used at the tunnel entrance. The type in the second row is used in the tunnel.

The format that Arcadis uses to show their ventilation designs is used to show the ventilation designs resulting from both approaches. This format has the capability to show differences between types of jet fans and the number of jet fans positioned along the tunnel width. This differs from the presentation style in this report, where the densities of jet fans at the nodes were shown, which does not specifically show the number or type of jet fans. In this report, this was not a concern since the same jet fan type was used for the entire tunnel, and the maximum number of jet fans along the tunnel width N_{max}, remained constant along the entire tunnel length.

5.2 Experience-Based Design Approach

The ventilation design obtained using the current design approach at Arcadis is based on an experience-based approach. The ventilation design by Arcadis is shown in Fig. 5.2. The blue squares with the two arrows attached show the ø800 jet fan. The two arrows indicate the capability of a reversible flow, which becomes relevant when considering a fire scenario in the other tunnel tube. However, for the purposes of this review, it will not be further discussed. At the tunnel entrance five jet fans of ventilator type ø1120 are positioned and are indicated by blue squares with one attached arrow. Within the tunnel eight jet fans of ventilator type ø800 are positioned. The grey jet fans in the figure show the redundant jet fans, which are not used to compare performance. The red rectangles show the positions of the escape doors.

5.3 Systematic Design Approach

The systematic approach to solve the problem is as presented in Chapter 4.4.1, which describes the scenario-based approach with the penalization objective. The solutions provided by the systematic

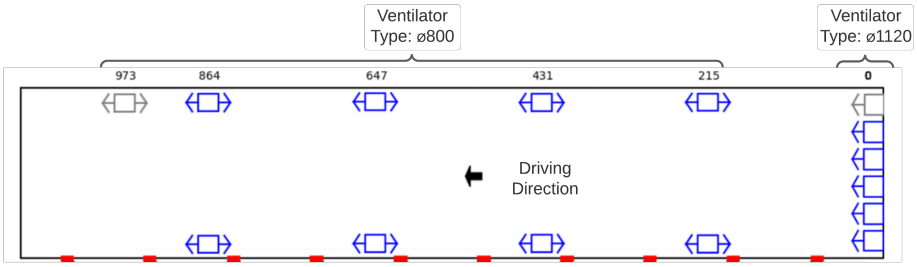

Figure 5.2: Ventilation design Arcadis Beveren Tunnel. The blue squares with two arrows attached indicate jet fan type ø800, with one arrow attached represent the ø1120 jet fan. The grey squares indicate redundant jet fans.

approach, are first presented in the format consistent with the rest of this report for showing the tunnel pressures, to assess the solution and the tunnel pressures. Subsequently, the solution is presented alongside the solution of Arcadis in Chapter 5.4, using the format shown in Fig. 5.2 to enable comparison. To carry out the optimization, the jet fan pressures at the nodes, P_{JFn}, are in accordance with the outlined jet fan specifications presented in Chapter 5.2. Accordingly, at the tunnel entrance, jet fans are associated with the characteristics related to jet fan ø1120 and a maximum of five jet fans can be positioned, thus $N_{max} = 5$ at this node. In the remaining part of the tunnel, jet fans with capacities related to ø800 can be positioned in clusters of two, thus $N_{max} = 2$. Nodes are separated by 10 m, and the weight allocation and penalization increment, ranging from 1 to 3, are in succession according to the conclusions in Chapter 3.4.

5.3.1 Discussion Solution

The results are shown in the left column of Fig. 5.3. As was observed in Chapter 4.4, the aim of f_s is to minimize the difference between the jet fans pressures and the tunnel resistance pressures. Consequently, this leads to results where the jet fan pressures do not operate above the required pressures for every fire scenario. For example, at 200 m the orange line (jet fan pressure) operates below the red line (resistances).

5.3.2 Further Refinement Ventilation Solution

As discussed in Chapter 4.4.4, this approach leaves some design freedom for the ventilation designer. The solution is viewed from the perspective of a ventilation designer, and in an effort to enhance it, the decision has been made to both decrease the number of jet fan clusters and increase the pressure generated by the jet fans. To achieve this, the ø800 jet fan located at 700 m, where $N_{max}(= 2)$ times $\rho_n(= 0.5)$ is equal to one jet fan, is replaced with a single jet fan of ø1120 type, which is added to the cluster at the tunnel entrance. This solution is provided in the right column of Fig. 5.3. Still not for every fire location, the jet fans operate above the resistances, for example at 100 m. However, the worst case wind scenario value was used to account for wind effects in the optimization process. For the comparative review, the probabilistic method in ProTuVeM is used which uses more realistic wind effects. This includes information regarding variations in wind, rather than solely relying on the worst-case scenario value. Therefore, the solutions presented in the right column are considered valid to use for the comparative review.

The solution shows six jet fans of type ø800, and five of type ø1120. With the exception of the larger jet fans positioned at the tunnel entrance, the remaining jet fans are positioned, as previously observed, in the part of the tunnel with a positive slope. When comparing it to the solutions presented in Chapter 4, it was found that approximately five jet fans were required to approach the equilibrium equation for each scenario. The higher number of jet fans needed in this case can be mainly attributed to the introduction of wind effects, as well as the longer tunnel section with a steeper negative slope, which results in an increased negative contribution from chimney effects.

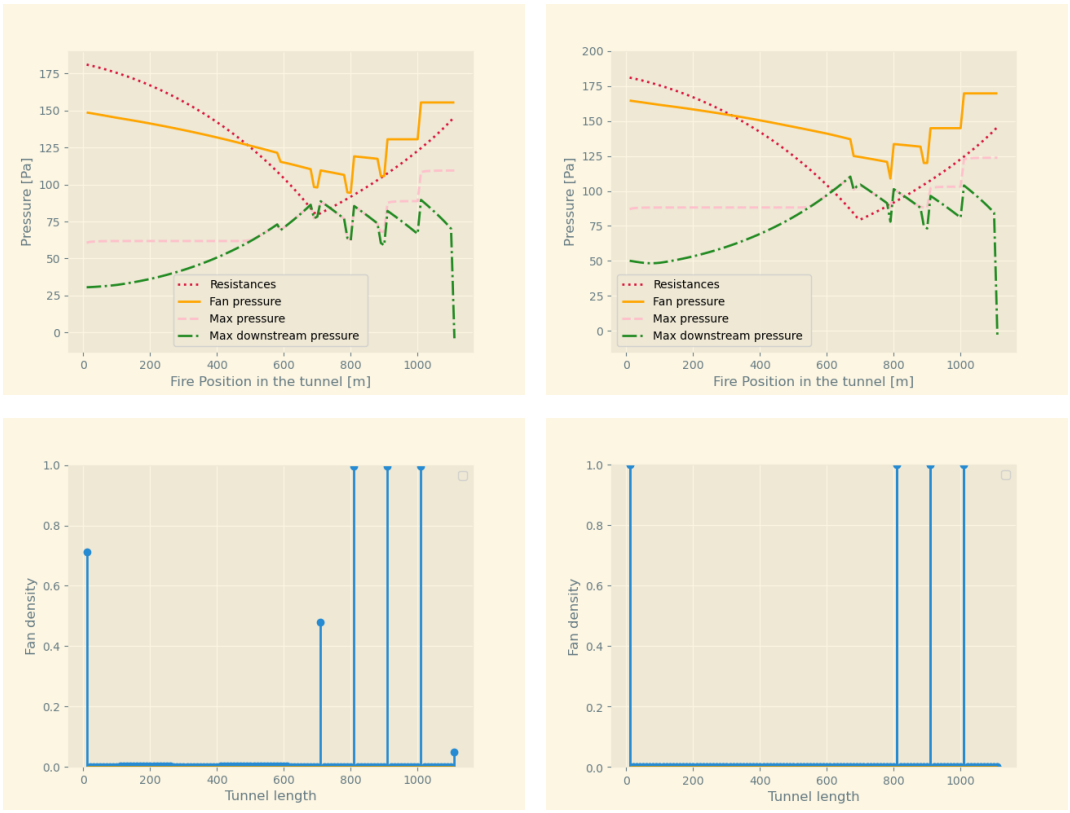

(a) The optimized jet fan layout.

(b) The adjusted optimized jet fan layout.

Figure 5.3: Ventilation design Beveren tunnel provided by the systematic design approach. Objectives f_s and f_q are optimized while meeting a volume constraint. Left column: solution obtained using the systematic design approach. Right column: adjusted solution by designer. A fire location every 10 m starting at the tunnel entrance is used with a HRR of 200 MW.

5.4 Longitudinal Ventilation Design Comparative Analysis

The ventilation designs of both approaches are comparatively shown in Fig. 5.4. A distinction in solutions is observed. First, the solution obtained using the systematic design approach provides two jet fans less. Second, although in both solutions there is a significant placement of jet fans at the tunnel entrance, the systematic approach positions jet fans in the tunnel part showing a positive slope, while the solution of Arcadis shows a more scattered positioning. At Arcadis, jet fans were strategically positioned with respect to escape doors and scattered throughout the tunnel to minimize the simultaneous influence of fire effects on the placed jet fans. However, when considering the objective of minimizing the number of jet fans and tunnel pressures using the systematic approach, it appears more beneficial to position jet fans in the part of the tunnel with a positive slope. This results in the alignment of jet fan pressures with the resistance pressures for the fire locations.

A description of the probabilistic calculations performed by ProTuVeM were outlined in Chapter 1.3.2. The calculations are performed for both ventilation designs. The failure probability for the design of Arcadis is 5.21e-02, while the systematic approach presents 4.92e-02. The systematic approach provides a design with two fewer jet fans, without an increase in the failure probability, and even showing a slight decrease. In the context of this comparison, the systematic approach offers an improved ventilation design.

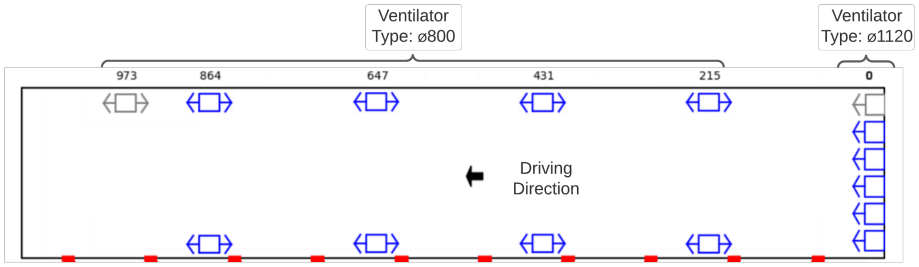

(a) Longitudinal Ventilation Design by Arcadis.

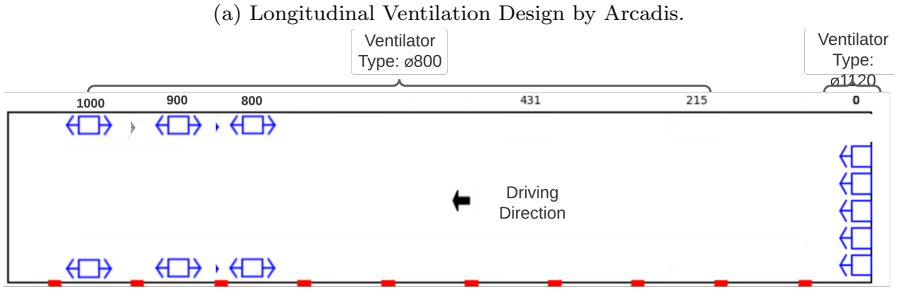

(b) Longitudinal Ventilation Design systematic approach Using ProTuVeM 2.

Figure 5.4: Ventilation design for the Beveren tunnel using the experience-based design approach (top figure) and using the systematic design approach (bottom figure).

5.4.1 Comparative Analysis Focused on Tunnel Pressures

To gain some insights in the effects of the solutions with respect to the final maximum tunnel pressures, the solutions are provided along side each other in the format used in Chapter 4. This is shown in Fig. 5.5. The left column shows the solution of Arcadis, the right column the solution provided by the systematic approach.

Observations reveal that the jet fan pressures resulting from the experience-based approach do not adhere to the resistances line. Instead, this solution consistently accumulates pressure within the tunnel, resulting in higher pressures than necessary for various fire locations. In contrast, the jet fan pressures obtained from the systematic approach closely approach the resistance pressure line. This suggests that the systematic design shows improved alignment with the actual requirements for jet fans at each fire location, in contrast to the solution obtained from the experience-based design approach. Therefore, the systematic approach achieves lower maximum pressures in the tunnel, which could benefit positive pressure ventilation design. It is important to note that this statement does not account for the positions of escape doors.

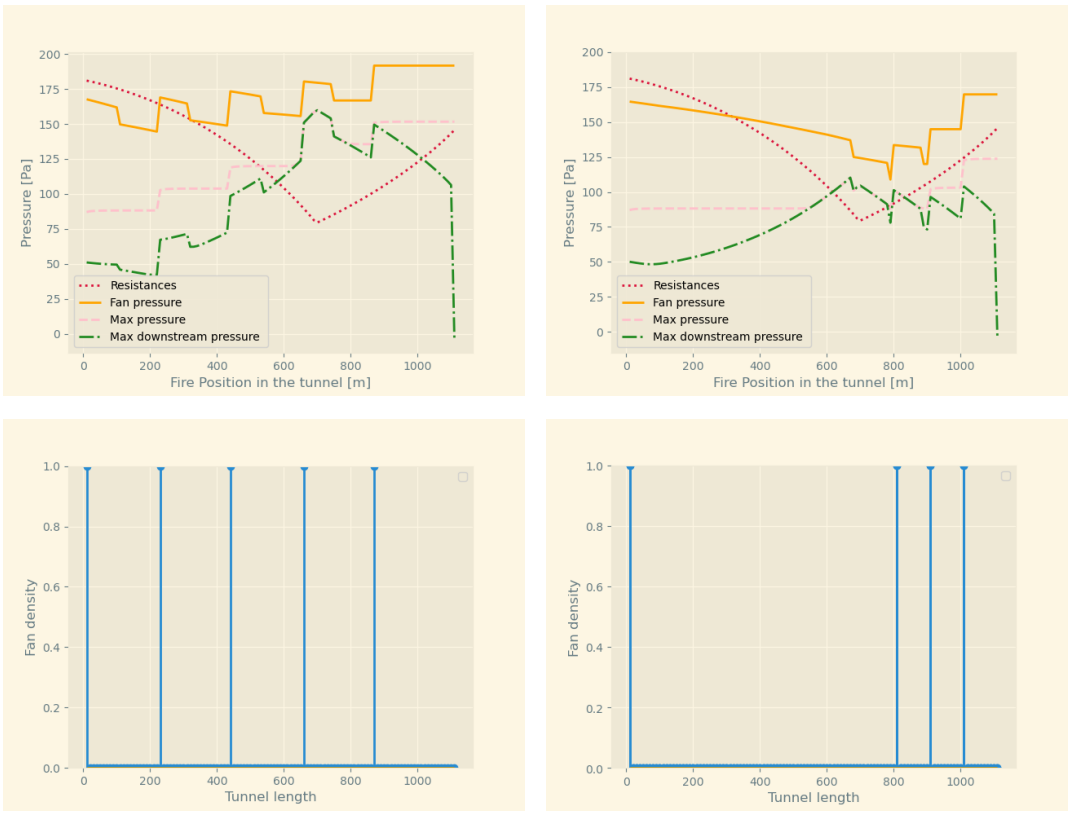

(a) Experience-based design approach.

(b) Systematic design approach.

Figure 5.5: Ventilation design Beveren tunnel generated by the experience-based design approach (left column) and the systematic design approach (right column). The first row shows the pressures resulting from the obtained solutions, the second row shows the final densities representing the jet fans.

6

Discussion

This report was dedicated to enhancing the longitudinal ventilation design at Arcadis. The main objective of this research was to transition from an experience-based design approach to a systematic methodology. ProTuVeM was rewritten in Python, referred to as ProTuVeM 2, to improve its usability and eliminate the need for a separate mathematical programming sheet to calculate cumulative pressures. The systematic approach aims to produce a longitudinal ventilation design that effectively prevents back-layering, minimizes unnecessary pressure buildup in the tunnel, addresses fire scenario uncertainties, and complies with jet fan placement requirements. The introduction of the systematic design approach has demonstrated effectiveness in optimizing jet fan placement for fire scenarios while addressing various objectives.

The introduction of a systematic design approach has demonstrated that, as anticipated, jet fans are placed where their performance remains unaffected by fire effects. However, when positioning all required jet fans at their maximum efficiency is unfeasible, due to requirements regarding jet fan placement, they are placed where they are least affected, as far from the fire as possible.

To accommodate the requirements of the positive pressure ventilation system within the deterministic longitudinal ventilation design, a second objective was established to minimize the maximum pressure within the tunnel. Consequently, this led to the placement of jet fans further down the tunnel, where the effects of tunnel and fire resistances introduced a pressure reduction. Leading to reduced maximum cumulative tunnel pressures.

The scenario-based approach, in addressing uncertainties, has revealed a positioning strategy distinct from the approach at Arcadis. The intuitive choice when designing for an uncertain fire scenario might be to position jet fans primarily near the tunnel entrance, where the chances of being affected by fire effects is minimized. However, the systematic design approach shows predominant placement in the tunnel part with a positive slope, and some placement near the entrance. The set up of the scenario-based approach is to minimize the difference between the jet fan performance and the tunnel resistances for every scenario. This is accomplished by strategically positioning jet fans so that in fire scenarios where lower total pressure values are needed, the total efficiency of the jet fans is lower, while in scenarios demanding higher performance from jet fans, the total efficiency is higher. This is accomplished by primarily locating jet fans in the tunnel part showing a positive slope. When the fire occurs at the tunnel entrance, the jet fans are located at a greater distance from the fire. Additionally, further down the tunnel, the further the fire location moves towards the tunnel ending, increased number of jet fans become located upstream of the fire. Which leads to increased jet fan pressures. Conversely, for fire locations leading to lower total resistance pressures, jet fans are located downstream and in closer proximity to the fire. Consequently, this positioning strategy seems to effectively align the positioning of jet fans with the specific pressure requirements for different fire locations.

While this report provides progress in enhancing the longitudinal ventilation design methodology, some promising aspects for future research remain.

Some limitations regarding ProTuVeM 2 were encountered. First, ProTuVeM was rewritten in Python to enhance usability. While alignment with resistance results was satisfactory, further improvement is needed in aligning fire-related results with ProTuVeM. Additionally, ProTuVeM 2 does not perform calculations of wind effects, leading to results without wind influences in this report. Second, ProTuVeM is constrained by a maximum of 49 segments. In contrast, ProTuVeM 2 allows flexibility in selecting segment sizes, but different schemes can lead to minor temperature variations and resistance value differences. The limited segment count and temperature variations originating from different discretization sizes not only hinder comparability between the two models

but also prove irregularities. Third, both ProTuVeM models are one-dimensional, assuming uniform behavior along the width of the tunnel. This simplifies usability but does not capture the full complexity of real-world tunnel systems. Incorporating complex physics, like tunnel width as an additional dimension, enhances the ventilation model. As ProTuVeM 2 continues to evolve, ensuring compliance with legal requirements is essential. Each enhancement complicates result comparison between ProTuVeM and ProTuVeM 2, requiring careful consideration.

A penalization objective designed to serve the distance requirement between jet fan clusters during optimization proves to provide the required distances between the jet fans. However, cautious application of this objective is essential to avoid excessive or insufficient influence, which could result in suboptimal solutions or failure to meet the distance requirement. A confined parameter study was carried out to evaluate the impact of different weight allocations in the optimization process and to explore the consequences of an evolving exponent penalty term. While these parameters, designed to facilitate the exploration of the design space while ensuring ventilation design feasibility, were examined in this initial investigation, certain aspects were left unexplored. For example, decisions were made regarding the focus of the analysis. The weight allocation was adjusted during every iteration, starting from the first iteration. However, the potential impact of different starting points for weight allocations or the frequency of allocation adjustments, such as every five iterations, was not investigated. The same considerations apply to the adjustment of the exponential factor. Furthermore, the analysis measured the influence of the penalization objective based on the downstream distances between the intended downstream jet fans, while other metrics and various volume fractions were not thoroughly examined. A more comprehensive exploration of these factors has the potential to provide deeper insights and further enhance the quality of the solutions.

Furthermore, as a result of the configuration of the uncertainty methodology, aimed at minimizing differences between jet fan pressures and resistances across various scenarios, the solution may not fully satisfy equilibrium requirements for every fire position for the specified tunnel and fire scenario. Presently, the ventilation design does not account for wind effects, and a worst-case scenario wind effect is used in the optimization. This approach has proven to meet the critical air velocity requirements. However, it is crucial to recognize that when actual wind effects are factored into the model, the scenario-based methodology may fail to meet the specified requirements. This consideration should be taken into account when incorporating actual wind effects into the design.

Additionally, the solutions retain certain intermediate densities. Although it was a deliberate choice for now, it implies that elements of experience-based decision-making still exist in the systematic design approach.

While this thesis focused on a specific number of fire scenarios, it is worth noting that the choice of the number of scenarios may impact the solutions. Future research could explore how varying scenario numbers affect design reliability and computational efficiency.

In this study, a fixed mesh size of 10 m between nodes was used. It should be noted that a proper investigation into the effect of different mesh sizes was not conducted. Certainly, with the introduction of an uncertain fire scenario and a penalization objective, the complexity of the design space increased, emphasizing the importance of precise jet fan placement. The potential influence of mesh dependency on result reliability should be considered. Although this study has provided valuable insights, it is important to acknowledge that the choice of mesh size impacted the optimized designs. This acknowledgment enables better understanding of the findings and their implications in design. For future research, a systematic exploration of mesh dependency is recommended. This could involve conducting mesh sensitivity analyses or comparing different mesh resolutions.

Additionally, the actual effects of solutions provided by the systematic approach with respect to the overpressure ventilation system requirements remain somewhat unexplored. An investigation should delve deeper into the effects on final cumulative tunnel pressures and what it means for the positive pressure ventilation systems. As the optimization formulation does not consider for example minimum pressures or the positions of escape doors.

In summary, this report presents an advancement in longitudinal ventilation design, providing valuable insights and strategies for systematic design. It serves as a foundation for ongoing research and improvements in the field of tunnel ventilation design.

7

Conclusion

This thesis aimed to enhance the ventilation design approach at Arcadis, focusing on improving fire safety and reducing ventilation design costs. A tunnel ventilation system comprises of two ventilation systems which prevent back-layering and smoke flow into the CEC. The two systems benefit from a contradictory jet fan layout and the fire scenario, which dominates the tunnel pressure, is uncertain during design. To facilitate design enhancement, a research question was formulated: *What systematic design approach can be used to solve the fire safety ventilation design problem dominated by an uncertain fire scenario and how can this approach be practically implemented to enhance fire safety and design efficiency?*

ProTuVeM was rewritten in Python and named ProTuVeM 2 to facilitate the development of a systematic design approach, offering enhanced control, automation, and optimization capabilities. This systematic approach enhances design flexibility and solves the multi-objective optimization problem under uncertain conditions. To solve the ventilation problem, a positioning method based on the fundamentals of topology optimization was established. Instead of providing the number of jet fans and their positioning, the necessary jet fan pressure is determined by inputting the critical air velocity. Two optimization methods were formulated: maximizing jet fan efficiency while adhering to a volume constraint, and minimizing the number of jet fans while meeting the equilibrium constraint. Both positioned jet fans where their performance is minimally influenced by fire effects. Additionally, ProTuVeM 2 calculates cumulative pressures, replacing a mathematical sheet for assessing pressure along the tunnel. This offers efficiency and flexibility, expanding insight possibilities. The systematic design approach uses the cumulative pressure information for a second objective: the minimization of the maximum tunnel pressure. This objective serves the requirements of the positive pressure ventilation system design during the longitudinal ventilation system design, thereby reducing the risk of redesign in later stages.

To improve the applicability of the results, it was necessary to promote the required distance between jet fans during optimization. A penalization objective was introduced into the optimization which takes the total sum over the nodes, where for every node the sum over the surrounding densities is taken within a defined distance. The surrounding densities are subjected to an exponential penalty factor which promotes the distance between jet fans and discourages intermediate densities. To effectively use the second objective, an investigation was performed to analyze the effects of various weight combinations, continuous weight allocation, the continuation method applied to the penalization factor, and their impacts when considered both independently and sequentially. The conclusion is that the use of a continuous weight allocation followed by a continuous penalization increment provided a stable convergence and demonstrated an improved exploration of the design space. It was proven that the desired distances between jet fans and improved binary solutions could be obtained by using the penalization objective.

A scenario-based method was used to address fire uncertainty by minimizing the uncertainty constraints represented as distinct scenarios. This method avoids excessive amounts of constraints or worst-case scenario optimization. Solutions indicate that a continuous jet fan solution can approach the required pressures for every fire scenario. This approach uncovers a positioning technique that primarily situates jet fans in the tunnel section displaying a positive slope. This prevents unnecessary pressure buildup in the tunnel and the installation of more jet fans than required. The introduction of the penalization objective, together with the constraint of not positioning jet fans in the last 100 m of the tunnel, increased the practical ability of the solutions. However, it was also observed that the introduction of these constraints led to an increase in the maximum tunnel pressures.

In conclusion, the systematic design approach aims to design for the required jet fan pressure,

preventing excessive pressure buildup in the tunnel and providing applicable longitudinal ventilation designs. This prevents over conservative longitudinal ventilation system design, resulting in reduced energy consumption and cost savings for both ventilation systems. Additionally, the improved model provides valuable insights. This leads to improved design decisions and increased safety for tunnel users. This was demonstrated through the comparison of the two ventilation design approaches. In the context of the defined comparative review, the new systematic design approach provided a ventilation design with two fewer jet fans, while still achieving the required failure probability. By systematically seeking the optimal jet fan layout, the new method introduces new designs that further enhance the knowledge and expertise of designers in tunnel ventilation design.

8

Recommendations

In the pursuit of further enhancing the tunnel ventilation design process, a series of recommendations are formulated. These recommendations aim to further automate the process, improve flexibility, enhance the usability of ProTuVeM 2, and further improve tunnel fire safety.

The first and most important recommendation for Arcadis is to integrate, automate, and optimize the positive pressure ventilation design. This design stage is performed after the longitudinal ventilation design and has great capacity to be further improved. Particularly, regarding potential synergy between the two ventilation systems design. Additional recommendations include:

- Enhance the automation of the longitudinal tunnel ventilation design process by further integrating ProTuVeM, to ensure compliance with the legal framework.
- Compared to ProTuVeM, ProTuVeM 2 misses the possibility of providing a changing tunnel intersection. This has a notable impact on tunnel ventilation design, especially in cases where tunnel geometry changes significantly. Therefore, this should be included when further developing ProTuVeM 2.
- Extend the optimization capabilities by enabling the use of a variety of jet fans within the design process. Instead of a single predefined jet fan type, provide a list of jet fans, allowing the optimization process to select the most suitable jet fans for the specific tunnel configurations and objectives.
- The ventilation design solutions could benefit from the exploration of alternative objectives which meet the requirements of different tunnel and ventilation assignments. For example, a cost reduction objective or an objective which considers the positions of escape doors.
- The penalization objective, which promotes the distance between jet fans, could benefit from further research. This includes investigating the effects of adjusting the penalization factor, the weight allocation, and step sizes. Moreover, analyzing different design spaces and considering different HRR is essential due to the significant influence on jet fan performance.
- It is worth exploring the introduction of, for instance, a Heaviside projection filter to further reduce the presence of intermediate densities. It is important to note that when implementing a projection filter to eliminate intermediate densities, it is beneficial to incorporate additional information related to the ventilation problem, such as considering the positions of escape doors. These analysis can enhance understanding of ProTuVeM 2 and the newly introduced design approach.
- The existing uncertainty approach considers only the uncertainty associated with the fire. Nevertheless, the tunnel ventilation model is also affected by uncertainties related to wind effects. Furthermore, future research should assess the influence of varying fire scenario numbers on design reliability and computational efficiency.
- Given the fixed mesh size used in this study and the impact on optimized designs, it is advisable to investigate mesh dependency systematically in future research. This exploration can involve conducting mesh sensitivity analyses or comparing different mesh sizes for specific cases to enhance result reliability and better understand the implications for design.
- Create a user-friendly design interface to ameliorate interaction between ProTuVeM 2 and designers would be a valuable development.

References

2004/54/EC. (2004, 04). Directive 2004/54/ec of the european parliament and of the council. *Official Journal of the European Union*.

Abraham, O., & Dérobert, X. (2003, 09). Non-destructive testing of fired tunnel walls: The mont-blanc tunnel case study. *Ndt & E International - NDT E INT*, *36*, 411-418. doi: 10.1016/S0963-8695(03)00034-3

Arnold, B. C. (1985). p-norm bounds on the expectation of the maximum of a possibly dependent sample. *JOURNAL OF MULTIVARIATE ANALYSIS*, *17*, 316-332.

AVV. (2005). Aanbevelingen ventilatie van verkeerstunnels [Computer software manual].

AVVb. (2005). Aanbevelingen ventilatie van verkeerstunnels, bijlagen [Computer software manual].

Bendsøe, M. P., & Kikuchi, N. (1988). Generating optimal topologies in structural design using a homogenization method. *COMPUTER METHODS IN APPLIED MECHANICS AND ENGINEERING*, *71*, 197-224.

Bruns, T. E., & Tortorelli, D. A. (2001). Topology optimization of non-linear elastic structures and compliant mechanisms. *Computer Methods in Applied Mechanics and Engineering*, *190*(26), 3443-3459. Retrieved from `https://www.sciencedirect.com/science/article/pii/S0045782500002784` doi: https://doi.org/10.1016/S0045-7825(00)00278-4

Dagbladet. (2009). *Dødsulykke i eiksundtunnelen.*

Dembo, R. S. (1991, 12). Scenario optimization. *Ann Oper Res*, *30*, 63–80. doi: 10.1007/BF02204809

Derikx, B., Janssen, W., & de Jong, L. (2011). *Handleiding protuvem v2.0.*

Ingason, H. (2016, 06). New challenges in tunnel fire safety. *Fire Technology*, *52*. doi: 10.1007/s10694-016-0607-1

Ingason, H., Li, Y., & Lönnermark, A. (2015). *Tunnel fire dynamics.* doi: 10.1007/978-1-4939-2199-7

Iowa environmental mesonet. (2021). Retrieved from `https://mesonet.agron.iastate.edu/`

Jansen, M., Lombaert, G., Schevenels, M., & Sigmund, O. (2014, 04). Topology optimization of fail-safe structures using a simplified local damage model. *Structural and Multidisciplinary Optimization*, *49*. doi: 10.1007/s00158-013-1001-y

Kreisselmeier, G., & Steinhauser, R. (1979). Systematic control design by optimizing a vector performance index. *IFAC Proceedings Volumes*, *12*(7), 113-117. Retrieved from `https://www.sciencedirect.com/science/article/pii/S1474667017655848` doi: https://doi.org/10.1016/S1474-6670(17)65584-8

Ntzeremes, P., & Kirytopoulos, K. (2022). Supporting decision-making processes for selecting fire safety measures for road tunnels. *Journal of Traffic and Transportation Engineering (English Edition)*, *9*(3), 473-489. Retrieved from `https://www.sciencedirect.com/science/article/pii/S2095756422000241` doi: https://doi.org/10.1016/j.jtte.2020.07.006

Osborne, W., Osborne, W., of Colchester Ltd, W., & Turner, C. (1954). *Woods practical guide to fan engineering.* Woods of Colchester Limited. Retrieved from `https://books.google.nl/books?id=CCOGAAAAIAAJ`

Pei, G., & Pan, J. (2014, 09). Numerical study on different series modes of jet fan in a longitudinal tunnel ventilation system. *Mathematical Problems in Engineering*, *2014*. doi: 10.1155/2014/194125

Pettersson, O., Magnusson, S., & Thor, J. (1976). Fire engineering design of steel structures. *Bulletin of Division of Structural Mechanics and Concrete Construction*, *Bulletin 52*, 232.

Rijkswaterstaat, & GPO. (2023). *Basisspecificatie tti rws tunnelsysteem.* (Manager Team: Fred Bouwmeester, Lead Architect: Hans Dijkema)

Scholten, R. (2016). *Nederlands kenniscentrum voor ondergronds bouwen en ondergronds ruimtegebruik.* Retrieved from `https://www.kivi.nl/uploads/media/583d4d3a06374/S204.pdf`

Svanberg, K. (1993). The method of moving asymptotes (mma) with some extensions. In G. I. N. Rozvany (Ed.), *Optimization of large structural systems* (pp. 555–566). Dordrecht: Springer Netherlands. Retrieved from `https://doi.org/10.1007/978-94-010-9577-8_26` doi: 10.1007/978-94-010-9577-8_26

van Oerle, N. (2016). *Verificatie en validatie overdruksystemen mtk wegtunnels, beschrijving methodiek.* (Company name: Peutz)

Weng, M., Obadi, I., Wang, F., Liu, F., & Liao, C. (2020). Optimal distance between jet fans used to extinguish metropolitan tunnel fires: A case study using fire dynamic simulator modeling. *Tunnelling and Underground Space Technology*, *95*, 103116. doi: https://doi.org/10.1016/j.tust.2019.103116

Zhu, B., Zhang, X., Zhang, H., Liang, J., Zang, H., Li, H., & Wang, R. (2020). Design of compliant mechanisms using continuum topology optimization: A review. *Mechanism and Machine Theory*, *143*.

Appendix A

A.1 Table Casualties of Tunnel Fires

Casualties of tunnel fires.

Case	No. of casualties	Tunnel	Length	Country	Year
1	289	Baku subway	2.2 km	Azerbaijan	1995
2	198	Daegu subway	25.9 km	South Korea	2003
3	155	Kaprun funicular tunnel	3.3 km	Austria	2000
4	39	Mont-Blanc tunnel	11.6 km	France/Italy	1999
5	12	Tauern tunnel	6.4 km	Austria	1999
6	11	Gotthard tunnel	16.9 km	Switzerland	2001
7	9	Viamala tunnel	750 m	Switzerland	2006
8	5	Gleinalm tunnel	8.2 km	Austria	2001
9	5	Eiksund tunnel	7.7 km	Norway	2009
10	3	Burnley tunnel	3.4 km	Australia	2007
11	2	Martino tunnel	4.8 km	Italy	2005
12	2	Fréjus tunnel	12.9 km	France/Italy	2005
13	2	Rotsethhorn tunnel	1.2 km	Norway	2000
14	1	Eidsvoll tunnel	1.2 km	Norway	2006
15	1	Baregg tunnel	1.1 km	Switzerland	2004

Figure A.1: Selection of life taking tunnel fires (Weng et al., 2020).

A.2 Automatic Clicker File to Enhance Comparability between ProTuVeM and ProTuVeM 2.0

Listing A.1: Made for ProTuVeM

```
# -*- coding: utf-8 -*-
"""
Created on Wed May 10 15:10:49 2023

@author: vanderds7457
"""

#Validation with ProTuVeM file
#Open ProTuVeM yourself, go to Segmentgegevens and then run this script to fill in t
import pyautogui # Control mouse and keyboard
import numpy as np

# Move the mouse to a specific location
# Get the current mouse position
x, y = pyautogui.position()
# Print the mouse position
```

```
print(f"Mouse position: {x},{y}")

###Provide information regarding the tunnel###
Slope = -0.3
Intersection = 64
Circumference = 32
Lanes = 2
Wall = 0.018
ORV = 80

Tunnel_length = 1000
segment_length = 100
seg_length = np.ones(int(Tunnel_length/segment_length))*segment_length

#######
SlopeV = np.ones(len(seg_length))*Slope
CircumferenceV = np.ones(len(seg_length))*Circumference
IntersectionV = np.ones(len(seg_length))*Intersection
LanesV = np.ones(len(seg_length))*Lanes
WallV = np.ones(len(seg_length))*Wall
ORVV = np.ones(len(seg_length)-1)*ORV
#Click defenitions
def click_L():
    pyautogui.moveTo(216, 191)
    pyautogui.click()
def click_H():
    pyautogui.moveTo(232,214)
    pyautogui.click()
def click_O():
    pyautogui.moveTo(223,237)
    pyautogui.click()
def click_D():
    pyautogui.moveTo(223,263)
    pyautogui.click()
def click_R():
    pyautogui.moveTo(228,279)
    pyautogui.click()
def click_Seg():
    """ These lines click on "Vaste gegevens" in ProTuVem"""
    pyautogui.moveTo(210, 114)
    pyautogui.click()
def click_W():
    """ These lines click on "Vaste gegevens" in ProTuVem"""
    pyautogui.moveTo(229,375)
    pyautogui.click()
def click_Op():
    """ These lines click on "Vaste gegevens" in ProTuVem"""
    pyautogui.moveTo(293,395)
    pyautogui.click()


click_Seg()
click_L()
```

```
pyautogui.press('backspace')
for i in seg_length:
    pyautogui.typewrite(str(i))
    pyautogui.press(['tab'])
pyautogui.press(['home']*2)
click_H()
pyautogui.press('backspace')
for j in SlopeV:
    new_j = str(j).replace('.', ',')
    pyautogui.typewrite(new_j)
    pyautogui.press(['tab'])
pyautogui.press(['home']*2)
click_O()
pyautogui.press('backspace')
for j in CircumferenceV:
    pyautogui.typewrite(str(j))
    pyautogui.press(['tab'])
pyautogui.press(['home']*2)
click_D()
pyautogui.press('backspace')
for j in IntersectionV:
    pyautogui.typewrite(str(j))
    pyautogui.press(['tab'])
pyautogui.press(['home']*2)
click_R()
pyautogui.press('backspace')
for j in LanesV:
    pyautogui.typewrite(str(j))
    pyautogui.press(['tab'])
pyautogui.press(['home']*2)
click_W()
pyautogui.press('backspace')
for j in WallV:
    new_j = str(j).replace('.', ',')
    pyautogui.typewrite(new_j)
    pyautogui.press(['tab'])
pyautogui.press(['home']*2)
click_Op()
pyautogui.press('backspace')
for j in ORVV:
    pyautogui.typewrite(str(j))
    pyautogui.press(['tab'])
```

A.3 Design Approach Deterministic and Uncertain Ventilation Design

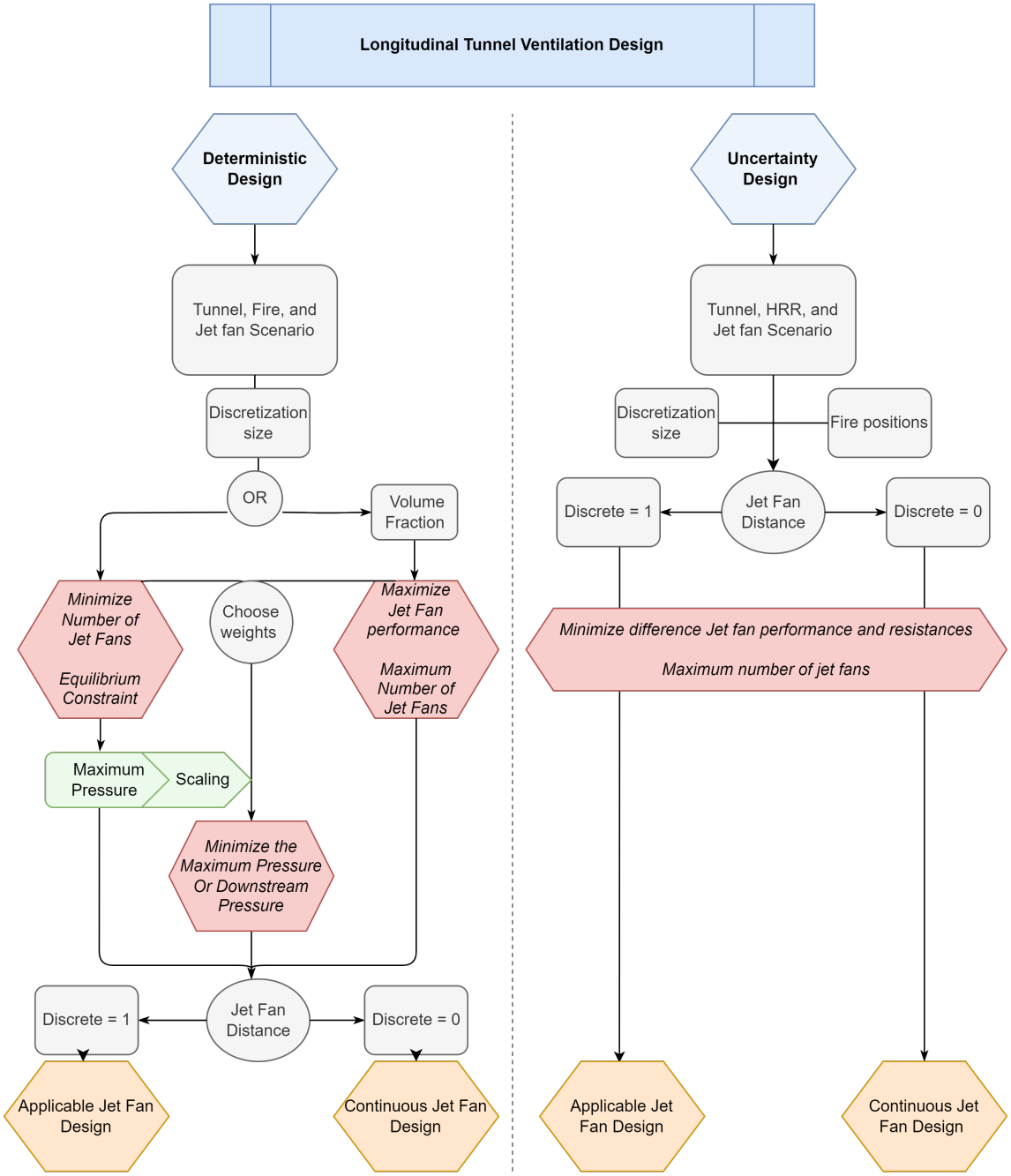

Figure A.2: Block diagram showing the deterministic design approach (left) and the uncertainty design approach (right).